A NUMERICAL DESIGN STUDY OF FULLY CAVITATING HYDROFOIL

SECTIONS HAVING PRESCRIBED PRESSURE DISTRIBUTIONS

B. R. Parkin, R. F. Davis and J. Fernandez

NAVY DEPARTMENT

NAVAL SEA SYSTEMS   MMAND

REPORT DOCUMENTATION PAGE		READ INSTRUCTIONS BEFORE COMPLETING FORM
1. REPORT NUMBER TM-75-170	2. GOVT ACCESSION NO.	3. RECIPIENT'S CATALOG NUMBER
4. TITLE (and Subtitle) A NUMERICAL DESIGN STUDY OF FULLY CAVITATING HYDROFOIL SECTIONS HAVING PRESCRIBED PRESSURE DISTRIBUTIONS.		5. TYPE OF REPORT & PERIOD COVERED Technical Memorandum
		6. PERFORMING ORG. REPORT NUMBER
7. AUTHOR(s) B. R. Parkin, R. F. Davis and J. Fernandez		8. CONTRACT OR GRANT NUMBER(s) N00017-73-C-1418
9. PERFORMING ORGANIZATION NAME AND ADDRESS Applied Research Laboratory P. O. Box 30 State College, PA 16801		10. PROGRAM ELEMENT, PROJECT, TASK AREA & WORK UNIT NUMBERS Program Element 62544N Task Area ZF43-421-001
11. CONTROLLING OFFICE NAME AND ADDRESS Naval Sea Systems Command Dept. of the Navy Washington, DC 20362		11. REPORT DATE 30 June 75
		13. NUMBER OF PAGES 136
14. MONITORING AGENCY NAME & ADDRESS(if different from Controlling Office) David W. Taylor Naval Ship R&D Center Department of the Navy Bethesda, MD 20084		15. SECURITY CLASS. (of this report) UNCLASSIFIED
		15a. DECLASSIFICATION/DOWNGRADING SCHEDULE

16. DISTRIBUTION STATEMENT (of this Report)

Approved for public release. Distribution unlimited.
Per NAVSEA - Nov. 25, 1975.

17. DISTRIBUTION STATEMENT (of the abstract entered in Block 20, if different from Report)

18. SUPPLEMENTARY NOTES

19. KEY WORDS (Continue on reverse side if necessary and identify by block number)

Hydrofoils, Numerical Design Study, Fully Cavitating.

20. ABSTRACT (Continue on reverse side if necessary and identify by block number)

Results of a study of fully cavitating hydrofoil sections are reported. All calculations are based upon the linearized theory of cavity flow in two dimensions. This report is the first detailed exploration of the consequences of the general inverse theory which permits the designer to specify the design values of the lift coefficient, cavitation number and the thickness of the upper surface of the cavity at the profile trailing edge as well as the shape of the pressure distribution on the wetted surface. The ordinates of the NEXT Pg

DD FORM 1473 1 JAN 73   EDITION OF 1 NOV 65 IS OBSOLETE

upper cavity contour and the wetted surface contour are calculated. The design angle of attack, the cavity length, the drag coefficient and the moment coefficient are also calculated. It is found for almost any cavitation number and any design lift coefficient that if the center of pressure is placed as closely as possible to the profile leading edge the resulting profile will have the most favorable lift-to-drag ratio. The study also includes off-design calculations, in accordance with the direct theory of cavity flows, to determine cavity interference with the upper nonwetted surface of the profile and the hydrodynamic forces of particular designs.

Abstract: Results of a study of fully cavitating hydrofoil sections are reported. All calculations are based upon the linearized theory of cavity flow in two dimensions. This report is the first detailed exploration of the consequences of the general inverse theory which permits the designer to specify the design values of the lift coefficient, cavitation number and the thickness of the upper surface of the cavity at the profile trailing edge as well as the shape of the pressure distribution on the wetted surface. The ordinates of the upper cavity contour and the wetted surface contour are calculated. The design angle of attack, the cavity length, the drag coefficient and the moment coefficient are also calculated. It is found for almost any cavitation number and any design lift coefficient that if the center of pressure is placed as closely as possible to the profile leading edge the resulting profile will have the most favorable lift-to-drag ratio. The study also includes off-design calculations, in accordance with the direct theory of cavity flows, to determine cavity interference with the upper nonwetted surface of the profile and the hydrodynamic forces of particular designs.

Table of Contents

Table of Contents (Cont.)

List of Tables

List of Figures

List of Figures (Cont.)

List of Figures (Cont.)

List of Figures (Cont.)

Nomenclature

Roman Symbols

a	-	cavity parameter
C_L	-	lift coefficient
C_D	-	drag coefficient
C_M	-	moment coefficient
K	-	cavitation number
ℓ	-	cavity length, $\ell = a^2 + 1$
L/D	-	lift-to-drag ratio
m	-	pressure amplification factor used in the second design method
p	-	nondimensionalized perturbation pressure
P_k	-	cavity pressure
P_∞	-	free stream pressure
s	-	peak pressure location, measured from the nose
$t(x)$	-	upper (non-wetted) surface of the hydrofoil
T	-	cavity thickness at the trailing edge
U	-	free stream velocity
$W(\varepsilon)$	-	function used to compute the angle of attack corresponding to the cavity-foil interference in the off-design calculations
x	-	absissa, taken as positive downstream, with the origin at the nose
$\bar{x}$	-	distance of the center of pressure from the nose
$y_u(x)$	-	cavity contour (upper surface)
$y_c(x)$	-	cavity thickness due to the complementary function (not total thickness)

Greek Symbols

α - angle of attack of the chord line with respect to the free stream

β - cavity parameter, $1 - \dfrac{1}{\sqrt{1+K}}$

$\eta(x)$ - wetted surface shape

ρ - density

$\Xi_1(a,x)$,

$\Xi_2(a,x)$ - functions used to compute the cavity contour in the off-design calculations

Superscript

$'$ - prime indicates differentiation with respect to x

INTRODUCTION

General:

In 1964, a method for calculating the shape of a fully-cavitating
hydrofoil section with prescribed pressure distribution was published
[1, 2, 3].* This work, which is based upon the linearized theory of
cavity flows in two dimensions, resulted in three profile design pro-
cedures. In all three, the shape of the pressure distribution on the
wetted surface of the profile is given, and the cavitation number, the
cavity thickness at the profile trailing edge, and the total section
lift coefficient are prescribed. Then the shape of the wetted surface
is calculated along with the cavity length, the drag coefficient, and
the moment coefficient about the profile nose. The lift-to-drag ratio
then follows. The three design procedures differ in the way that the
cavity thickness requirement is satisfied. Because of this difference,
the design attack angle is an outcome of the calculations in the first
and second procedures. In the third method, the attack angle is
prescribed from the outset.

In the first design procedure, the cavity thickness is obtained by
use of the complementary function for the problem. This complementary
function is commonly called the "point-drag-solution" [4] of cavity flow
theory. In our procedure, the profile is taken to be at the attack
angle for "shockless entry" so that the prescribed pressure distribution
defines completely the pressure distribution on the wetted surface.
Thus, profile design at the ideal attack angle provides the designer with

_____

*Numbers in brackets refer to citations in the list of references.

the greatest control over every detail of the pressure distribution; and for this reason we might be justified in regarding the first design procedure as the proper embodiment of the linearized inverse hydrofoil problem. The analogous method of thin airfoil theory is given in [5, 6, 7], for example. The fact that the designer can now control the cavity thickness allows him to make sure that the upper surface of the cavity does not interfere with the hydrofoil, and thereby to make some provision for the structural adequacy of his design from the start.

The second design procedure accounts for the fact that interference between the hydrofoil and the cavity can also be eliminated by increasing the attack angle of the profile above the ideal angle, instead of by means of the complementary function. In this case, one prescribes the value of C_L as before. However, now one cannot control all details of the pressure distribution. Only the shape of that part of the pressure distribution which is associated with the wetted-surface camber is subject to the designer's pleasure. The pressure distribution now has two parts: the first part which is due to the nose singularity (or incremental attack angle), and the second part which is due to camber of the wetted surface. The shape of the first part is fixed, but we can vary its magnitude by changing the angle of attack. Once the shape of the second part is specified; one can adjust its amplitude so that the value of the lift coefficient originally specified is met by the sum of contributions from the first and the second parts of the pressure distribution.

The third design procedure is more general than the first and

second procedures, because the complementary function and the incremental

attack angle are both used to meet prescribed cavity-thickness require-

ments. Now, one specifies the value of attack angle along with the lift

coefficient, cavitation number, cavity thickness at the trailing edge,

and the shape of that part of the pressure distribution due to camber.

Then, the remaining properties of the profile can be determined. The

third design procedure has not been worked out in detail, so that no

calculations have been made in with this procedure.

On the other hand, some calculations have previously been made with

the first two design procedures. However, those calculations were carried

out only to illustrate the efficacy of the theory [2, 3]. No attempt has

yet been made to put forward specific profile designs or to use these

two procedures to explore the outcome of various design philosophies.

The purpose of the present study is to remedy this deficiency. In order

to update the numerical procedures of References 2 and 3 so that the

computer program is compatible with the IBM 370 computer, the entire

program, as described in Reference 3, has been reviewed, all necessary

corrections and modifications have been made, and all analytical results

of Reference 2 have been checked to be sure that the calculated results

are accurate. This work has been carried out by R. F. Davis and J.

Fernandez. They have documented their work in a companion report [8].

It should be emphasized that the present study explores only the

consequences of various hydrodynamic design strategies on profile

performance and geometry. The only consideration relating to profile

structural requirements is expressed in terms of the cavity thickness.

This hydrodynamic variable is treated parametrically in order to show

systems and structural engineers possible hydrodynamic consequences of

structural or other systems requirements. The important design inter-

actions between detailed structural and hydrodynamic requirements are

outside the scope of this study.

Flow Geometry and Nomenclature:

Before turning to the study of numerical results from the first an

second design procedures, we will define the flow geometry and the maj r

parameters which are basic to our considerations with the help of Fig re 1.

Although this schematic illustrates the way one might load a profile or

calculations in accordance with the first design procedure, the esse :ial

geometric aspects of the hydrofoil, the cavity and the free-stream f ow

apply to both the first and the second design procedures. In the ca e of

the second design procedure the region of secondary perturbation pr ssure

between the primary peak and the trailing edge, shown in Figure 2, would

be deleted. As we have already noted, the second procedure make use of

an angle of attack increment above that needed for shockless er ry to

provide for the prescribed cavity thickness T. In this case ae complete

pressure distribution consists of two parts and the first pa t, due to

the nose singularity resulting from the incremental attack ngle above

that for shockless entry, provides automatically that the ofile wetted

surface will have a non-zero perturbation pressure everywh e, except at

the trailing edge where it must be zero. Thus, one needs prescribe

only the primary pressure peak of the second part in order to determine

the shape of the wetted surface when the second design pr cedure is used.

As Figure 1 shows, the free-stream velocity and static pressure are U and P_∞, respectively. The cavity pressure is P_k, a constant, and if the density of the liquid is ρ the cavitation number for the flow is

$$K = \frac{P_\infty - P_k}{1/2\ \rho\ U^2} \quad . \tag{1}$$

If the static pressure at any point in the flow is $P(x,y)$, we shall define the perturbation pressure as

$$p(x,y) = \frac{P(x,y) - P_k}{1/2\ \rho\ U^2} \quad , \tag{2}$$

with the understanding that at points on the wetted surface of the hydrofoil we have $p(x,o) = p(x)$, where now $0 \leq x \leq 1$. On the upper and lower surfaces of the cavity, $p(x,y) = 0$. The angle of attack is α, the cavity length is ℓ and the peak pressure location, measured from the nose of the foil is s. Note also that the hydrofoil has a unit chord and that the cavity thickness, T, is defined at the point x=1 only. Figure 1 also shows the positive senses of the lift, cavity drag and the pitching moment referred to the nose of the hydrofoil. The term cavity drag is used to emphasize that skin friction on the profile wetted surface is excluded from the present considerations. If the Reynolds number for the flow is known this added drag can be estimated separately. It is much smaller than the cavity drag. The three hydrodynamic coefficients assume their customary definitions for two dimensional flow:

$$C_L = \frac{L}{1/2 \, \rho \, U^2} \quad , \tag{3}$$

$$C_D = \frac{D}{1/2 \, \rho \, U^2} \quad , \tag{4}$$

and

$$C_M = \frac{M}{1/2 \, \rho \, U^2} \tag{5}$$

provided the chord length is unity. In this study the upper contour of

the cavity is denoted by $y_u(x)$, the wetted surface contour (or camber

function by $\eta(x)$; and the strength of the nose singularity corresponding

to an attack angle above shockless entry by A. The relationship between

the strength of the point drag singularity E, and the incremental cavity

thickness provided by the complementary function, $y_c(1)$, is

$$E \equiv y_c(1)/\sqrt{\ell-1} \tag{6}$$

where ℓ is the cavity length as illustrated in Figure 1. This notation

is consistant with that used in References [1], [2] and [3]. Additional

information on this and related theoretical topics are given in those

sources.

<div align="center">FIRST DESIGN PROCEDURE–SUMMARY OF RESULTS</div>

Preliminary Remarks:

In order to explore design trends to be obtained with the first

design procedure a series of inverse calculations have been made which

use the pressure distribution of Figure 2. In these first calculations

the location of the peak pressure is restricted mostly to values of s between

.1 and .5 chord. For the present this limitation will not impose any essential drawback to this preliminary investigation. More complete correlations, corresponding to the range $.1 \leq s \leq .9$, are discussed later in this report, and a tabulation of coefficients for the entire range is given in Appendix A. The range of C_L values in this tabulation has been chosen to correspond to those likely to be encountered in the design of cavitated foils for a high speed hydrofoil boat.

Figure 2 shows a double ellipse pressure distribution having a peak pressure magnitude of h and a secondary peak of λh where $0 < \lambda << 1$. The secondary ellipse is used simply to insure that the disturbance pressure on the profile will exceed zero everywhere on the wetted surface of the profile except at the nose and at the trailing edge. The elliptical distribution has the form $p(x) \sim \sqrt{1-x}$ near $x=1$ in accordance with function-theoretical requirements appropriate to the boundary value problem [2]. For this pressure distribution the primary semi-ellipse always starts at the point $x=0$ for all values s of the horizontal semi-axis for which $0 \leq s \leq .5$ as indicated in Figure 2. In those cases for which $.5 \leq s \leq 1.$, the semi-axis of the primary elliptical distribution is $(1-s)$ and this loading is anchored to the trailing edge for all values of s corresponding to this rearward loading of the profile. Thus, the primary semi-ellipse occupies the interval $(2s-1) \leq x \leq 1$ and the quarter ellipse of the secondary loading would occupy the interval $0 \leq x \leq (s2-1)$. That is, if we reflect the contours of Figure 2 in the vertical axis so that the positions of nose and trailing edge are reversed we will have the loading configuration for tail-loaded profiles. If C_L, s and λ are prescribed, it follows at

once that

$$h = \frac{2C_L}{\pi[s + \lambda(1-2s)]} \quad , \quad 0 < s \leq 1/2 \quad . \tag{7}$$

When $1/2 \leq s < 1$ one has the case of aft loading on the foil and

$$h = \frac{2C_L}{\pi[1-s + \lambda(2s-1)]} \quad . \tag{8}$$

Equation (7) determines the value of h for the various lift coefficients considered in the initial phases of our study of nose-loaded profiles.

Hydrodynamic Performance:

The best value of λ to be used for foil design is somewhat uncertain because the designer needs only enough positive pressure in the secondary ellipse to provide him some assurance that premature wetted surface cavitation will not occur within some range of attack angles less than the ideal design value in any particular case. On the other hand if λ is too large then it becomes less convenient for one to shift the center of pressure location to whatever value may be desired. Clearly, $\lambda = 0$ is the best choice in this latter respect. In order to examine the effect of the value of λ a series of calculations were made at zero cavitation number and fixed cavity thickness, $T = 0.15$, for $\lambda = 0$, .025 and .05. Values of s were selected at $s = .3$, .4 and .5. Values of C_L were chosen to be at $C_L = .08$, .10, .12, .15. The important parameter for performance considerations is the lift-to-drag ratio. The result of these calcula-

tions is shown in Figure 3 in which L/D versus s curves are given for $\lambda=0$ and $\lambda=.05$. The curves for $\lambda=.025$ lie between the curves for $\lambda=0$ and $\lambda=.05$ and they were omitted for the sake of clarity. For future reference this illustration also shows a curve obtained from calculations made with the second design procedure. The first point to be noticed from this illustration is that a value of λ as large as .05 does not affect the value of L/D too drastically and yet it should provide some margin for error in the operating attack angle. Therefore, the value $\lambda=.05$ has been selected as the standard value for use in subsequent calculations by the first design procedure.

Another trend shown by Figure 3 is the increase in L/D as the peak pressure moves toward the nose for all C_L values. This is an important point to note because in the past, designers have often tried to place the peak pressure as near to the trailing edge as possible in order to obtain foils of low drag. This design philosophy originated with Tulin [9] and it was further reinforced by the more general considerations of Reference [2]. However, those recommendations ignore the fact that the upper surface of the cavity must clear the wetted surface of the hydrofoil. In the present calculations this fact is explicitly accounted for in the design procedure and it results in a trend with respect to the location of the peak loading which is directly contradictory to the previous result — but at the cost of less favorable lift-to-drag ratios.

A further exploration of these preliminary trends shows the effect of cavitation number on lift-to-drag ratio when the cavitation number varies from 0 to 0.2. The cavity thickness, $T=.15$, and location of peak

pressure at s=.3 were held fixed. The same values of C_L were selected
as before. The result of these calculations is shown in Figure 4.
Evidently the lift-to-drag ratio is strongly affected by cavitation
number with the most favorable values being found at K=0.

Figure 5 shows the lift-to-drag ratio as a function of peak pressure
location for various lift coefficients at a cavitation number, K=.2.
Note that the cavity thickness for this case is T=.1 so that for s=.3
one can compare this illustration with Figure 4 and see that increasing
T at K=.2 increases the cavity drag. This trend is obviously true at
all K values. Moreover, we see from these curves that when K=.2 and
T=.10 the best position for the peak pressure varies with C_L. For
example at C_L=.15 the best value of s appears to be at s=.42 and that
it apparently moves toward the trailing edge as C_L decreases.

In Figure 6 the lift-to-drag ratio has been plotted against peak
pressure location, s, at a constant C_L=.15 and at constant T=.15 for
various cavitation numbers between K=0 and .2. One can compare the
curve for K=.2 with the curve for C_L=.15 of the preceding figure to
see again how increasing the cavity thickness from T=.10 to T=.15
decreases the lift-to-drag ratio from about 8.5 to about 6. For the
thicker cavity considered in Figure 6 it appears that the most favorable
location for the peak pressure is near the profile nose.

The foregoing results from the first design procedure have revealed
the following trends. For most cases one will obtain more favorable
lift-to-drag ratios if he concentrates the pressure loading as near to
the leading edge of the profile as he can. The cavitation number has a

large effect on the lift-to-drag ratio. The larger the value of K

becomes, the less favorable is the resulting lift to drag ratio. This

is a direct consequence of the fact that one requires a fixed value of

cavity thickness, T, at the design point regardless of the cavitation

number. But as the cavitation number increases the cavity length

decreases and if left to itself the cavity thickness would tend to

decrease too. However, our design method requires a constant cavity

thickness at the trailing edge. Therefore, it is necessary that we

increase the strength of the point drag function to meet this require-

ment. Accordingly, the lift-to-drag ratio must decrease because the

cavity drag is increased while we hold the lift constant. This situation

should be true for all locations of the peak pressure. The preceding

examples also show that the design lift coefficient has an appreciable

effect on the lift-to-drag ratio. For nose-loaded profiles the lift-to-

drag ratio increases with increasing values of lift coefficient. This

effect seems to become stronger as the peak pressure location is moved

toward the nose. Now it is known for a delta function pressure at the

trailing edge [2, 1] that

$$\frac{L}{D} = \frac{8\pi(1+K)}{C_L} \frac{\ell(\ell-1)}{(\ell-2)^2} \quad , \tag{9}$$

where

$$\sqrt{\ell-1} = \frac{C_L}{4\pi(1+K)\beta} + \sqrt{\left[\frac{C_L}{4\pi(1+K)\beta}\right]^2 - 1} \quad , \tag{10}$$

and

$$\beta = 1 - \frac{1}{\sqrt{1+K}} \quad . \tag{11}$$

As $K \to 0$, $\ell \to \infty$ and equation (9) reduces to Tulin's result [9] in which $L/D = 8\pi/C_L$. The important thing to note is that these formulae indicate that the lift-to-drag ratio should decrease as C_L increases which is opposite to the trend found by means of the first design procedure. Thus, if structural limitations allow it, the present study suggests that the designer should use heavily loaded foils in order to secure the most favorable values of L/D at the design condition. The "delta function rule" suggests that lightly loaded foils are preferred. We have already noted that the delta function rule does not control the position of the cavity upper surface with respect to the wetted surface of the profile. Evidently, the control of the cavity location incorporated into the present design procedure changes the direction of the trend of L/D with respect to design C_L in a most significant way. However, we will see that as the location of the peak pressure moves nearer to the trailing edge the increase of L/D with increasing C_L becomes less, although this trend is not reversed for profiles defined by the first design procedure. Another general trend resulting from the foregoing calculations is that as the cavitation number increases, changes in the peak pressure location have less effect on the value of L/D. For example, Figure 6 shows that the lift-to-drag ratio of nose loaded profiles in the range $.1 \lesssim \xi \lesssim .5$ is hardly changed by the location of the peak pressure when $K = .2$, although the change is appreciable when $K = 0$.

Hydrodynamic Equivalence and Performance Summary:

All of the preceding analysis of trends have been made for various
peak pressure locations, denoted by the parameter s of the double ellipse
pressure distribution. While this has been a convenient procedure, the
foil loading quantity of fundamental interest is $\bar{x}$, the chordwise distance
from the hydrofoil nose to the center of pressure. Values of $\bar{x}$ for all
cases calculated for the double ellipse pressure distribution are tabulated
in Appendix A. Now, one has considerable freedom in the specification
of the pressure distribution for calculations in accordance with the
first design procedure. It is certainly possible to prescribe several
distributions which will have the same value of $\bar{x}$ even though their
shapes may differ in detail. One would anticipate that as long as all
of these distributions have the same value of $\bar{x}$, C_L, T and K at the
design point, the remaining hydrodynamic performance design parameters
should differ very little from one another. In order to test this con-
jecture a series of calculations have been made with the first design
procedure for a modified three-term [2] and a reversed three-term pressure
distribution at a C_L = .12, as shown in Figure 7. The reversed three-
term distribution has $\bar{x}$ = .3647, corresponding to a nose-loaded design.
The modified three-term distribution has $\bar{x}$ = .6685, corresponding to a
tail-loaded design. Hydrodynamic performance data from these two distri-
butions are compared with data from equivalent double-ellipse distributions
in Tables I and II. It can be seen that differences in performance
between equivalent profiles are very small indeed. In fact we believe
that part of the differences shown may be due to the fact that data for

the elliptical distributions were obtained from those of Appendix A
by linear interpolation.

The foregoing is a useful result because it permits one to summarize
all of the hydrodynamic trends considered above for the double ellipse
family of pressure distributions with the understanding that this summary
will also be valid for other distributions having different shapes. All
that we require is that the pressure distributions are hydrodynamically
equivalent in the sense that the value of $\bar{x}$ be the same for each and that
the same design point (C_L, T and K) applies to all of them. As a result
of these considerations a series of "performance maps" have been prepared
from the data of Appendix A. These are given in Figures 8, 9, 10, 11
and 12, which show plots of L/D vs C_D with contours of constant C_L and
s. Each one of these maps shows three designs, corresponding to three
values of T, and each map is valid for the value of K noted on it.
Evidently, all C_L contours are equilateral hyperbolas. Note that the
plot for T=.10 shows intersecting contours for certain values of s.
This occurrance is a consequence of the trends shown already in Figure
5. As we have seen, when the cavitation number is high enough and T is
sufficiently small, the best location for the peak pressure moves from
the nose toward the trailing edge. Evidently the nose location is not
always the best location. However, this is the only case found so far
in which the nose location is not the best choice. The chart of Figure
13 is a plot of C_M vs $\bar{x}$, with contours of constant C_L and s as before.
This chart provides the connection between $\bar{x}$ and s so that if the design
C_L and $\bar{x}$ are known the resulting value of s can be used to enter the

charts of Figures 8 through 12 to find the design L/D, etc. for distri-
butions having other than the double ellipse shape. Note that Figure
13 applies to all values of K and T so that only one such chart is needed.
The value λ, the secondary quarter-ellipse parameter, for these charts
is .05.

Profile Geometry:

The foregoing paragraphs give a fairly comprehensive overview of
the hydrodynamic performance of fully cavitating hydrofoil sections
designed by the first procedure. It is now necessary to explore the
geometric properties of the profiles as the design point and the peak
pressure location are varied. The graphs of Figures 14 through 23 show
to scale the profile wetted surfaces and the upper cavity contours in
accordance with the nomenclature defined in Figure 1. In these figures
the chord lines of all profiles are on the x-axis from x=0 to x=1.0.
The y-axis shows contour ordinates to the same scale as the abscissa of
each point. Note that only that portion of the cavity upper surface
which lies directly above the wetted surface of the profile is plotted
in these graphs. The trailing edge of the wetted surface is located at
the point x=1.0 on all plots and the lower surface of the cavity, which
would extend beyond the trailing edge is not shown at all. The cavity
thickness, T, for each design can be measured directly from the graphs
as the vertical distance from the trailing edge of the profile (1.0, 0)
to the upper surface of the cavity (1.0, T). The space between these
two contours from the profile nose at (0, 0), and on into the cavity
beyond the trailing edge of the wetted surface if need be, is available

for the hydrofoil structure. We have not drawn in any foil structure
in these plots, preferring to restrict our attention to the hydrodynamics
of these flows. Of course, we assume that there would be some clearance
space between the upper surface of the cavity and the uppermost parts of
the profile structure.

The profiles of Figures 14, 15, 16, 17 and 18 have all been designed
for $T=.15$, $K=0$, $C_L=.15$. Values of s vary from $s=.2$ to $s=.8$. (Note that
s should be listed as an input quantity in these figures.) This sequence
of profiles shows how the maximum camber of the profile moves toward the
trailing edge as the peak pressure point moves toward the trailing edge.
Moreover, as the peak pressure point moves to the rear, the rounding of
the profile nose increases, corresponding to an increase of the point-
drag singularity at the nose. This increase is required in order to
maintain the value $T=.15$ as s increases, thereby shifting the peak
pressure to the rear. It can be seen that the cavity drag almost doubles
as s increases from .2 to .8. In the following graphs we will explore
the effect on profile geometry when s is held fixed and the design point
is varied.

The effect of varying cavity thickness, T, when $s=.5$, $K=0$ and
$C_L=.15$ is shown by Figures 17, 19 and 20 for $T=.10$, .15 and .20 respec-
tively. Notice that the cavity drag nearly triples and that the profile
nose becomes more rounded as T increases over this range.

Comparison of Figures 17 and 21 shows the effect of increasing the
cavitation number from 0.0 to 0.2 at the fixed values of $T=.15$, $C_L=.15$
and $s=.5$. We see that the shorter cavity, denoted by L in the figures,

corresponding to the higher value of cavitation number requires an

increase of the point-drag function to maintain a thick cavity and this

results in greater rounding of the profile nose.

Figures 17 and 22 show the effect of reducing C_L from .15 to .08

respectively. Notice that as C_L decreases the amount of undercamber

decreases and the nose curvature seems only slightly affected. In this

comparison the fixed parameters are T=.15, K=0.0 and s=.5.

Figure 23 illustrates the kind of a design one produces when he

specifies a thick cavity, fairly high C_L, forward loading and high cavi-

tation number. As also indicated from the performance map, the lift-

to-drag ratio is not very good. As a general comment, it has been

found in this series of calculations that profiles having a far-foward

loading or a far-rearward loading such as s=.1 or s=.9 require a higher

point density over the pressure distribution so that the profile wetted

surface will be accurately calculated. This behavior results from the

sharp pressure peaks which require fairly dense point distribution for

an adequate number of points in the steep regions of the distribution.

Less "peaky" pressure distributions can be defined with fairly good

precision by 50 equal intervals between x=0 and x=1. The contours

shown in this report generally result from this spacing and close

inspection of Figures 14, 19 and 23 which have s-values of .2, .5 and

.8 respectively, show the onset of the behavior noted above when only

50 points are used.

Finally, we note that the region of undercamber on the wetted

surface of all designs illustrated is quite dependent on the position

of the peak pressure. For example, if one consi(rs a nose-loaded profile and he studies the region between x=0 and x=2s, he will note that the undercamber is concentrated in this re on. Of course, the nose rounding required by the point-drag func\i on modifies this behavior in the vicinity of the nose. However, near t point x=2s the curvature of the wetted surface reverses and beyond this point the wetted surface shows no undercamber. In the case of tail-loaded profiles the situation is the same except that the influence of th point-drag function is farther away and one can now make the same general observations if he replaces the interval, $0 \le x \le 2s$ by $2(1-2s) \le \le 1$. It appears therefore, that while the hydrodynamic performance o. the profile depends primarily on the location of the center of pressu , the geometry of the wetted surface is sensitive to the peak pressu location and other details of the pressure distribution shape.

<center>SECOND DESIGN PROCEDURE · SUMMARY OF RESULTS</center>

Preliminary Remarks:

The exploration of design tren derived from the second design procedure start with the modified p essure distribution shown in Figure 24. These pressure distributions re obtained from those defined by Equations (7) and (8) simply by p ting $\lambda=0$. As we have already explained, the secondary pressure distribution which is used in the first design procedure to insur that $p(x)>0$ except at the leading edge and trailing edges of the profi e is not needed for this case. In the second design procedure, this equirement is automatically satisfied by the added pressure distributi n resulting from the departure of the

attack angle from the ideal angle.

Hydrodynamic Performance:

As before, the important performance parameter for design purposes is the lift-to-drag ratio. A series of calculations made in accordance with the second design procedure has given the results plotted in Figure 25. This figure shows the effect of peak pressure location on lift-to-drag ratio at K=0 for a range of section lift coefficients and for two cavity thicknesses. Note the similarities between the trends shown in this graph and those obtained from analogous calculations by the first design procedure in Figure 3. Note also that the range of C_L and T values in Figure 25 is somewhat narrower than those used in our exploration of the first-design-procedure. This narrowed scope is caused by the fact that C_L and T cannot always be specified independently. Reasons for this behavior have been discussed in a more quantitative but somewhat different way in Reference 1. For the present discussion, it is sufficient to note that if C_L is fixed and T is also prescribed, then situations can occur in which the value of α required to meet the required cavity thickness will cause higher lift than the C_L specified. The use of the point drag function as in the third design procedure is needed to overcome this difficulty. Thus, Figure 25 shows that the lowest C_L value which could be attained when T=.1 is about .12 and when T=.15 the lowest C_L is about .15. When T=.20 it was found that the lowest value of C_L exceeds .16.

In spite of the limitations discussed above, one can still draw useful conclusions about the trends produced by the second design

procedure and these trends can also be compared with corresponding results from the first procedure. Of course we have already seen in the case of the first design procedure that profile performance relates primarily to center of pressure and that while the center of pressure is related to peak pressure location, s, this parameter tends to have an important influence on wetted surface geometry. Therefore comparisons of performance trends from the two design procedures in terms of s are suggestive only. It remains to be seen how they compare on the basis of center of pressure location.

For example, let us compare the curve for C_L=.15 and T=.15 from Figure 25 with corresponding curves of the first design method in Figure 3 above. This comparison suggests that for nose loaded foils (s<.3) the first design procedure provides profiles having more favorable lift-to-drag ratios. On the otherhand, when the peak pressure moves toward the trailing edge, the second design procedure is better. In fact, Figure 8, the first design procedure performance map for K=0, shows that L/D=7.09 when s=.9, T=.15 and C_L=.15. This is only about 60% of the corresponding L/D value at s=.9 in Figure 25. Thus, when location of the peak pressure is the chief concern and a tail-loaded profile must be used (s<.4) the second design procedure is probably the better design procedure. However, if securing the most favorable, L/D is one's primary goal then it would seem that nose loading is to be preferred and the first design procedure should be employed. In order to reinforce this point, Figure 26 compares L/D for nose-loaded profiles for s=.2, with T=.10 and .15, for a range of C_L values. The curves for s=.3 are included in Figure 25 simply for reference. If for some reason one needs to design a tail-loaded profile

in spite of the L/D penalties noted here, the elliptical pressure

distribution may not be the best choice. For sufficiently high values

of C_L and s, turbulent separation could be produced. A means of avoiding

this occurrence for profiles which use the first design method is given

in Appendix C. We note in passing that Appendix C illustrates how one

can avoid separation but still have the steepest possible pressure rise.

Should it be needed, this approach aims to prescribe appropriate pressue

distributions without requiring extensive turbulent boundary layer

calculations and a turbulent separation model, thus avoiding the sort of

calculations described in Reference 11, for example.

The foregoing comparisons summarize the chief design factors to

be observed in connection with prescribed peak pressure locations for

the second design procedure. Other performance trends parallel those

of the first procedure at least qualitatively. This fact is illustrated

within the parameter-range limitations of the second procedure by the

performance map of this method of profile design. But first, the matter

of hydrodynamic equivalence in the sense defined above for the first

foil[*] will be examined for the present case of the second design procedure.

Two-Term Profiles, Hydrodynamic Equivalence and Performance Maps:

As a preliminary to the main body of the theory, Reference 1 contains

a discussion of hydrofoils at zero cavitation number and related airfoils

which extends the ideas originated by Tulin [9]. As an example of optimum

design, a "two-term" profile is found which has the most favorable lift-

to-drag ratio and which has a cavity which clears the wetted surface.

---

[*] p. 24.

The cavity clears the wetted surface because the pressure distribution
on the foil contains an angle of attack term besides the two terms due
to camber. Moreover, there is no complementary function in the solution
so that the example treated resembles the more general second design
procedure. As a matter of fact we can put the "optimum" results from
Example 3 of Reference 1 in a form which permits comparison with the
present results. In order to facilitate this comparison and to make this
document more nearly self-contained, Appendix D gives an excerpt form
Reference 1 which contains these preliminary considerations. For
example, we find from Equations (16) and (36) of Reference 1 that

$$C_M = - \frac{33\pi}{160} \alpha \qquad (12)$$

and from Equations (16) that

$$C_D = \frac{\pi}{2} \alpha^2 \quad \text{and} \quad C_L = \frac{7\pi}{10} \alpha \qquad (13)$$

at the condition for most favorable lift-to-drag ratio. Since $\bar{x}C_L = C_M$
it follows for this foil that $\bar{x} = .2946$. Moreover, at a prescribed
value of C_L we can write the lift-to-drag ratio as

$$\frac{L}{D} = \frac{\pi}{2C_L} (1 + \frac{24}{25}) \qquad (14)$$

The corresponding result for a flat plate is $L/D = \pi/2C_L$. We can also
use Equations (39) and (40) of Reference 1 to write the cavity thickness

at the trailing edge (x=1) as

$$T=1.5764\alpha \tag{15}$$

which permits one to determine C_L, C_D and C_M for any desired cavity thickness. Table III shows two-term profile performance for three values of cavity thickness.

From this example one sees that the designer has more freedom if he uses the more general second design procedure because the "optimum" condition selected in Reference 1 results in a fixed portion of the total lift which is carried by that part of the pressure distribution due to camber. For example, in the second design procedure we express that fraction of C_L which is carried by the prescribed pressure distribution as

$$C_L' = m\, C_L \quad . \tag{16}$$

Then that part of C_L carried by the extra angle of attack, or the effect of a_o in Example 3 of Reference 1, is $(1-m)C_L$. We can make use of Equations (36) and (27) from Reference 1 to determine that

$$m = 6/7 \quad , \tag{17}$$

which holds for all values of α. That is to say, m is fixed once and for all and this result is consistant with the fact that $\bar{x}$ is also

independent of α for this particular example of an "optimum" profile. This is not the case for the second design procedure as can be seen from the data of Appendix B. In the second design procedure, we specify C_L, T and K as well as the shape of the pressure distribution due to camber. As a result the parameter m shows considerable variation within its permissible range, $0 \leq m \leq 1$.

In spite of the differences just discussed, it seems useful to compare the performance of a two-term profile with an equivalent profile obtained from the second design procedure. To do this we compare the results of Table III with C_L and T values in Appendix B for K=0. We see that if T is greater than .10, the values of C_L in Table III are outside the range of cases studied in Appendix B. However, when T=.10 the two-term foil has C_L = .1395. But C_L = .14 is one of the lift coefficients tabulated in Appendix B. These C_L values differ by 1.1% and if one considers the effect of this C_L variation on the data of Appendix B for $s \approx .3$, he will conclude that L/D would suffer a corresponding variation of about 0.5%. Therefore, it seems reasonable to interpolate for that value of s corresponding to $\bar{x}$ = .2946. This corresponding value is s=.2834. Other quantities relating to both two-term and elliptical pressure distributions are compared in Table IV. From this table one can conclude for K=0, at least, that shape variations among hydrodynamically equivalent pressure distributions will have little effect on the hydrodynamic performance of the resulting profiles. Note that the value of m for the two cases shows a significant difference.

Of course, the foregoing results apply strictly to the second design procedure at zero cavitation number. These findings need to be extended

to other values of the cavitation number such as K=.05 and K=.10 and to other cavity thicknesses, such as T=.10 and T=.15. A convenient choice for the lift coefficient is C_L = .16 because Appendix B shows a good range of $\bar{x}$ at both values of K. For the comparison calculations, we will use the modified three-term and reversed three-term pressure distributions of Figure 7 except that the ordinates of that illustration must be scaled in the ratio 16/12 in order to give the design C_L in the event that m=1. The results of all calculations are given in Tables V and VI. As in previous comparisons, the performance of the equivalent elliptic pressure distribution is obtained by linear interpolation from values in Appendix B.

Tables V and VI show again that the performance of hydrodynamically equivalent profiles is insensitive to detailed variations of pressure distribution shape. An interesting aspect shown by these tabulations and Table IV also is that the m-values for the elliptical distribution are always somewhat smaller than those for the three-term or the two-term profiles. As was found in the case of the first design procedure, it also appears in the case of the second design procedure that profile performance estimates can be based on data from the elliptic pressure distribution as long as the pressure distributions are hydrodynamically equivalent. The practical problem for the application of this rule to the second design procedure, is that one now needs to carry out the design calculation for the new profile in order to establish the equivalence between it and one having an elliptic pressure distribution. This situation is caused by the fact that now the pressure distribution

has two parts and we can specify only that part which affects the camber of the profile whereas the center of pressure coordinate depends upon the relative magnitude of both parts. This fact prevents us from using a summary of results, such as that presented for the first design procedure in the charts of Figures 8 through 13, as rather precise guides for profile design performance.

On the other hand, performance maps which summarize the properties of profiles having elliptic pressure distributions do provide a convenient overview of trends to be expected from the second design procedure and they can give the designer qualitative guidance. Figures 27, 28 show the forces and Figures 29, 30 and 31 show the pitching moment. These figures illustrate the results tabulated in Appendix B, except that moment data for $T=.15$ have not been plotted in order to simplify these illustrations. As discussed previously, the range of parameters for the second design procedure is not as extensive as it is for the first design procedure and so there are fewer charts of L/D versus C_D in this case. However, there are more charts of C_M versus $\bar{x}$ because now these contours depend upon K and T.

Center of Pressure Location and Comparison of First and Second Design Procedures:

All of the preceding comparisons have used, s, the position of the peak prescribed pressure on the wetted surface as the primary foil design parameter. This has been a convenient choice because it can be prescribed quite independently of the final performance parameters; and, as we have seen in the case of foils derived from the first design procedure, it is important with respect to the wetted surface geometry. However, the hydrodynamic performance of profiles designed by both procedures has

been found to depend on $\bar{x}$, the location of the center of pressure. This parameter is certainly related to the value of s, but for the second design procedure the added pressure distribution caused by the increase in attack angle above the ideal angle makes this relationship somewhat indirect. It remains, therefcre, to see how the idea of hydrodynamic equivalence applies to comparisons between the first and second design procedures.

Figures 32, 33 and 34 present plots of L/D against $\bar{x}$ for profiles obtained from the two design procedures. The points on the curves show various s-values given in Appendices A and B. In Figure 32, those points nearest the L/D axis on the curves for the first design procedure correspond to s=.1 and on the curves for the second design procedure, the points plotted nearest to the L/D axis are for s=.2 when C_L=.12 and s=.3 when C_L=.15. This situation is also true for Figures 33 and 34, except that now the C_L=.15 curves for the second design procedure start at s=.2 also. These figures show that the use of $\bar{x}$ for comparing first- and second-foil performance only exhibit rather small L/D differences over the range of $\bar{x}$ for which they are comparable. Of course these differences are much larger than those displayed in Tables I through VI above. But those data compare foil designs within a given procedure so that relatively minor variations of pressure distribution shape are considered. When we compare a profile from the first design procedure with an equivalent profile from the second design procedure, the pressure distributions for the two cases differ significantly. Therefore, we expect to see more of a difference for the present comparisons than we

found above. The fact that these differences are as small as they are

is noteworthy. Finally, we note that if one accepts the differences shown

as being significant, we can state that theoretically the first design

procedure generally leads to profiles having the lower drag. The practi-

cal importance of this slight advantage is questionable.

The limited range of center of pressure travel of the second design

procedure compared to the first design procedure is another feature

which deserves comment. For example, when K=0, it is known that $\bar{x} = 5/16$

for the flat-plate hydrofoil at all angles of attack. But the added

pressure distribution due to attack angle found in the second design

procedure is the flat-plate distribution. Therefore, its presence

inhibits the degree by which the designer can vary $\bar{x}$ by changing the

value of s. Thus, we see that all of the $\bar{x}$ values for the second design

procedure are less than .5 even though s values as large as .9 are

included in Figures 32, 33 and 34. We also see that the forward travel

of $\bar{x}$ available to the designer is similarly limited although this

restriction is not as severe as it is for rearward travel. This behavior

explains the apparent superiority of the second procedure compared to

the first procedure for large values of s noted in Figure 3.

Geometric Properties:

Discussion of performance trends for the first and second procedures

are now complete. The remaining aspect of the second design procedure

requiring discussion is the profile geometry obtained by this method.

The necessary results are contained in Figures 35, 36, 37 and 38 which

show wetted surface and upper cavity contours for four representative

flows at zero cavitation number. These plots conform to the same rules

given previously for the first design procedure. Figures 35 and 36 show

how the undercamber of the wetted surface is increased as the design C_L

increases from .12 to .15. This trend was also observed in the case of

foils resulting from the first design procedure. Figures 36 and 37 show

how the region of undercamber moves toward the profile trailing edge as

the peak pressure location is changed from s=.3 to s=.7. This trend

has also been observed for contours derived from the first design method.

Finally, a comparison of Figures 37 and 38 illustrates how the wetted

surface changes for s=.3 when C_L increases from .15 to .16 and at the

same time T increases from .10 to .15. It does not seem necessary to

show the effect on wetted surface shape of increasing K above zero while

other parameters are fixed because this trend is essentially the same

as that illustrated for the first design method. In fact, the essential

difference between the two procedures as far as foil geometry is con-

cerned is that the leading edge of profiles obtained from the second

design procedure will be sharp instead of rounded. This can cause some

problems structurally, particularly for a situation as illustrated in

Figure 36. In fact if one selects s=.1 or .2 and does not require a

large enough value of T the cavity surface will intersect the wetted

surface contour. This occurrence is not as likely with the first

design method. However, in either case one will not always produce

acceptable designs if the peak pressure is moved too far forward. More-

over, previous remarks concerning computational accuracy needed to define

the wetted surface for peak pressure locations very close to the leading

edge or very close to the trailing edge also apply to the second design procedure.

OFF-DESIGN CALCULATIONS

Suppose the wetted surface and upper cavity contours have been determined from inverse calculations by means of the first or second design procedure. The next step is to examine the off-design performance and critical flow geometries of the candidate hydrofoil section. In this study, we shall carry out such calculations by means of the linearized direct theory of cavity flows [10]. Of course, we know that linearized theory lacks the precision of the nonlinear theory. Nevertheless, since the present inverse theory is linearized it is consistant to use the linearized direct theory with it. In this way, one obtains a consistant set of preliminary results for both design and off-design flow states. Once a few promising candidates for a particular application have been found from the linearized theory, one can complete the design process by recourse to nonlinearized cavity-flow calculations.

Linearized calculations for hydrofoil-cavity interference can be carried out if one uses the direct theory of Reference 8 to determine the upper cavity contour at any attack angle α. In these calculations, the slope of the wetted surface, $\eta'(x)$, resulting from an inverse calculation will be tabulated numerically over the interval $0 \leq x \leq 1$. This slope function, the cavity length, ℓ, and the attack angle, α, will be inputs to the calculation. In the direct theory, the cavitation number follows from the cavity closure condition. We can express this condition as

$$\alpha = a\beta + W(a) \quad , \tag{18}$$

where $a = \sqrt{\ell-1}$ and β is defined by Equation (11). The precise form of all terms in this equation is given in Reference 2. This reference also shows that the upper cavity contour at any off-design condition can be expressed as

$$y(x) = \beta \Xi_1 (x,a) + \Xi_2 (x,a) \quad , \tag{19}$$

where the functions Ξ_1 and Ξ_2 are obtained from $y(x)$ in Reference 2 by grouping its terms so that β is a coefficient of Ξ_1 as shown.

Suppose next that one selects a contour $t(x)$ which lies within the area bounded by the wetted surface of the profile and the upper cavity contour at the design flow state. The contour $t(x)$ is the upper surface of the foil structure will simply be given by table of ordinates over the interval $0 \leq x \leq 1$. Then a critical off-design flow state will exist when the cavity contour $y(x)$ is tangent to $t(x)$. This flow state can be found if one puts $y(x)=t(x)$ in the off-design cavity contour equation above and solves for β:

$$\beta = \frac{t(x) - \Xi_2 (x,a)}{\Xi_1 (x,a)} \quad . \tag{20}$$

Then if one chooses a value of a, he can calculate a value of β for each x in (o,x). He can select the largest value of β from among these values. Then, he can use this same value of a and this greatest value of β in the closure equation to find the corresponding α. One can then

calculate β from Equation 11. The three values (a, K and α) define an off-design flow state at which the cavity is just tangent to the upper (non-wetted) surface of the hydrofoil. This calculation can be repeated for a sequence of a-values which divides an α-K plane into two regions, in the region above this curve the flow will be at a permissible state. Points on or below this curve correspond to states having interference between the foil and the cavity. The actual equations employed and the numberical methods used in these calculations are given in Reference 3.

An example of results obtained from the calculations described above has already been given in Reference 2. Nevertheless it is useful to give further examples which correspond to flow conditions typical of this study. Accordingly, we have selected the parameters s=.3, C_L=.12, K=0 and T=.10 for the design flow state for two profiles: one from the first and one from the second design procedure. The results of these calculations are plotted in Figures 39 and 40 in an α-K plane. The design attack angle for these profiles is plotted on the υ-axis. Points in this plane above the curves are permissible flow conditions. Those which are on or below the curves are not permissible flow states. In these figures "alpha critical" refers to the locus of points defining the conditions of cavity tangency. In these calculations the upper surface of the foil has been derived from the upper cavity surface in each case by putting

$$t(x) = \theta y(x) \quad , \quad 0<\theta<1 \quad . \tag{21}$$

In both examples we have put θ=.9 and .8. Thus, the hydrofoil sections have a wedge-like shape.

To continue these examples we have also included the general off-design calculation method of Reference 8. The two wetted-surface slope functions $\eta'(x)$ noted above are also inputs to these calculations which are carried out for a range of K and α values. They permit us to calculate k, C_L, C_D, C_M and L/D for the prescribed values of ℓ and α. Results for the two profile designs are shown in the curves of Figures 41 to 48. It will be noticed that we have also superimposed the locus of interference conditions from Figures 39 and 40 when $\theta=.9$ in Figures 41 and 45 to show how interference can cut off the available range of off-design performance. Aside from the interference data, general trends shown in these illustrations follow those which have been noted in many previous investigations of the direct-theory of cavity flows. No further discussion of those found here seems necessary.

CONCLUSIONS

Perhaps the most important general conclusion to emerge from this study is that the most favorable lift-to-drag ratios are most often found when the profile is designed to have its center of pressure placed as near to the leading edge of the profile as possible. Only one exceptional combination of T=.10 and K=.2 has been found so far. This result holds for profiles designed with either the first or the second design procedure. Of course, this finding must be applied with geometric and other modifying factors kept in mind. Consequently, this result will seldom, if ever, be applied to the fullest extent.

For foils resulting from either design procedure, it is found that at the design point (prescribed values of lift coefficient, cavitation

number, and cavity thickness) and with a pressure distribution fixed in

shape but having variable amplitude, the lift-to-drag ratio increases

with increasing lift coefficient. That is, within structural limita-

tions, the profile should be designed to be as heavily loaded as possible.

The cavity thickness at the design point has a powerful effect on

the lift-to-drag ratio. For either design procedure, as the the thick-

ness increases the cavity drag increases.

The cavity thickness at the design point also influences the lift-

to-drag ratio for a given design. Increasing the cavitation number

decreases the lift-to-drag ratio for foils obtained from both design

procedures for most attack angles of practical interest.

Another result found in this study is that the location of the

center of pressure is the most important property of the pressure

distribution as far as hydrodynamic performance is concerned. As long

as the center of pressure is held fixed, variations in the shape of

the pressure distribution have almost no effect on the hydrodynamic

forces on the profile. Of course, fixing the center of pressure does

not allow for very large variations in pressure distribution shape

because this result was found to be true when the design point is also

fixed. When the design point is fixed and two profiles have the same

center of pressure they are said to be hydrodynamically equivalent.

This equivalence is particularly precise when the two profiles result

from the same design procedure but have differing pressure distribution

shapes.

Hydrodynamic equivalence has also been found to be a useful concept

when one profile designed by the first procedure is compared with a foil

designed by the second procedure. If both have the same design point

and center of pressure the hydrodynamic forces are nearly the same.

While this equivalence is less exact than it is for profiles obtained

by the same design procedure it appears that agreement of the forces is

close enough for many practical purposes. Of course fairly small

differences were found in the forces and if one wishes to attach

importance to them he could say that the first design procedure leads

to slightly more efficient profiles than the second procedure. We do

not believe this to be a very important point.

Finally it was found that the shape of the wetted surface is most

sensitive to the location of the peak pressure. Although the peak

pressure location is related to the center of pressure location, its

influence on the undercamber of the wetted surface appears to be most

direct and its influence on profile forces seems somewhat less direct

than does the center of pressure location.

The limited scope of this study suggests that although we have

established desirable design goals from a purely hydrodynamic. viewpoint,

structural considerations may not always permit their fullest exploitation.

We have seen that enhancement of lift-to-drag ratios is accomplished by

a reduction in the cavity cross-sectional area available for the

profile structure. This is especially true near the leading edge where

chordwise and spanwise bending stresses in a three dimensional hydrofoil

may become too high to meet strength requirements. From this viewpoint

it might be better to compre lift-to-drag ratios against an appropriate

strength criterion instead of using the parameters of cavity thickness and lift coefficient. Therefore, the present study is not a complete guide for the use of inverse theory in hydrofoil design. However, we hope that the hydrodynamic trends are well enough established to make the union of hydrodynamic and structural design considerations less difficult.

Table I - Performance Comparison for Nose Loading, First Design Procedure

| T | K = .05 | | | K = .10 | | | Notes: $\bar{x}$ = .3647 |
	C_D	$\alpha°$	L/D	C_D	$\alpha°$	L/D	C_L=.12, C_M=−.04376
.10	.00704	3.2808	17.0557	.00893	3.2618	13.430	3-TERM, REVERSED
	.00702	3.2266	17.0944	.00893	3.2101	13.430	DOUBLE ELLIPSE
.15	.01338	4.7132	8.9672	.01575	4.6942	7.619	3-TERM, REVERSED
	.01336	4.6590	8.9841	.01574	4.6425	7.623	DOUBLE ELLIPSE
.20	.02174	6.1456	5.5201	.02461	6.1266	4.8762	3-TERM, REVERSED
	.02171	6.0914	5.5285	.02459	6.0749	4.880	DOUBLE ELLIPSE

Table II - Performance Comparison for Tail Loading, First Design Procedure

| T | K = .05 | | | K = .10 | | | Notes: $\bar{x}$ = .6685 |
	C_D	$\alpha°$	L/D	C_D	$\alpha°$	L/D	C_L=.12, C_M=−.08022
.10	.00914	2.4476	13.1299	.01063	2.4666	11.2887	3-TERM
	.00909	2.4126	13.2019	.01060	2.4331	11.3224	DOUBLE ELLIPSE
.15	.01632	3.8800	7.3529	.01838	3.8990	6.5291	3-TERM
	.01626	3.8500	7.3842	.01833	3.8655	6.5481	DOUBLE ELLIPSE
.20	.02551	5.3124	4.707	.02812	5.3313	4.2675	3-TERM
	.02542	5.2774	4.721	.02805	5.2979	4.2788	DOUBLE ELLIPSE

Table III – "Two-Term" Profile Performance at Zero Cavitation Number

T	$\alpha°$	C_L	C_D	L/D	C_M
.10	3.6346	.1395	.00632	22.07	-.04110
.15	5.4519	.2092	.01422	14.71	-.06166
.20	7.2692	.2790	.02528	11.04	-.08221

Table IV – Performance Comparison of Equivalent Two-Term and Elliptical
Pressure Distributions: T=.10, K=0 and x=.2946

C_L	C_D	L/D	$\alpha°$	PRESSURE DISTRIBUTION
.1395	.0063	22.07	3.635	TWO-TERM, m=.8571
.1400	.0064	21.87	3.602	ELLIPTICAL, m=.6529

Table V – Performance Comparison for Aft-Loaded Profiles, Second Design Precedure, Design C_L=.16

K	T	C_M	$\bar{x}$	C_D	L/D	$\alpha°$	m	PROFILE
.05	.10	-.0690	.4312	.0085	18.73	3.254	.3331	ELLIPTICAL
				.0086	18.59	3.255	.3407	3-TERM, REVERSED
	.15	-.0522	.3263	.0142	11.23	5.126	.3630	ELLIPTICAL
				.0143	11.22	5.126	.3709	3-TERM, REVERSED
.10	.10	-.0588	.3675	.0096	16.61	3.487	.1398	ELLIPTICAL
				.0096	16.58	3.488	.1434	3-TERM, REVERSED

Table VI – Performance Comparison for Nose-Loaded Profiles, Second Design Procedure, Design C_L=.16

K	T	C_M	$\bar{x}$	C_D	L/D	$\alpha°$	m	PROFILE
.05	.10	-.0540	.3375	.0076	20.92	3.544	.5396	ELLIPTICAL
				.0077	20.74	3.557	.5731	3-TERM
	.15	-.0506	.3162	.0141	11.33	5.157	.0587	ELLIPTICAL
				.0141	11.32	5.159	.0625	3-TERM
.10	.10	-.0524	.3275	.0093	17.15	3.607	.2247	ELLIPTICAL
				.0093	17.12	3.611	.2390	3-TERM
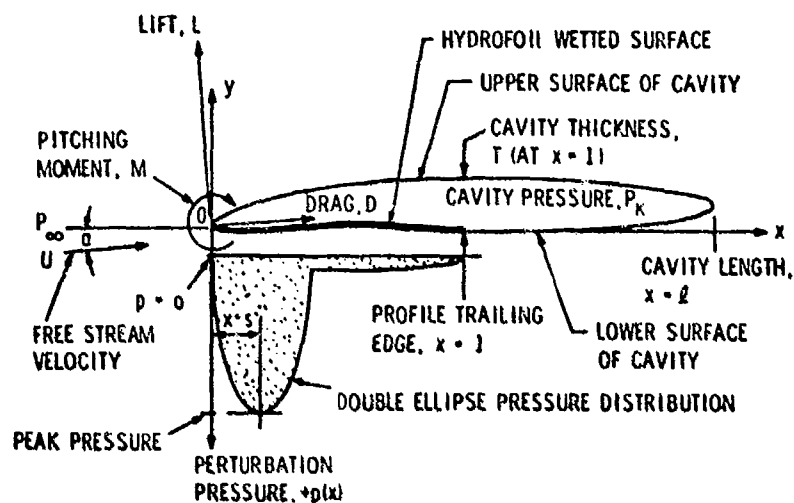
Figure 1 – Schematic Diagram of Two-Dimensional Flow Geometry
and Prescribed Pressure Distribution for the First
Hydrofoil Design Process
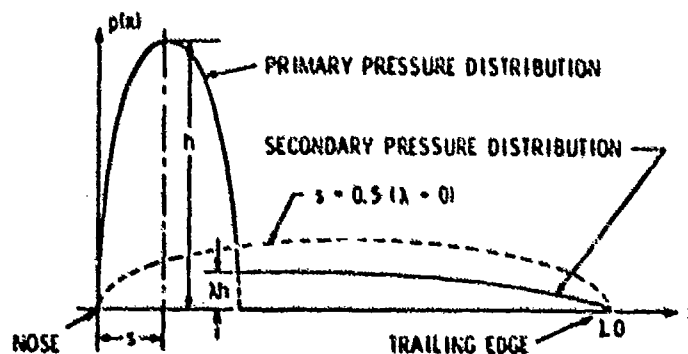
Figure 2 – Double-Ellipse Pressure Distribution for Use with
the First Design Procedure

FIRST DESIGN PROCEDURE
PEAK PRESSURE LOCATION, s = 0.3
CAVITY THICKNESS, T = 0.15
λ = 0.05

$C_L = 0.15$
0.12
0.10
0.08

CAVITATION NUMBER

LIFT-TO-DRAG RATIO, C_L/C_D
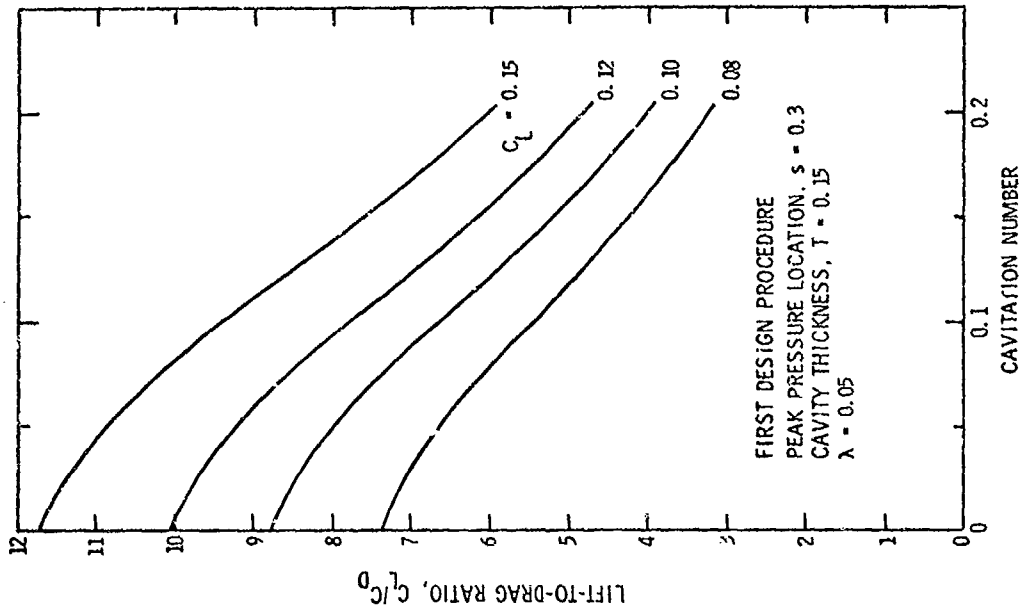
Figure 4 — Effect of Cavitation Number and Lift Coefficient on Profile Lift-to-Drag Ratio

2nd DESIGN PROCEDURE
λ = 0, C_L = 0.15

λ $\begin{cases} 0.1 \\ 0.05 \end{cases}$

$C_L = 0.15$
0.12
0.10
0.08

SHOWING THE EFFECT OF λ VARIATIONS
FIRST DESIGN PROCEDURE
CAVITATION NUMBER = 0
CAVITY THICKNESS, T = 0.15
FIRST DESIGN PROCEDURE

NOSE

PEAK PRESSURE LOCATION, s

LIFT-TO-DRAG RATIO, C_L/C_D
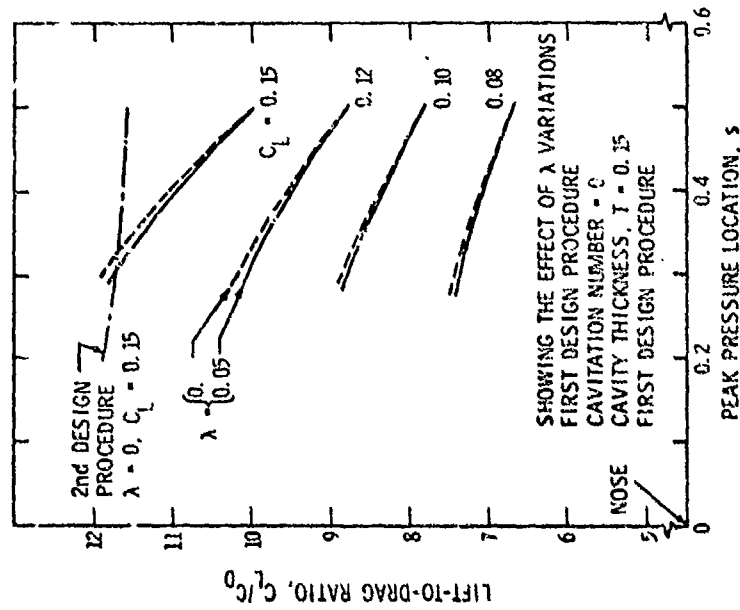
Figure 3 — Effect of Secondary Pressure Loading on Hydrofoil Lift-to-Drag Ratio

Figure 6 – Effect of Cavitation Number and Peak Pressure Location on Profile Lift-to-Drag Ratio
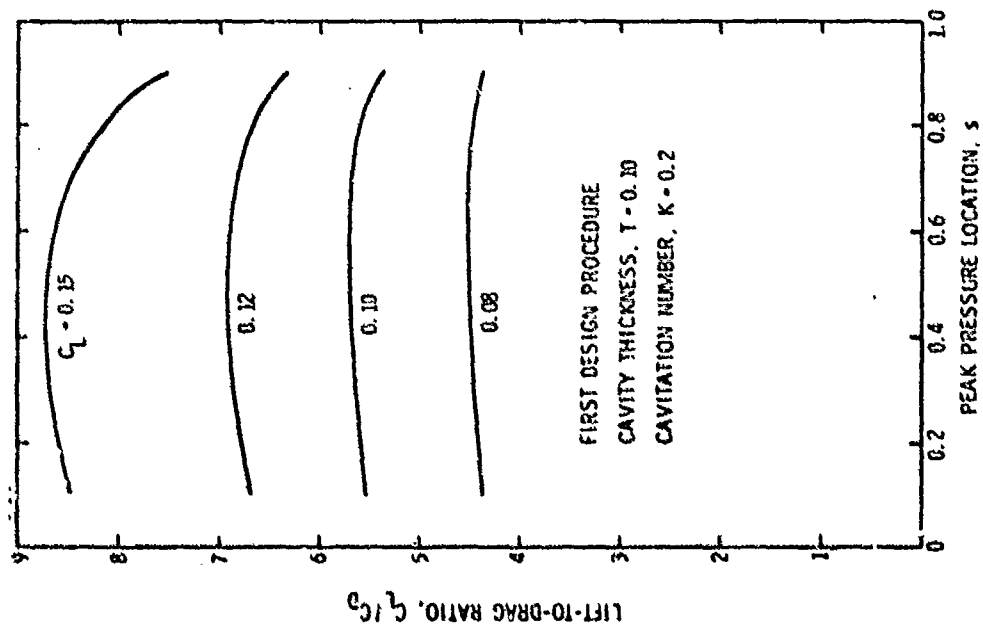
Figure 5 – Influence of Peak Pressure Location and Lift Coefficient on Profile Lift-to-Drag Ratio
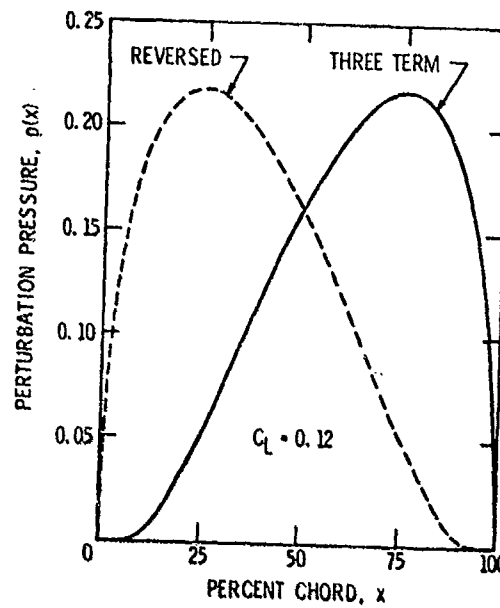
Figure 7 — Three-Term and Reversed Three-Term
Pressure Distributions for Comparison
of Results with Results from Elliptic
Distributions
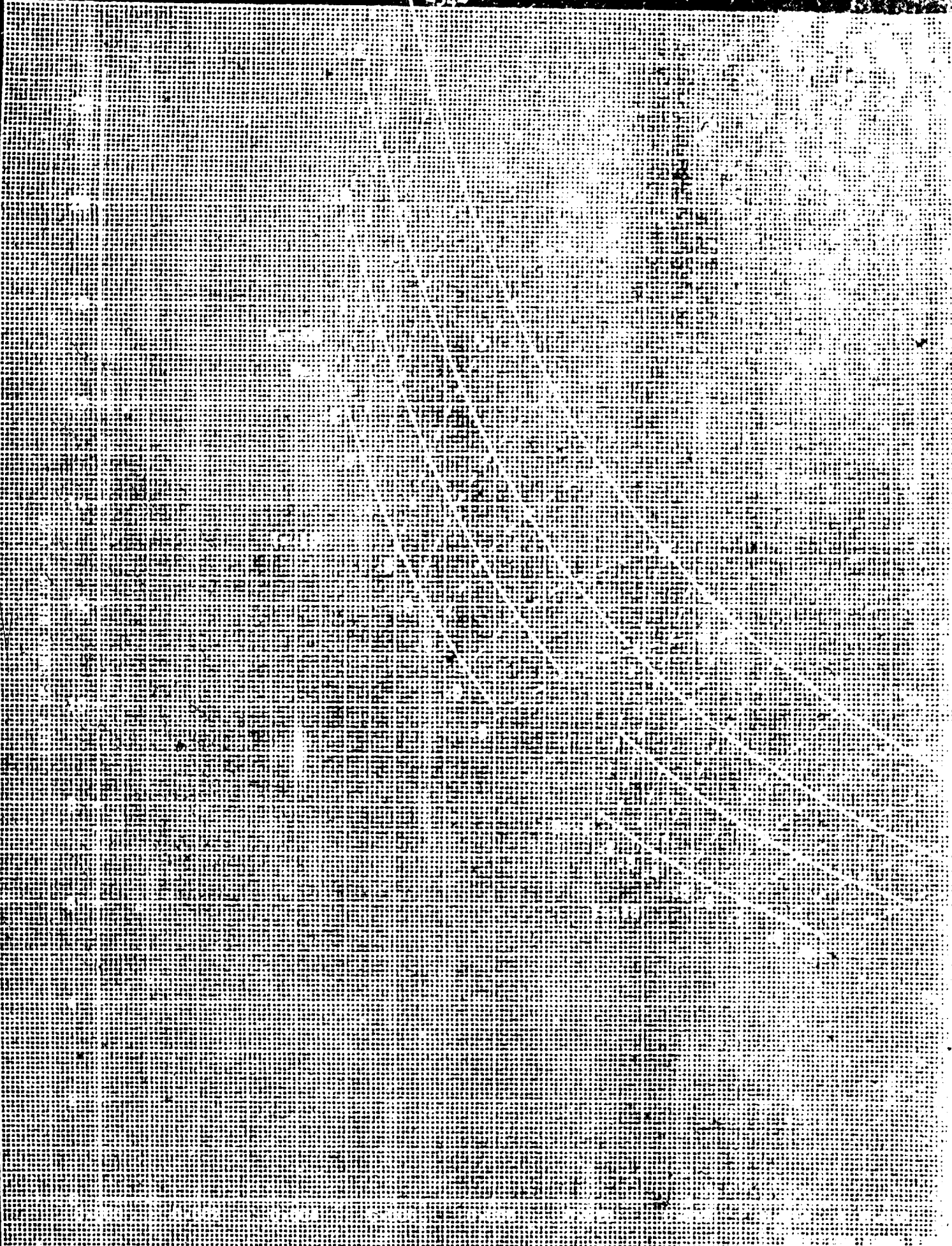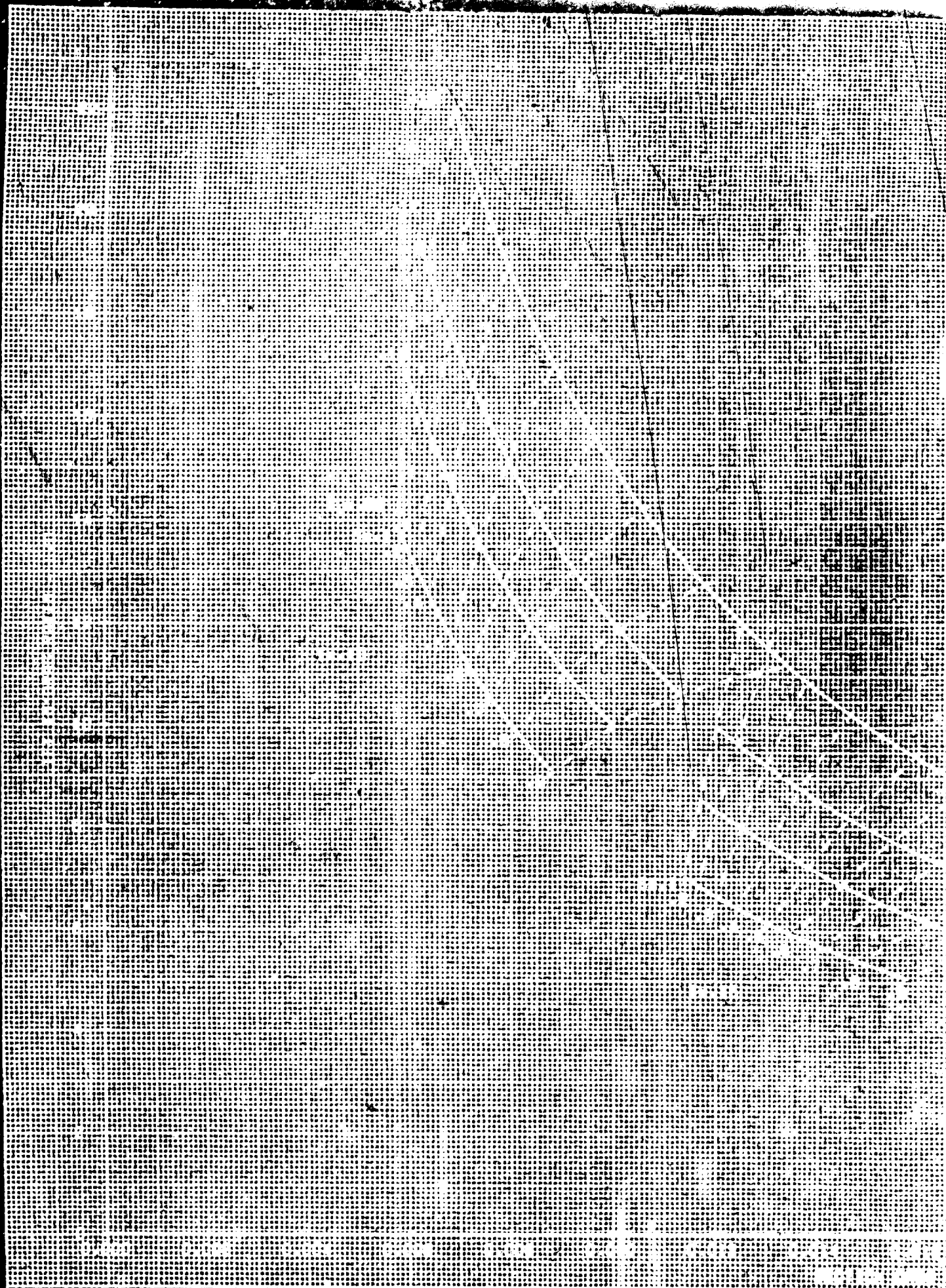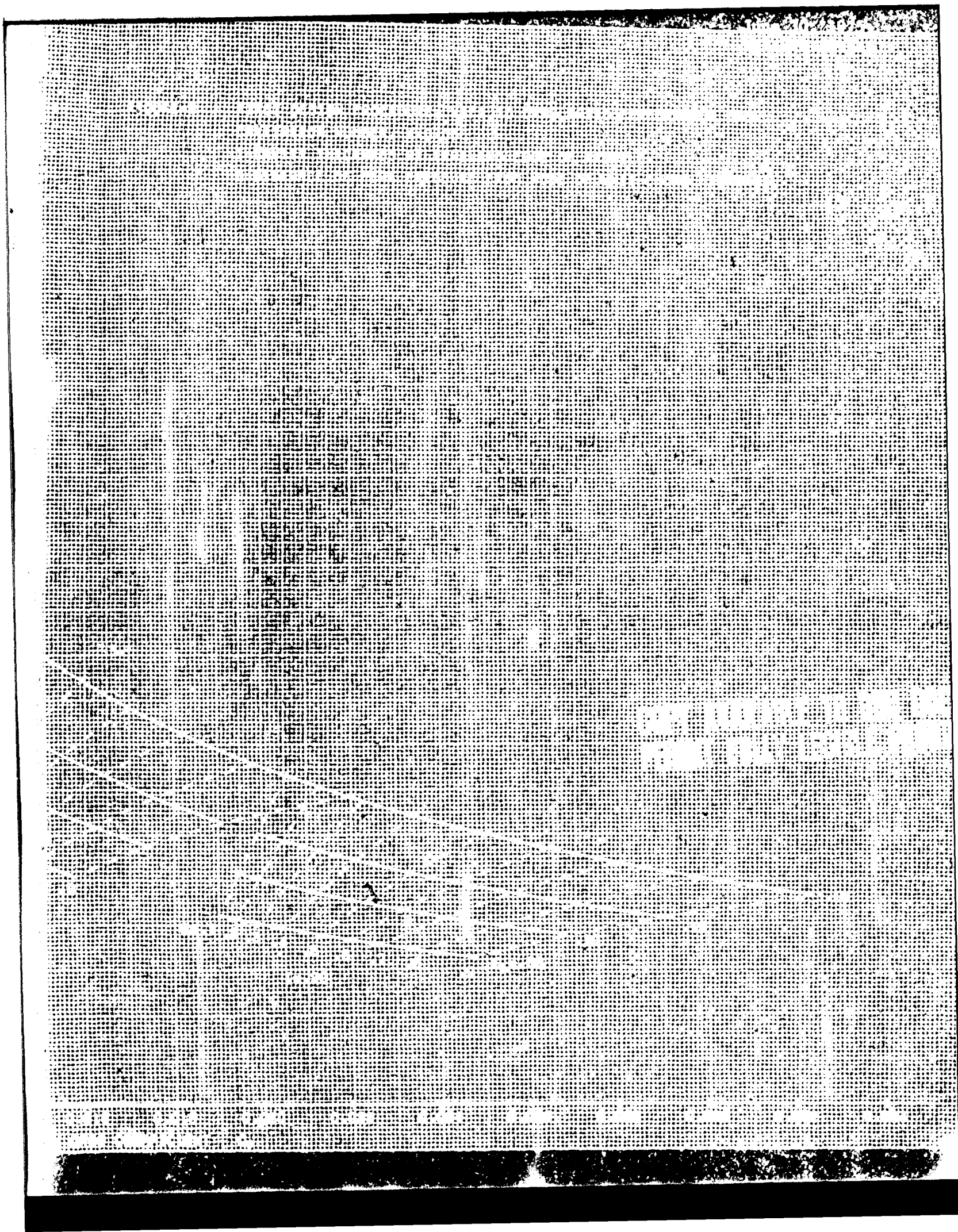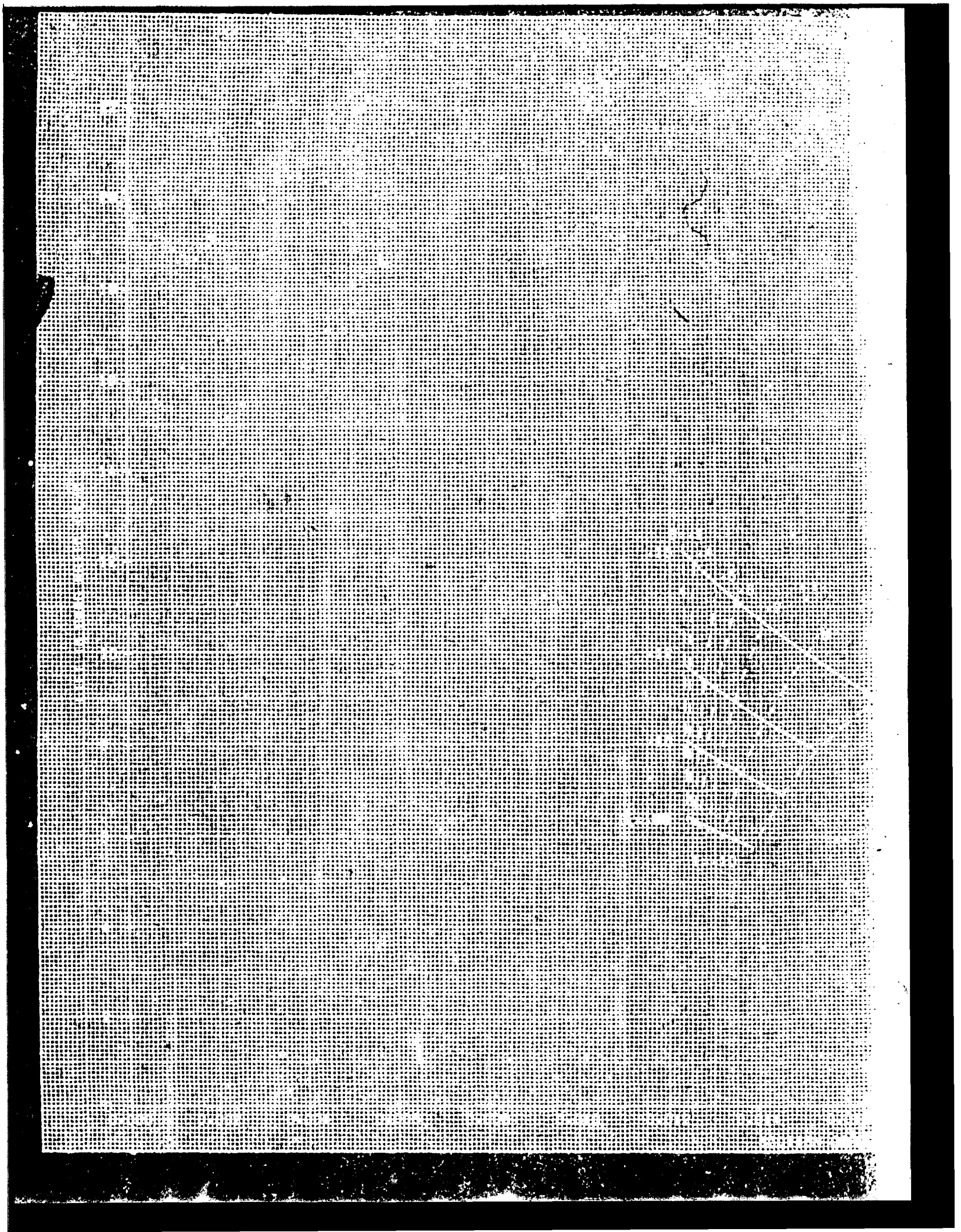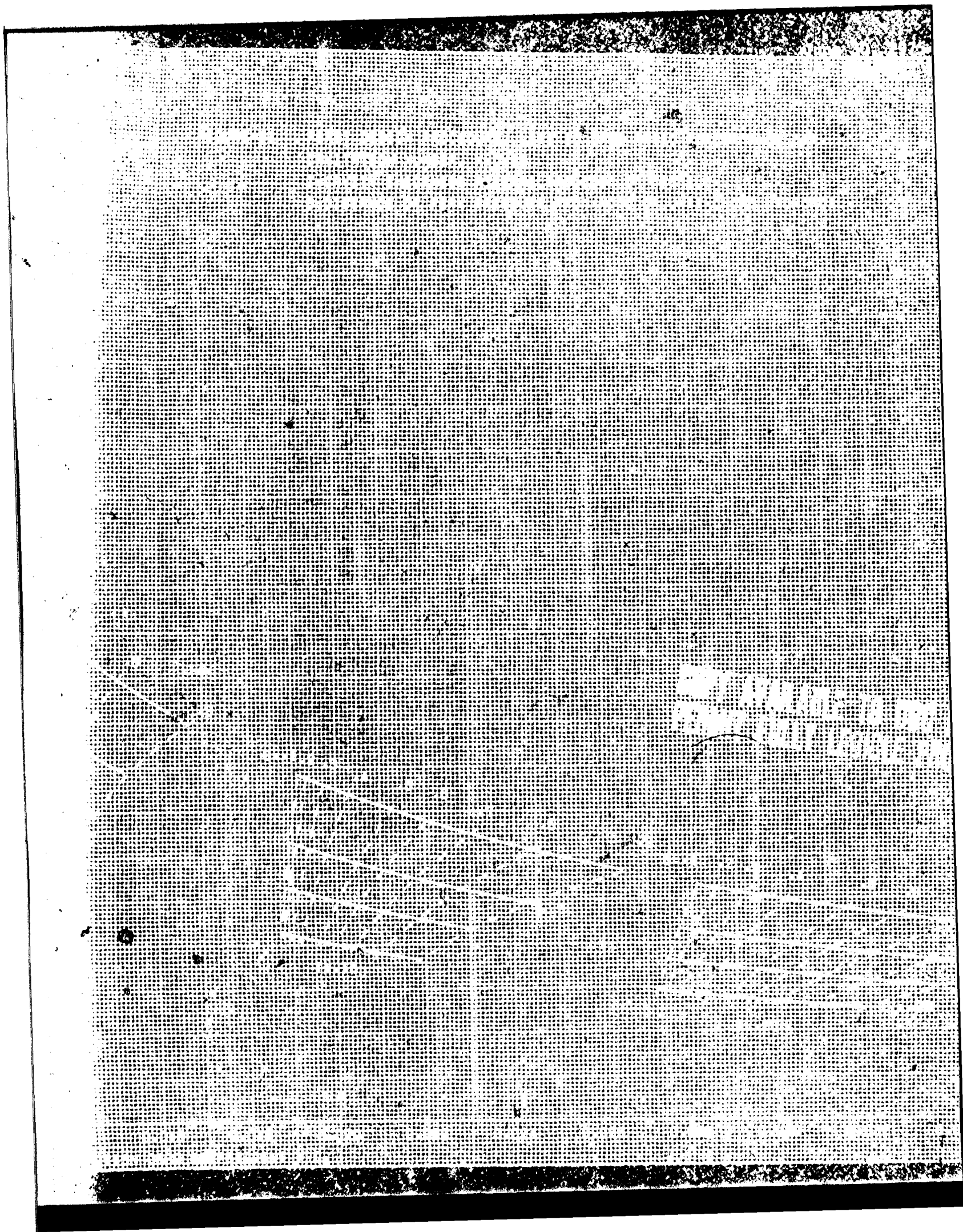
FIGURE 13. PITCHING MOMENT PERFORMANCE MAP
FIRST DESIGN PROCEDURE
DOUBLE ELLIPSE PRESSURE
DISTRIBUTIONS, $\lambda = .05$
VALID FOR ALL VALUES OF T AND K

INPUT	T	0.1500
	K	0.0000
	CL	0.1500
	L	∞
OUTPUT	ALPHA	5.2502
	CD	0.0120
	CM	-0.0343
	L/D	12.5349
INPUT	S	0.2000

Chord Line

SURFACE ORDINATES
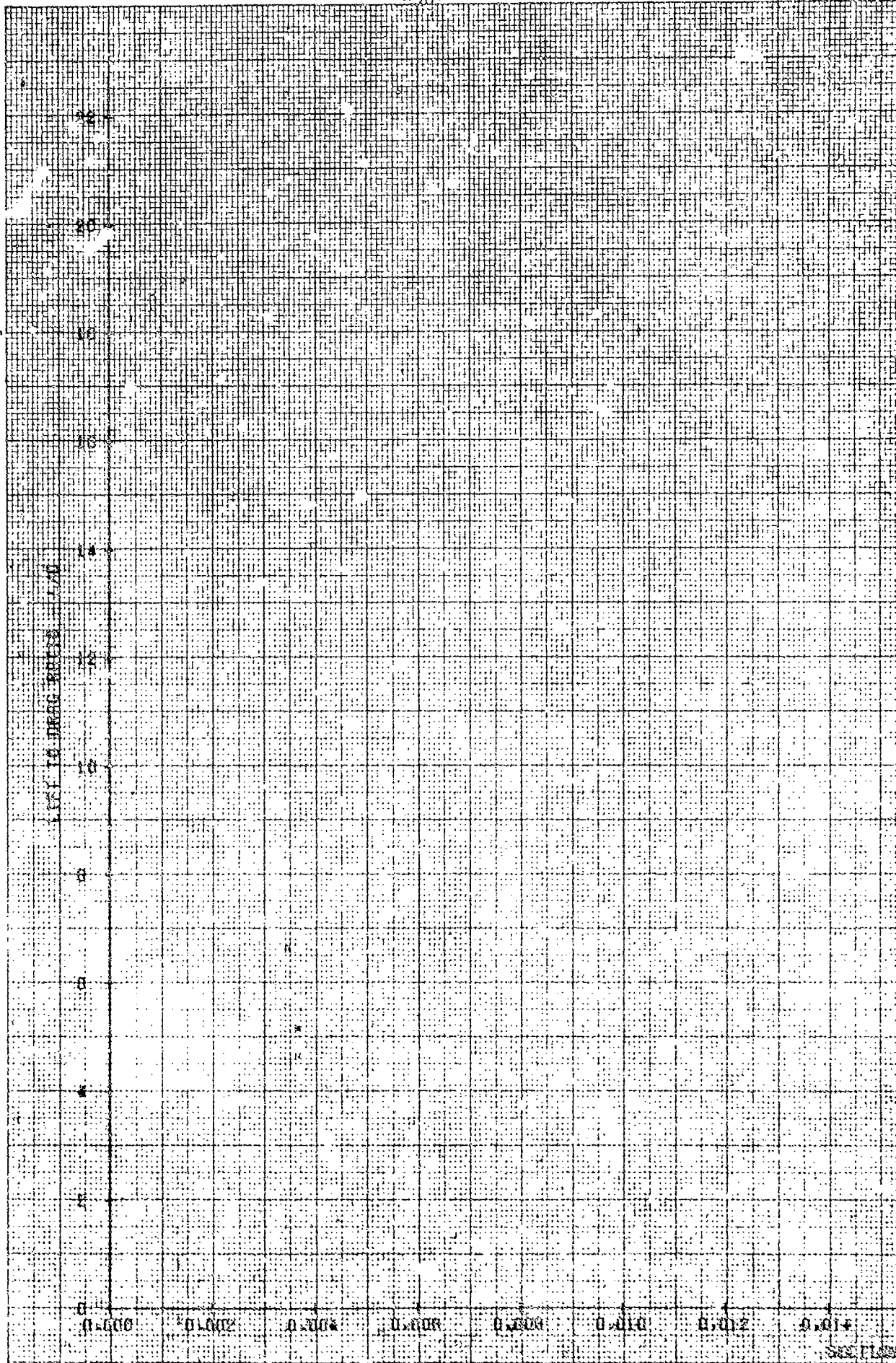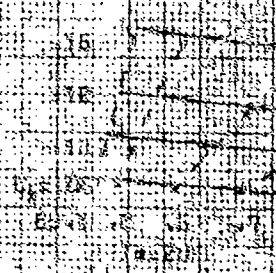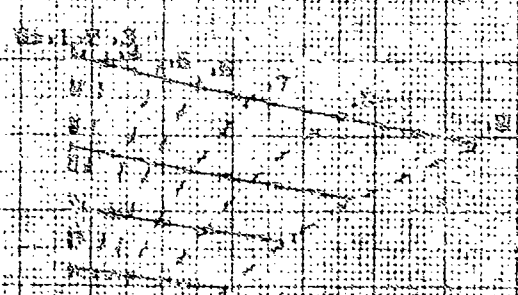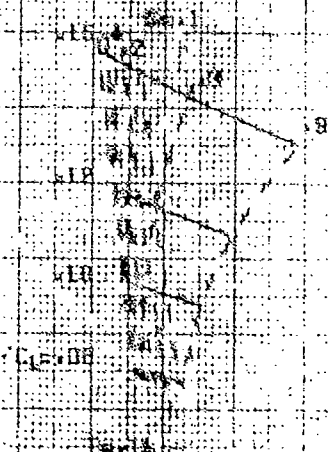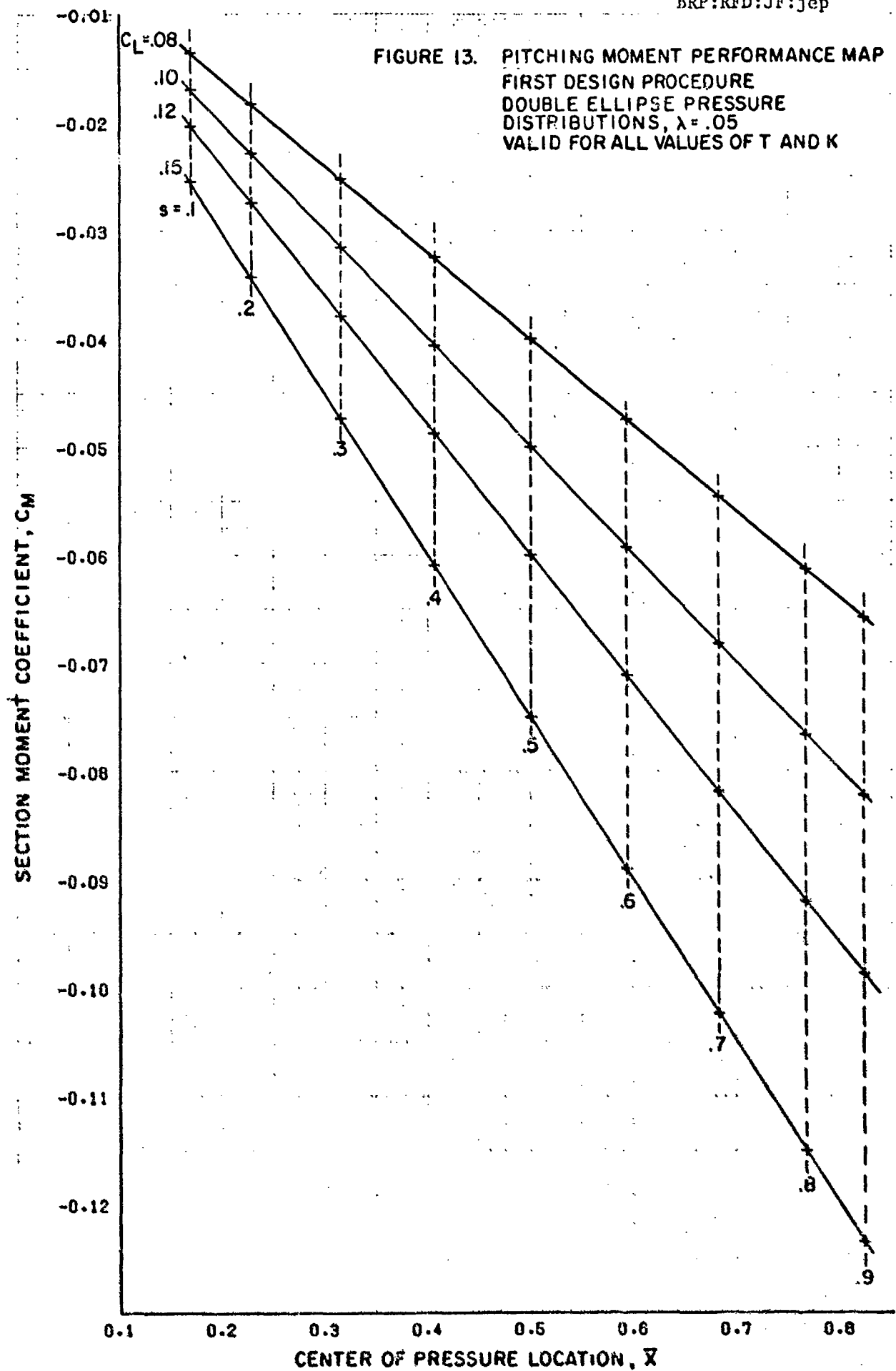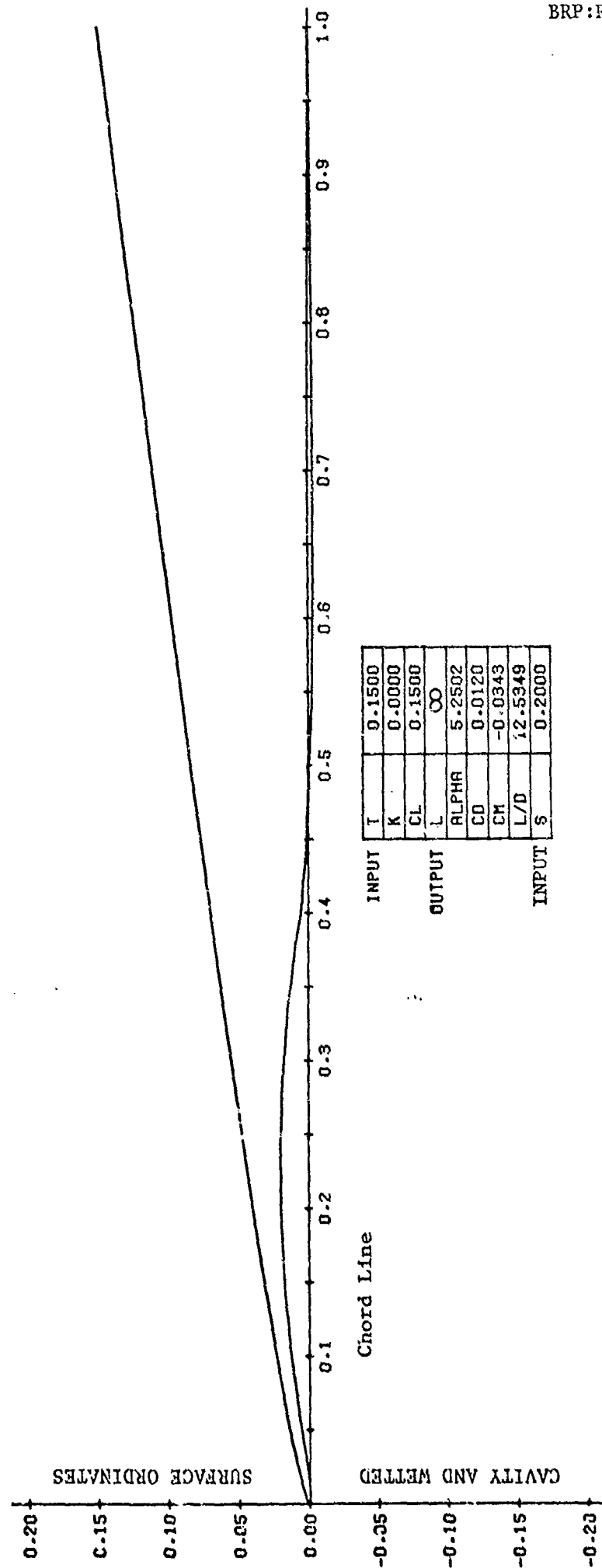
CAVITY AND WETTED

Figure 14 — Cavity and Wetted Surface Geometry
Double Ellipse Pressure Distribution, λ = .05, First Design Procedure

INPUT	T	0.1500
	K	0.0000
	CL	0.1500
	L	∞
OUTPUT	ALPHA	4.9339
	CD	0.0128
	CM	-0.0479
	L/D	11.7497
INPUT	δ	0.3000

Chord Line

SURFACE ORDINATES
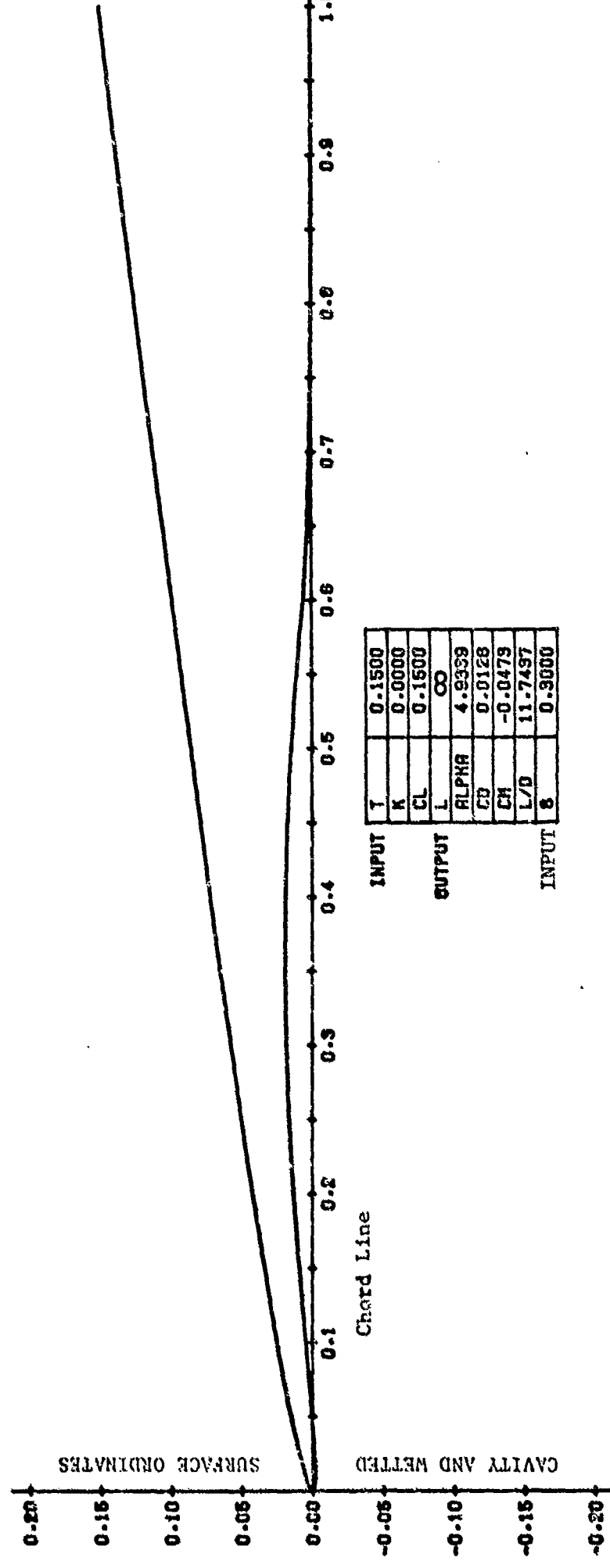
CAVITY AND WETTED

Figure 15 — Cavity and Wetted Surface Geometry
Double Ellipse Pressure Distribution, λ = .05, First Design Procedure

INPUT	T	0.1500
	K	0.0000
	CL	0.1500
OUTPUT	L	CO
	ALPHA	4.6358
	CO	0.0137
	CM	-0.0609
	L/D	10.9555
INPUT	B	0.4000

Chord Line

SURFACE ORDINATES
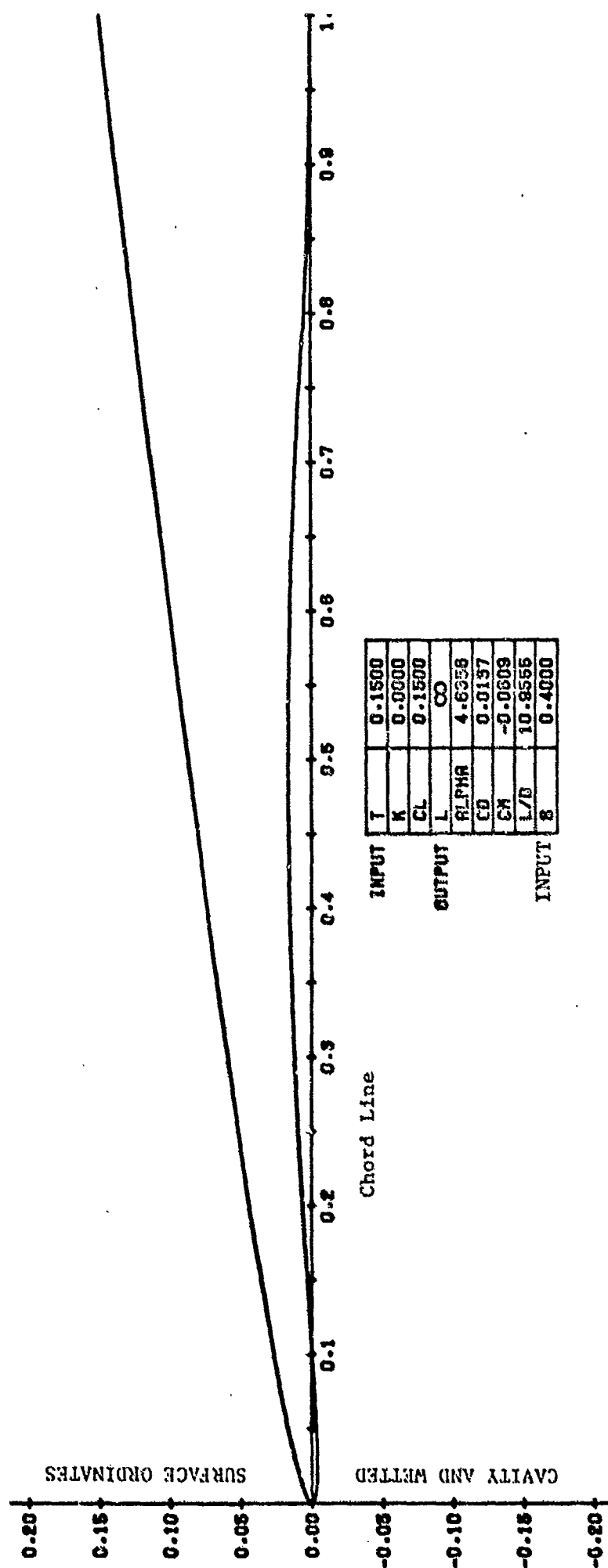
CAVITY AND WETTED

Figure 16 - Cavity and Wetted Surface Geometry
Double Ellipse Pressure Distribution, $\lambda = .05$, First Design Procedure

INPUT	T	0.1500
	K	0.0000
	CL	0.1500
OUTPUT	L	∞
	ALPHA	4.2366
	CD	0.0160
	CM	-0.0750
	L/D	9.8250
INPUT	S	0.5000
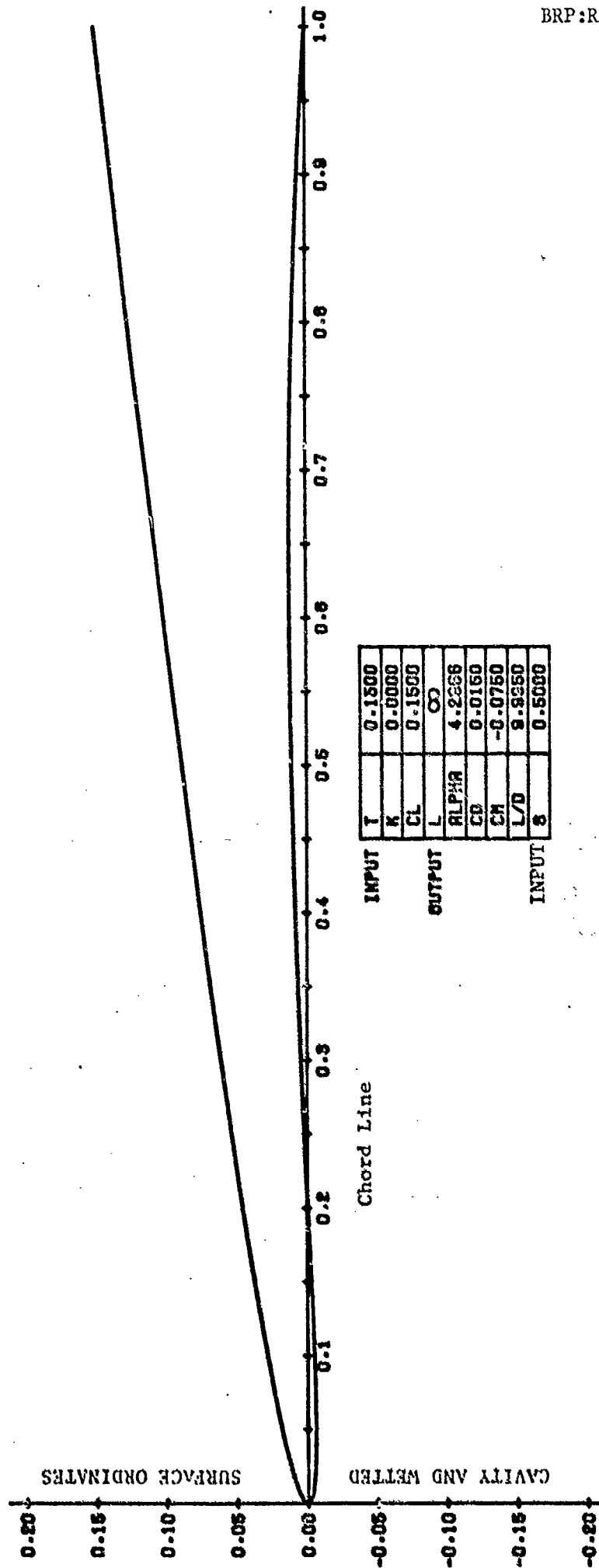
Figure 17 — Cavity and Wetted Surface Geometry
Double Ellipse Pressure Distribution, $\lambda = .05$, First Design Procedure

Figure 18 – Cavity nad Wetted Surface Geometry
Double Ellipse Pressure Distribution, $\lambda = .05$, First Design Procedure

INPUT	T	0.1500
	K	0.0000
	CL	0.1500
OUTPUT	L	∞
	ALPHA	3.3421
	CD	0.0190
	CM	-0.1150
	L/D	7.8745
INPUT	S	0.8000

Chord Line

SURFACE ORDINATES
CAVITY AND WETTED
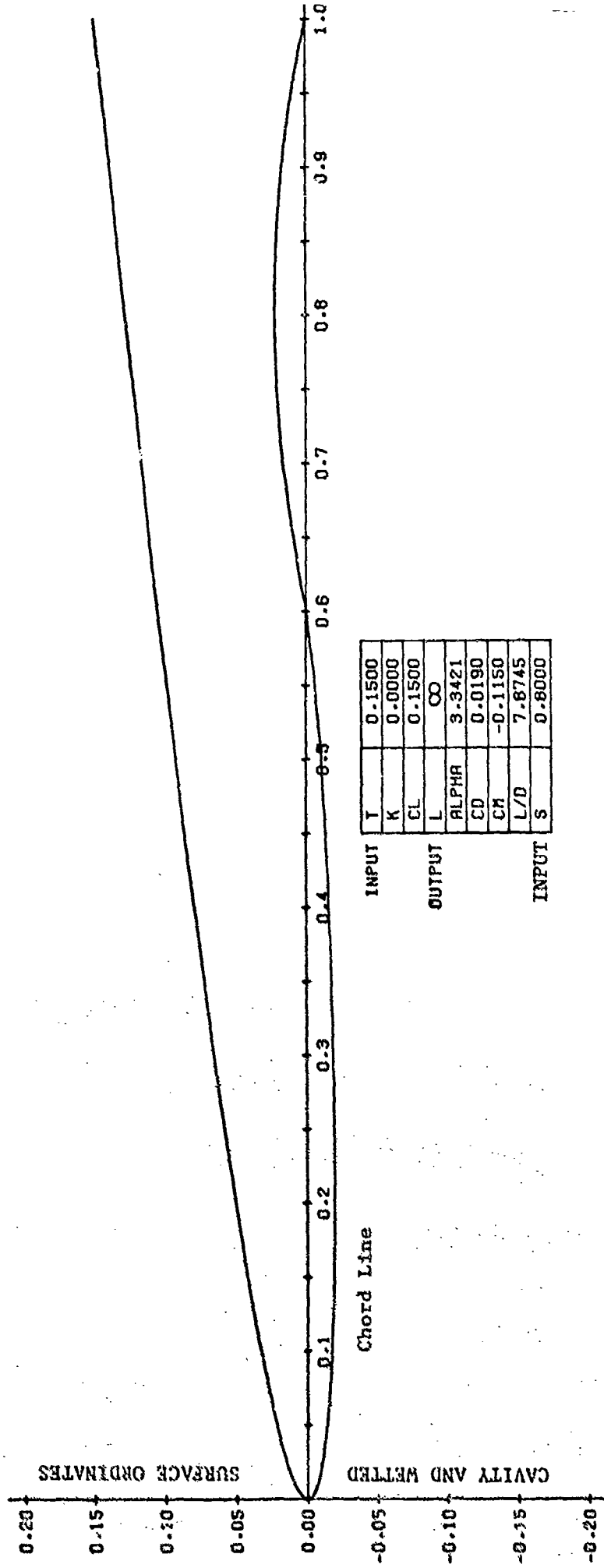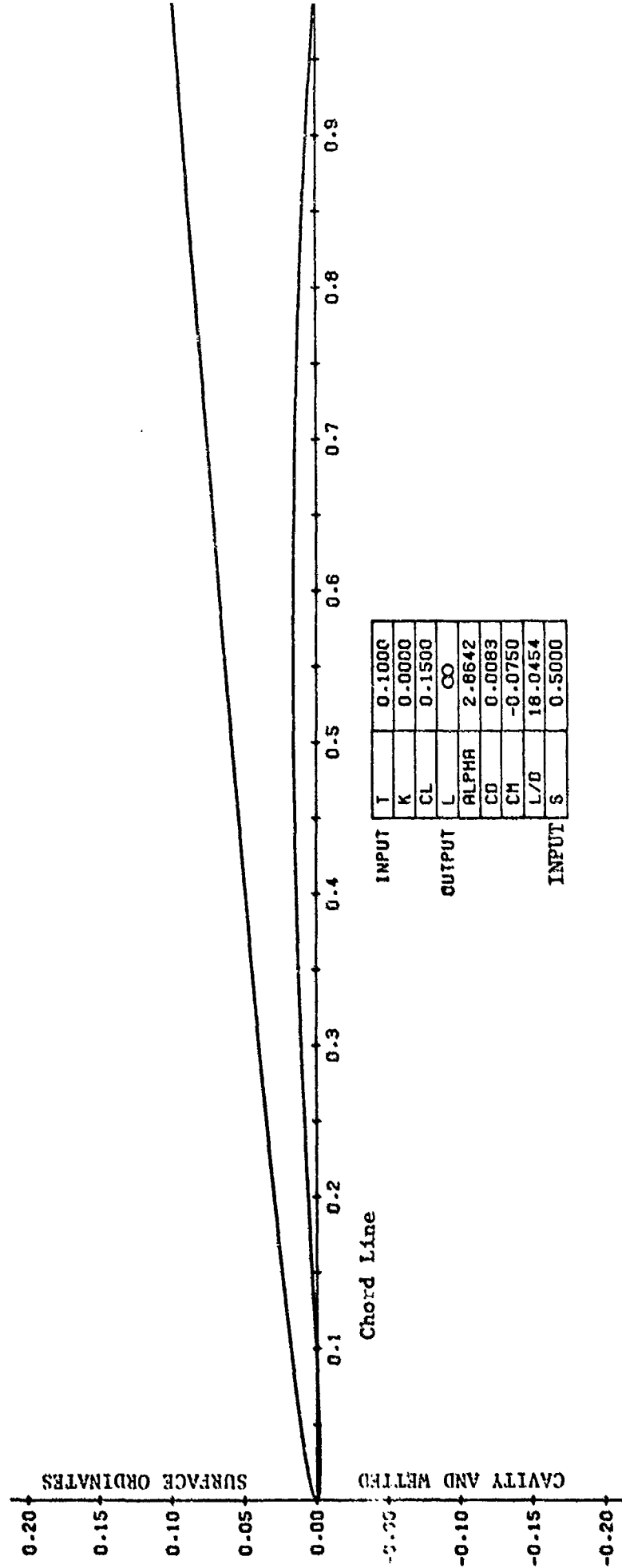
Figure 19 - Cavity and Wetted Surface Geometry
Double Ellipse Pressure Distribution, $\lambda = .05$, First Design Procedure

INPUT	T	0.1000
	K	0.0000
	CL	0.1500
OUTPUT	L	∞
	ALPHA	2.8642
	CD	0.0083
	CM	-0.0750
	L/D	18.0454
INPUT	S	0.5000

Chord Line

CAVITY AND WETTED SURFACE ORDINATES

0.20 0.15 0.10 0.05 0.00 -0.05 -0.10 -0.15 -0.20

0.1 0.2 0.3 0.4 0.5 0.6 0.7 0.8 0.9

Chord Line

INPUT	T	0.2000
	K	0.0000
	CL	0.1500
OUTPUT	L	∞
	ALPHA	5.7290
	CD	0.0237
	CM	-0.0750
	L/D	6.3382
INPUT	S	0.5000

SURFACE ORDINATES — CAVITY AND WETTED
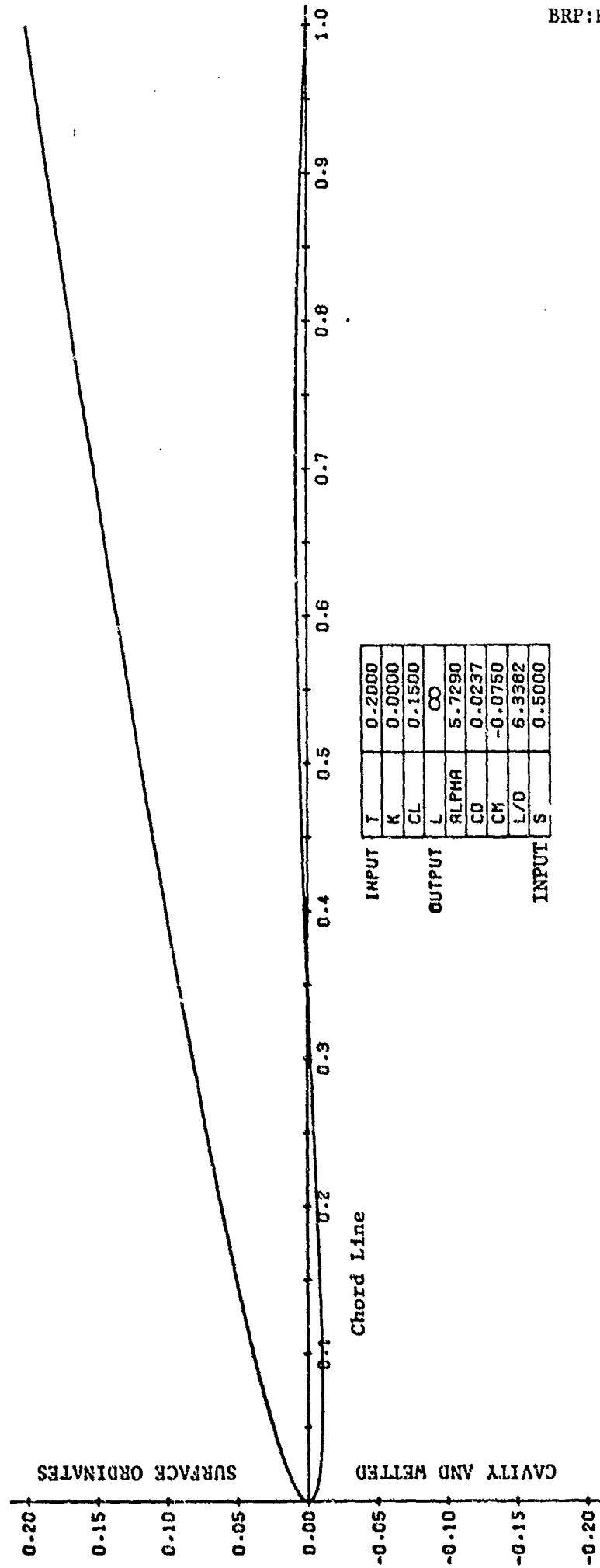
Figure 20 - Cavity and Wetted Surface Geometry
Double Ellipse Pressure Distribution, λ = .05, First Design Procedure

INPUT	T	0.1500
	K	0.2000
	CL	0.1500
OUTPUT	L	2.0621
	ALPHA	4.2967
	CD	0.0260
	CM	-0.0750
	L/D	5.7796
INPUT	S	0.5000
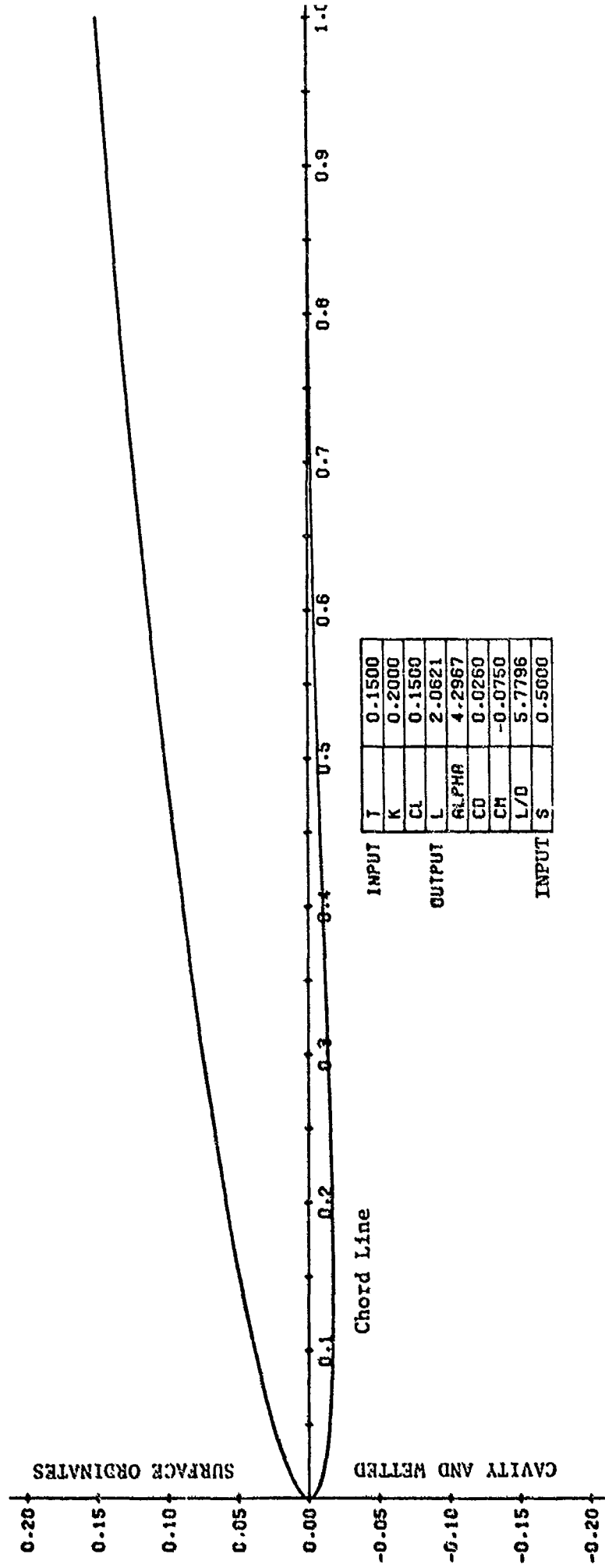
Figure 21 – Cavity and Wetted Surface Geometry
Double Ellipse Pressure Distribution, λ = .05, First Design Procedure
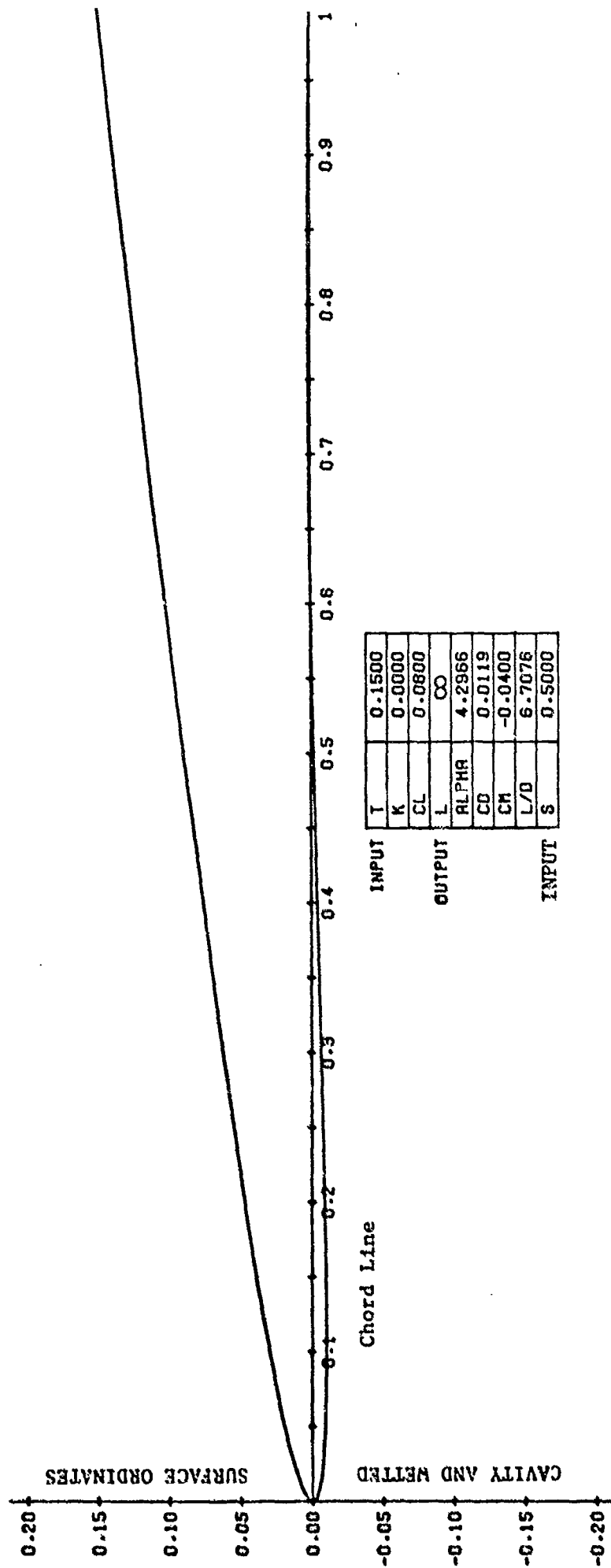
Figure 22 - Cavity and Wetted Surface Geometry
Double Ellipse Pressure Distribution, λ = .05, First Design Procedure

INPUT	T	0.2000
	K	0.2000
	CL	0.1500
OUTPUT	L	3.0899
	ALPHA	4.9337
	CD	0.0406
	CM	-0.1150
	L/D	3.6987
INPUT	S	0.8000
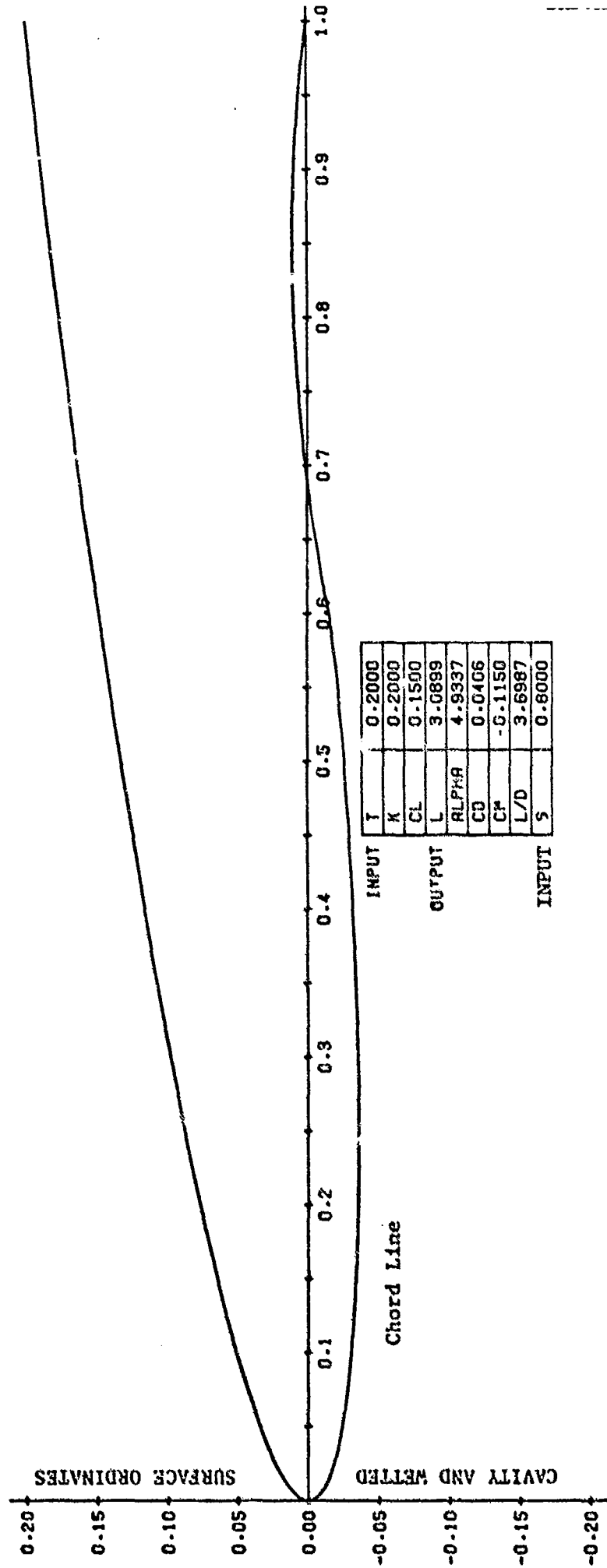
Figure 23 – Cavity and Wetted Surface Geometry
Double Ellipse Pressure Distribution, $\lambda = .05$, First Design Procedure
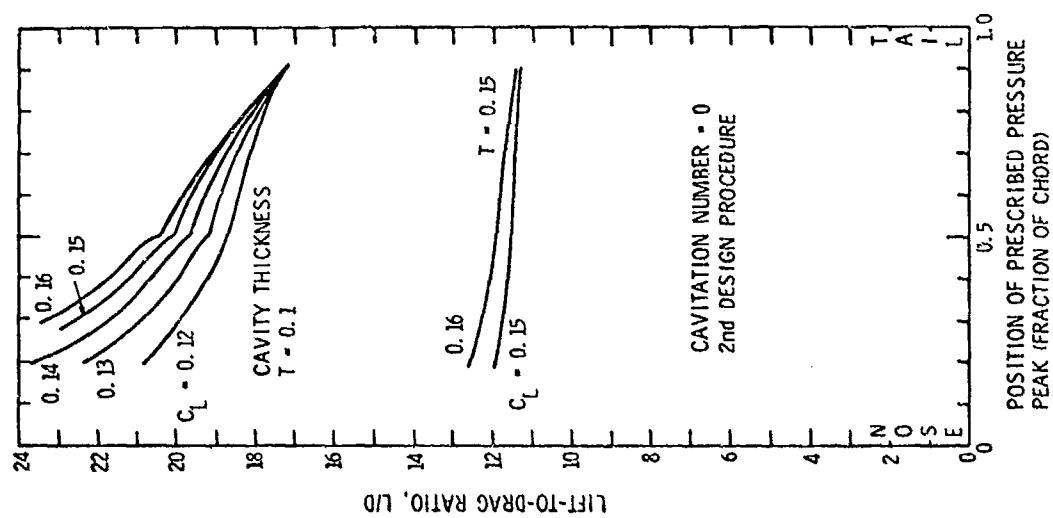
Figure 25 — Effect of Peak Pressure Location
of Performance of Hydrofoils
Designed with the Second Procedure
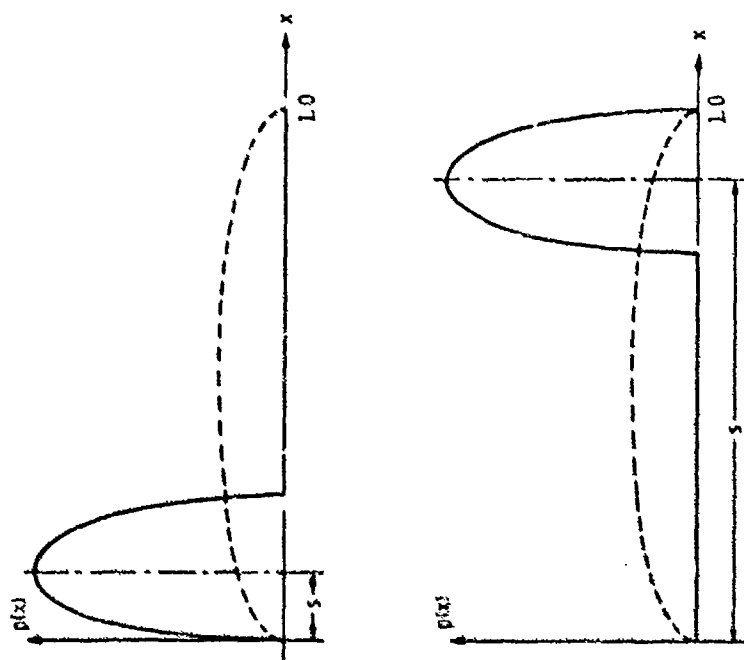
Figure 24 — Nose- and Tail-Loaded Pressure
Distributions for Use with the
Second Design Procedure
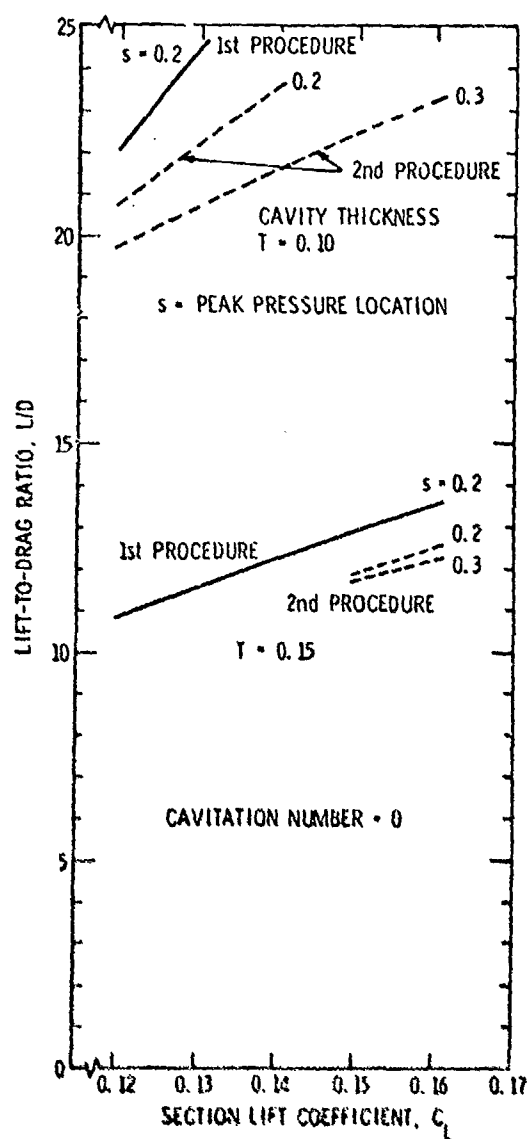
Figure 26 — Further Comparisons of Results from
First and Second Design Procedures for
Nose-Loaded Hydrofoils

FIGURE 29. SECOND DESIGN PROCEDURE, PITCHING
MOMENT PERFORMANCE MAP

CAVITATION NUMBER, K = 0

T = CAVITY THICKNESS AT TRAILING
EDGE OF PROFILE

s = DISTANCE OF PEAK PRESSURE FROM
NOSE OF UNIT-CHORD HYDROFOIL

FIGURE 30. SECOND DESIGN PROCEDURE, PITCHING
MOMENT PERFORMANCE MAP

CAVITATION NUMBER, K = .05

T = CAVITY THICKNESS AT TRAILING
EDGE OF PROFILE

s = DISTANCE OF PEAK PRESSURE FROM
NOSE OF UNIT-CHORD HYDROFOIL

CENTER OF PRESSURE LOCATION, $\bar{x}$
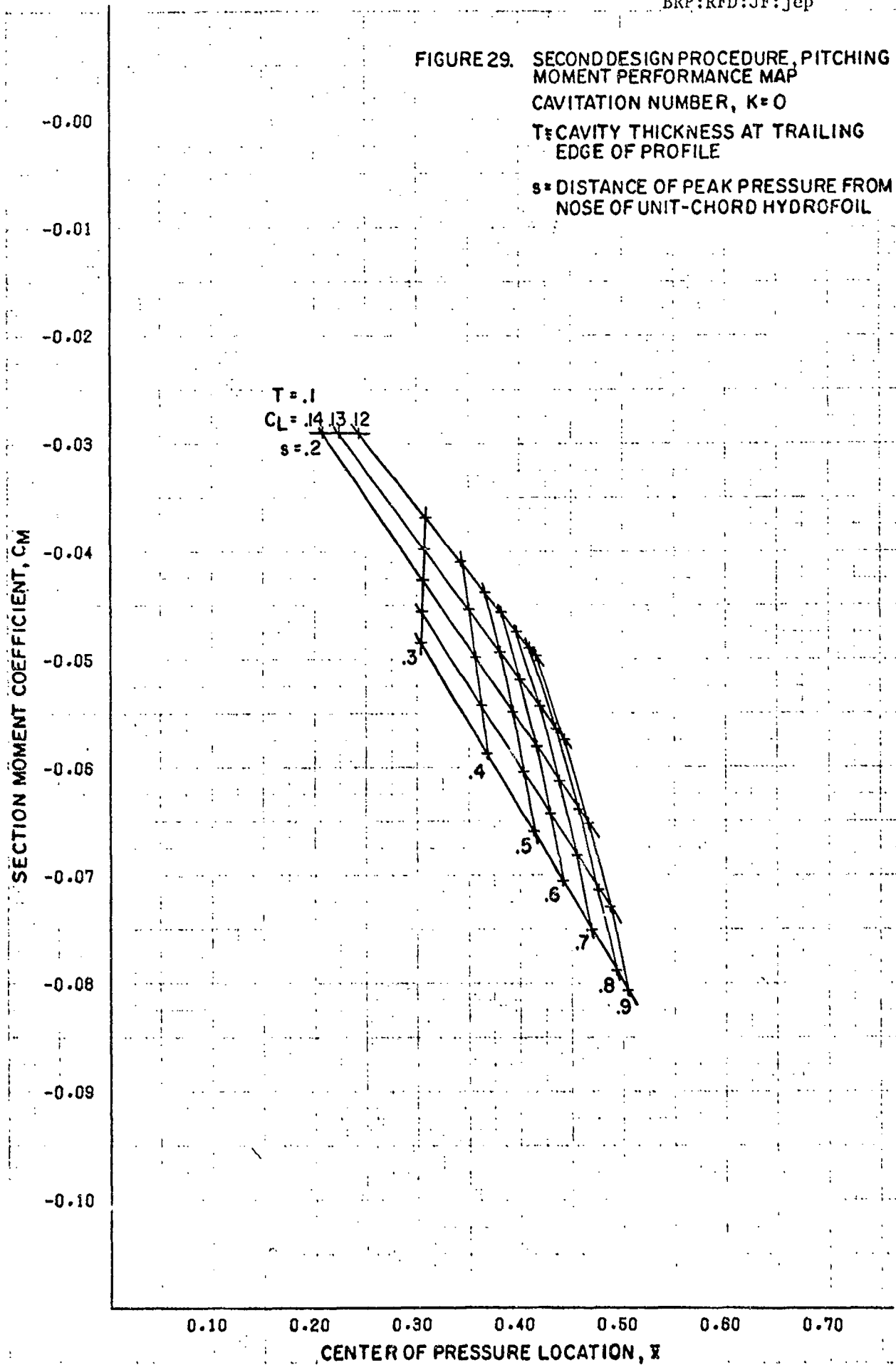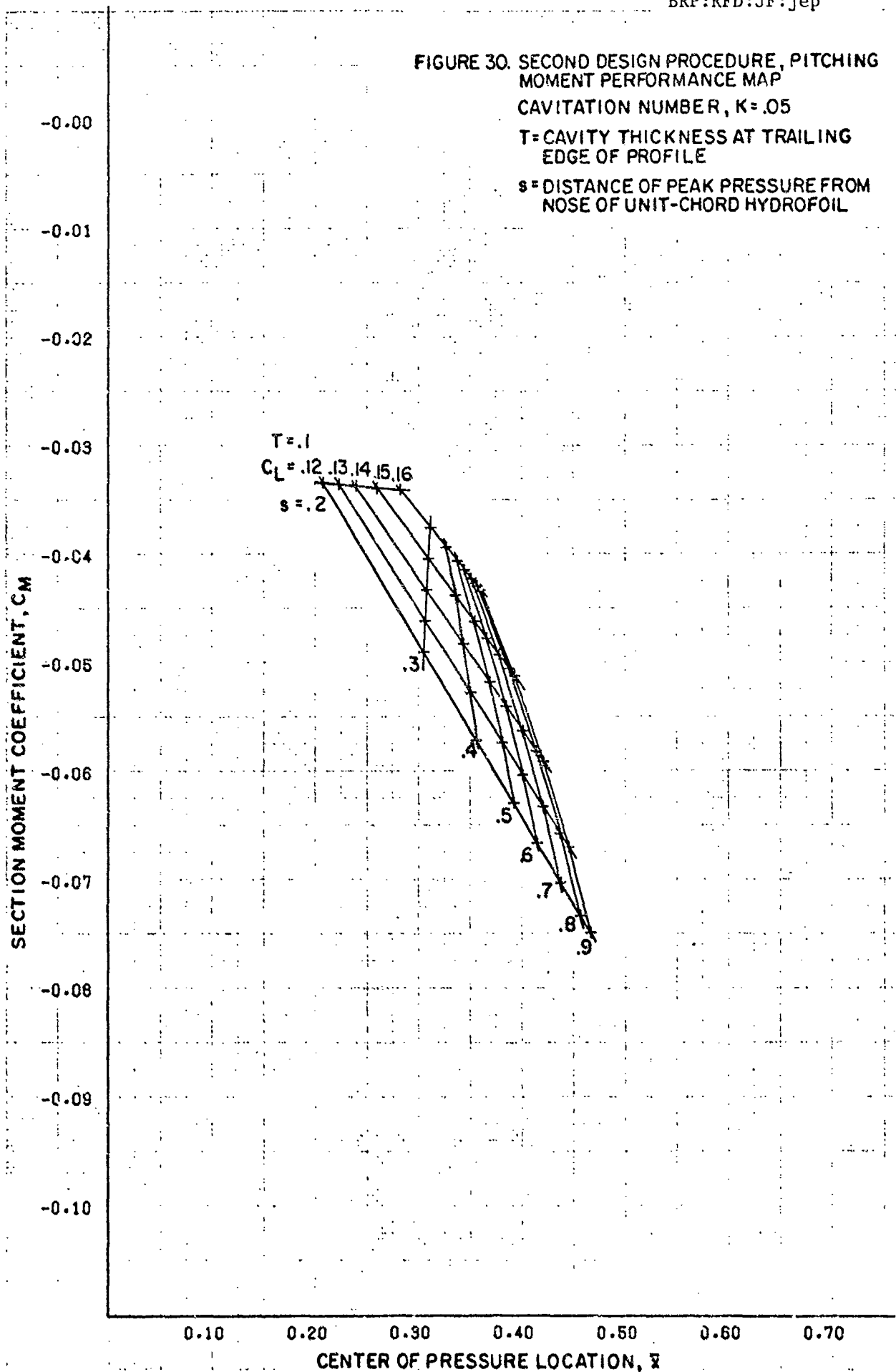
FIGURE 31. SECOND DESIGN PROCEDURE, PITCHING MOMENT PERFORMANCE MAP

CAVITATION NUMBER, K=.1

T = CAVITY THICKNESS AT TRAILING EDGE OF PROFILE

s = DISTANCE OF PEAK PRESSURE FROM NOSE OF UNIT-CHORD HYDROFOIL
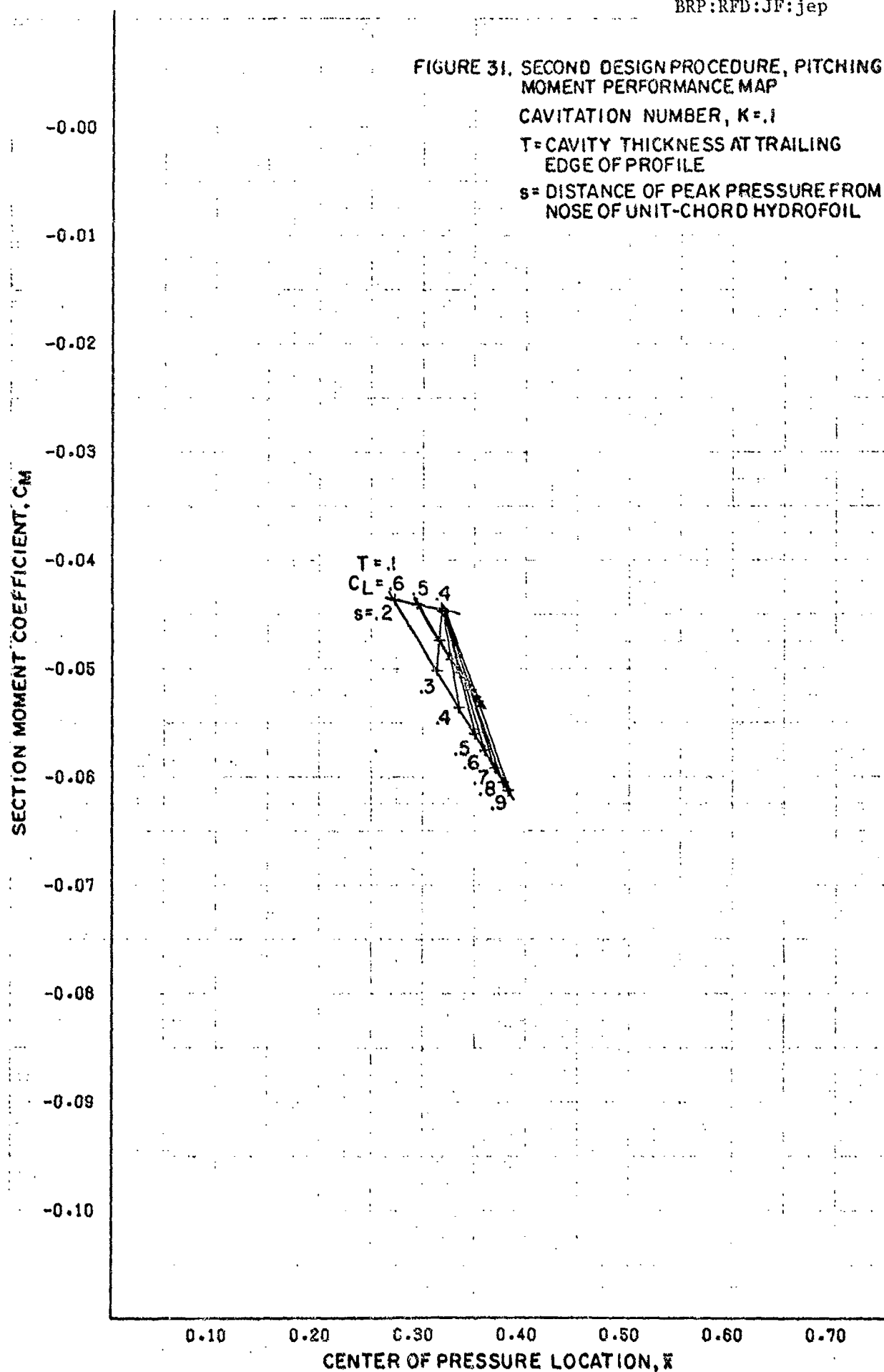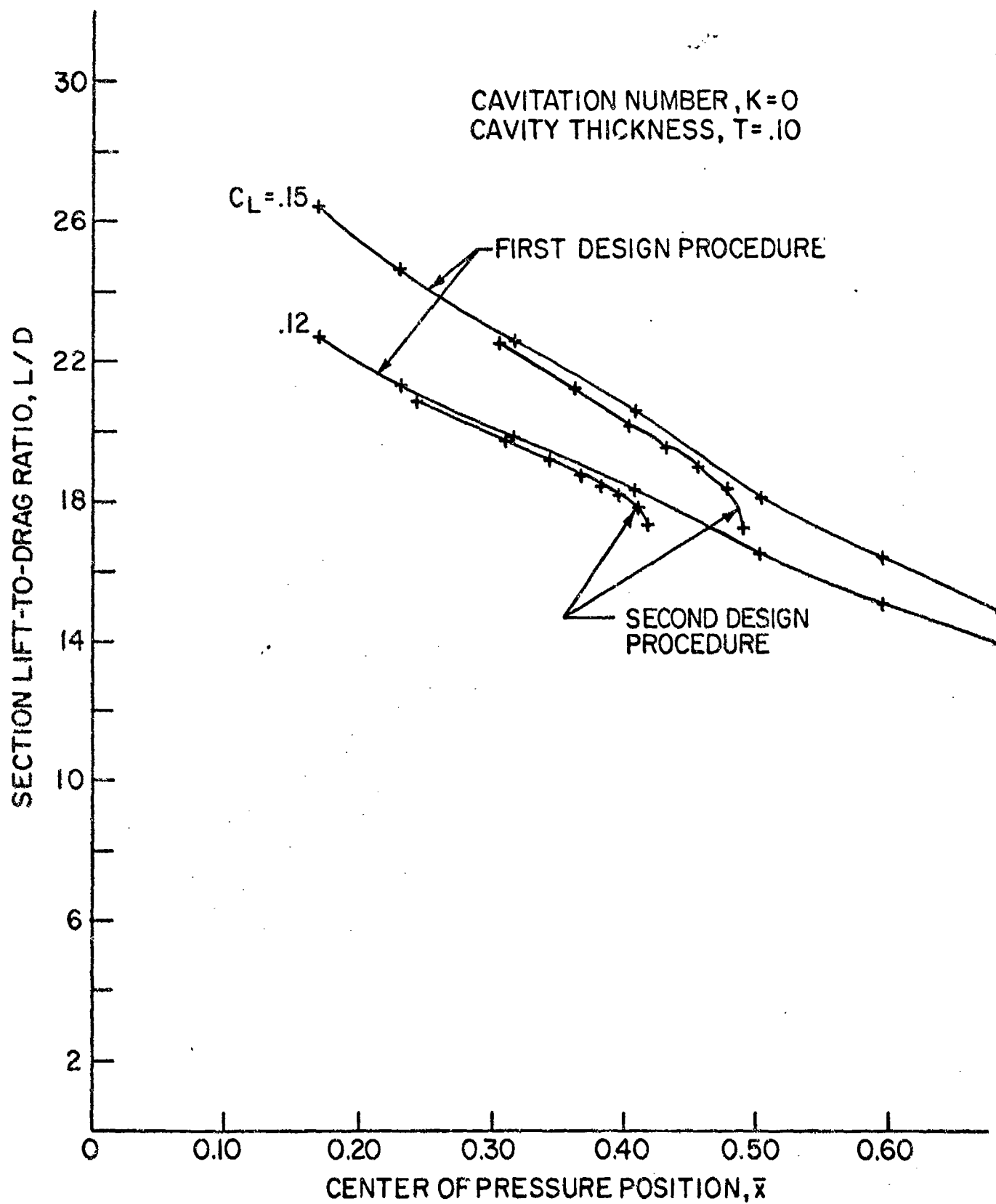
Figure 32 – Comparison of Performance Obtained from First and Second Design
Procedures at Two Design Lift Coefficients, K = 0
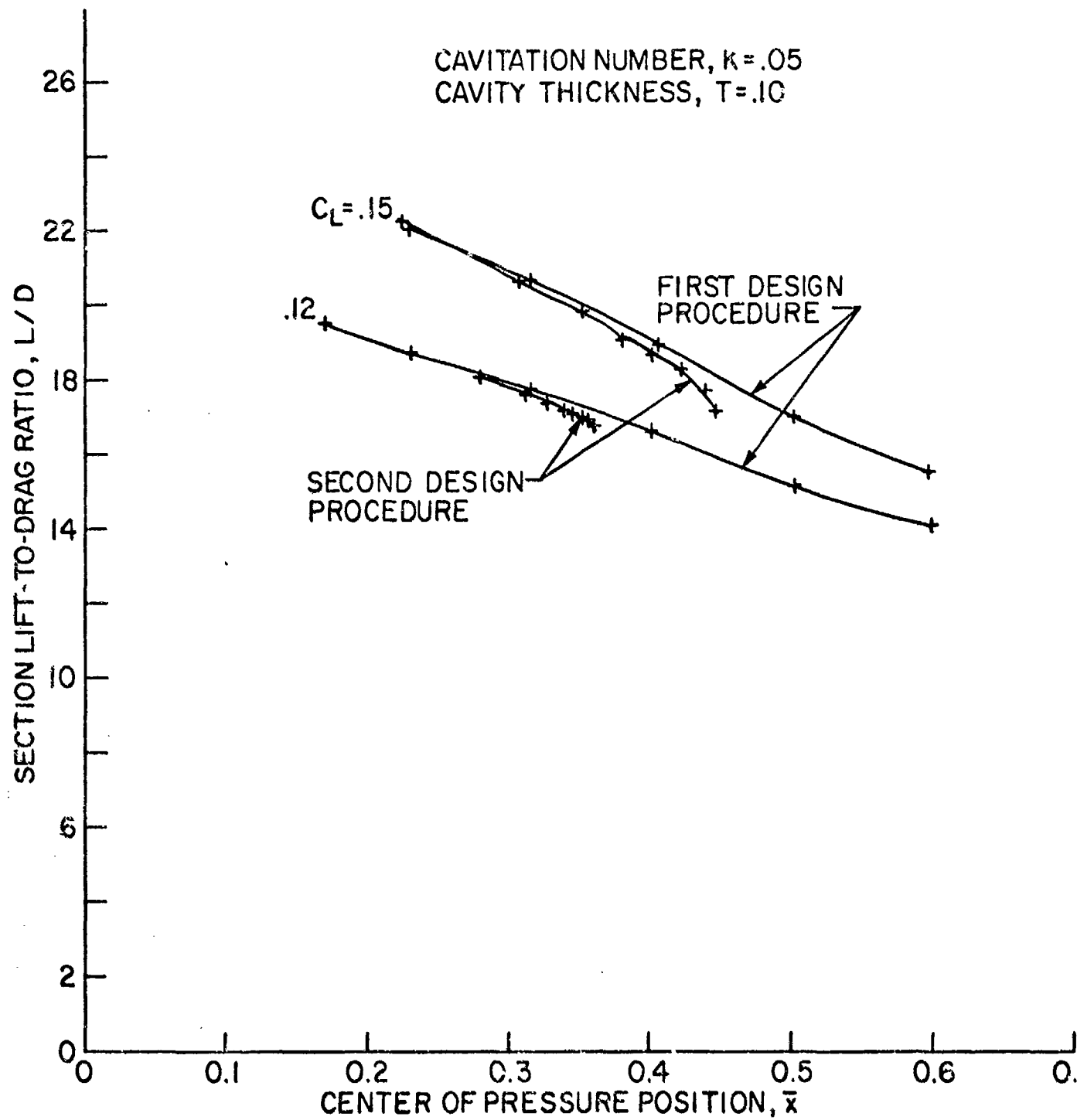
Figure 33 – Comparison of Performance Obtained from First and Second Design
Procedures at Two Design Lift Coefficients, K=.05
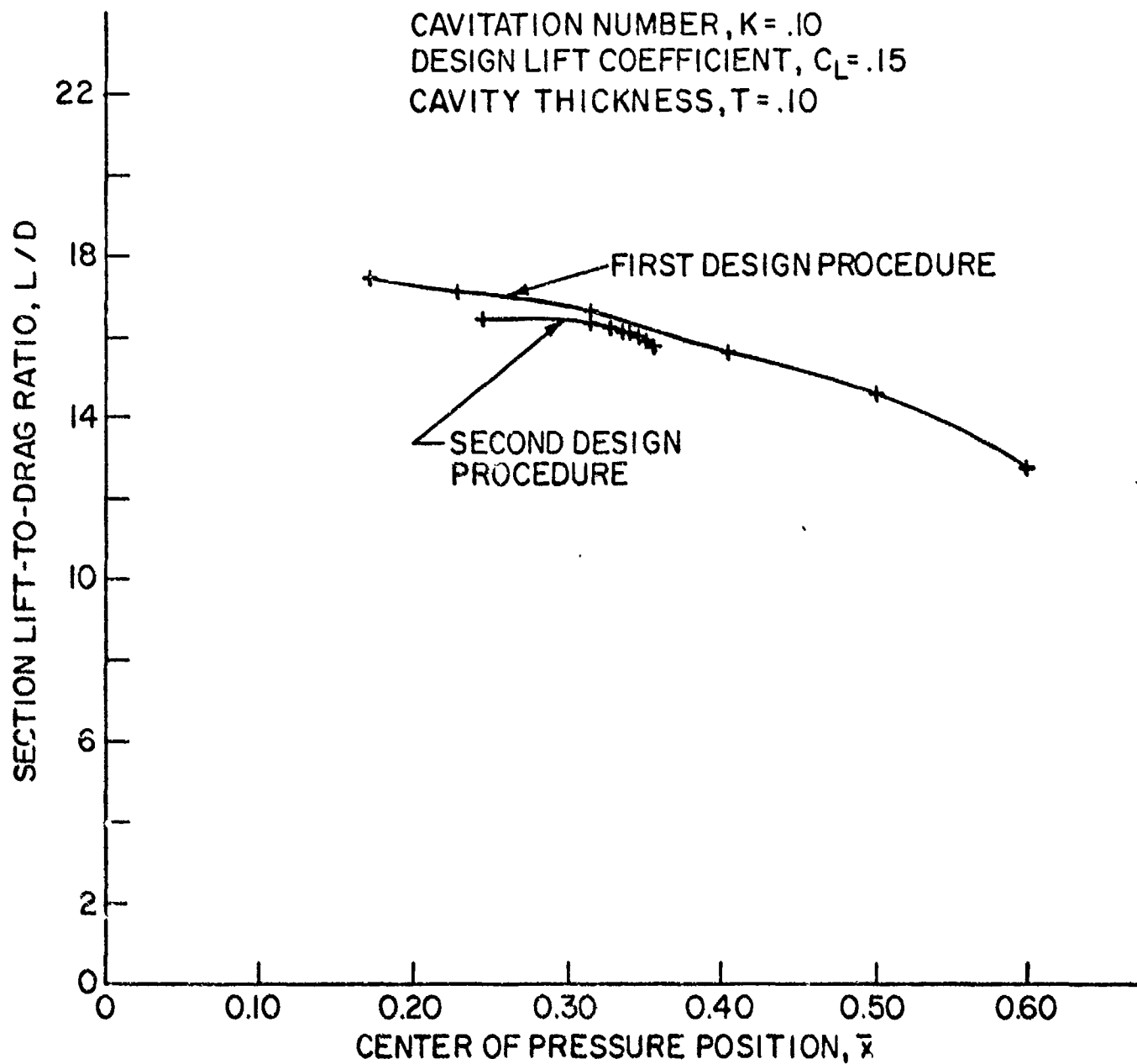
Figure 34 - Comparison of Performance Obtained from First and Second
Design Procedures, K=.10

INPUT	T	0.1000
	K	0.0000
	CL	0.1200
	L	∞
OUTPUT	ALPHA	0.0811
	CD	0.0051
	CM	-0.0389
	L/D	18.7785

Chord Line

CAVITY AND WETTED SURFACE ORDINATES
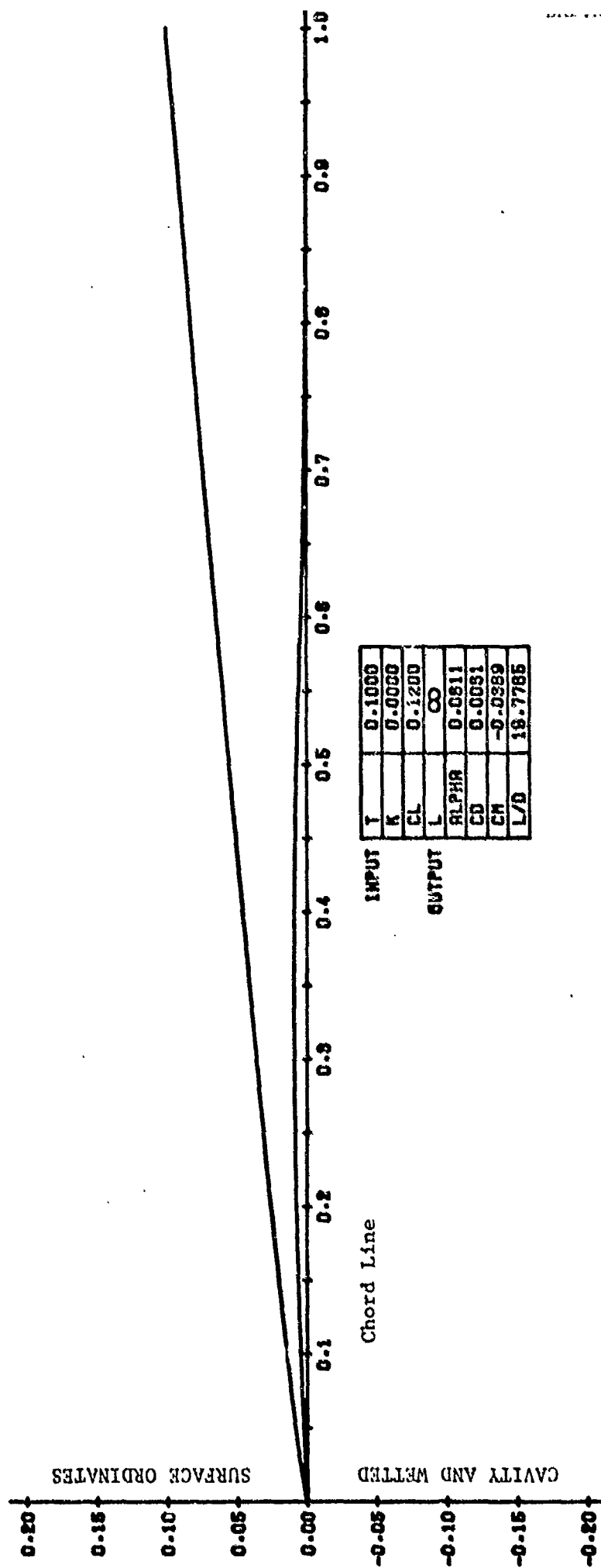
Figure 35 - Cavity and Wetted Surface Geometry
Elliptic Pressure Distribution, Peak Pressure Location s = .3.
Second Design Procedure
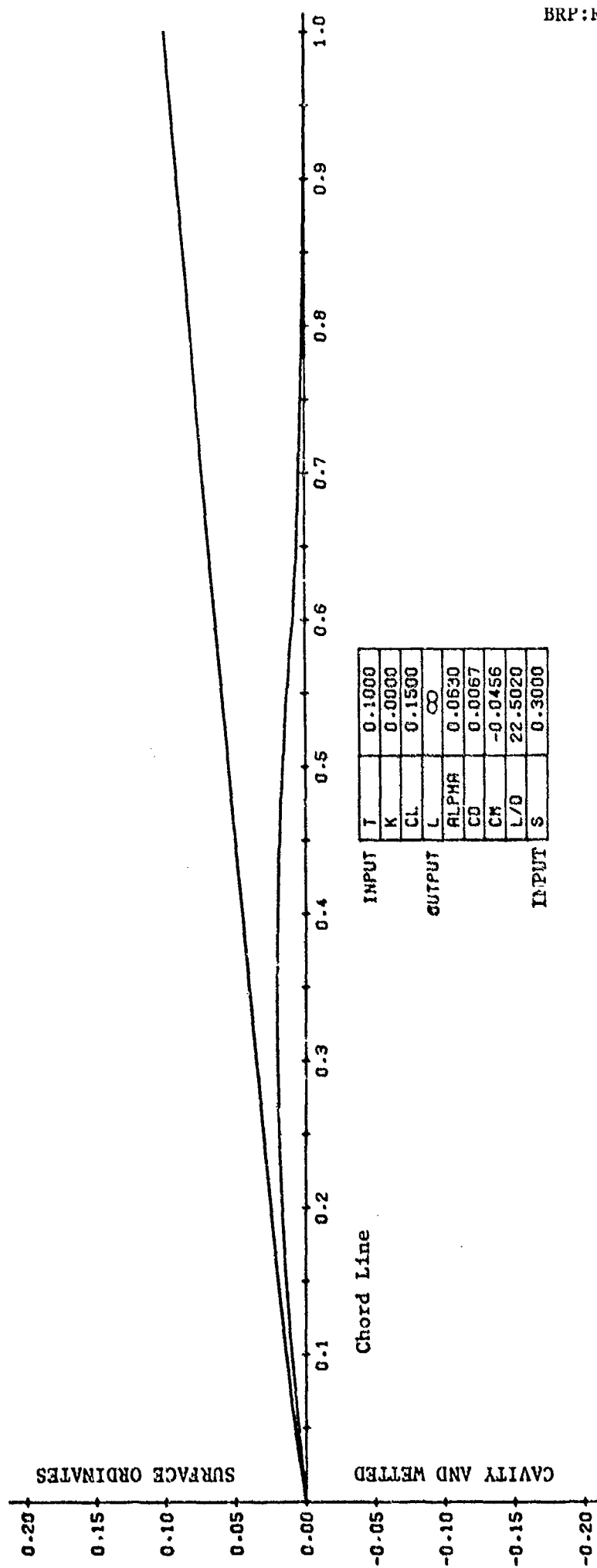
Figure 36 - Cavity and Wetted Surface Geometry
Elliptic Pressure Distribution, Peak Pressure Location s = .3.
Second Design Procedure

INPUT	T	0.1000
	K	0.0000
	CL	0.1500
	L	∞
OUTPUT	ALPHA	0.0630
	CD	0.0067
	CM	-0.0456
	L/D	22.5020
INPUT	S	0.3000

Chord Line

CAVITY AND WETTED SURFACE ORDINATES

BRP:RFD:JF:jep

INPUT	T	0.1000
	K	0.0000
	CL	0.1500
	L	∞
OUTPUT	ALPHA	0.0552
	CD	0.0079
	CM	-0.0682
	L/D	18.9443
INPUT	S	0.7000

Chord Line

SURFACE ORDINATES
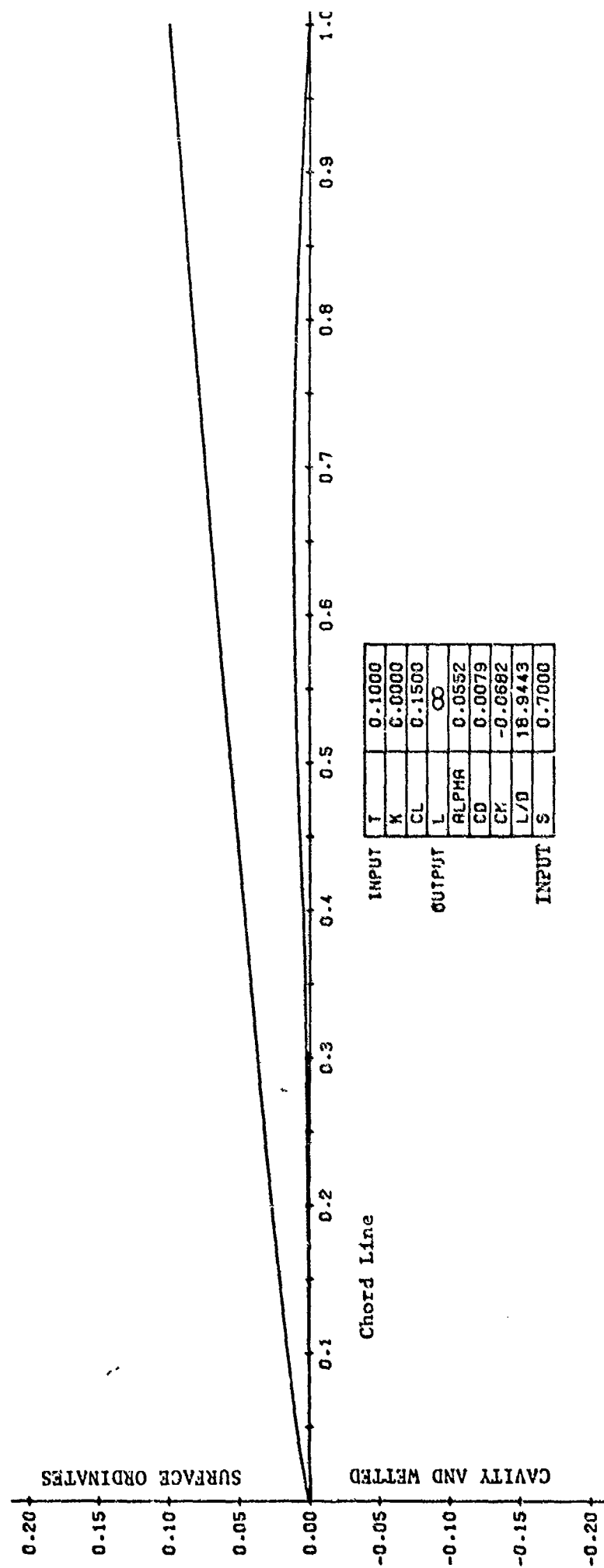
CAVITY AND WETTED

Figure 37 — Cavity and Wetted Surface Geometry
Elliptic Pressure Distribution, Peak Pressure Location s = .7.
Second Design Procedure

INPUT	T	0.1500
	K	0.0000
	CL	0.1600
	L	∞
OUTPUT	ALPHA	0.0805
	CD	0.0191
	CM	-0.0485
	L/D	12.2284

Chord Line

SURFACE ORDINATES
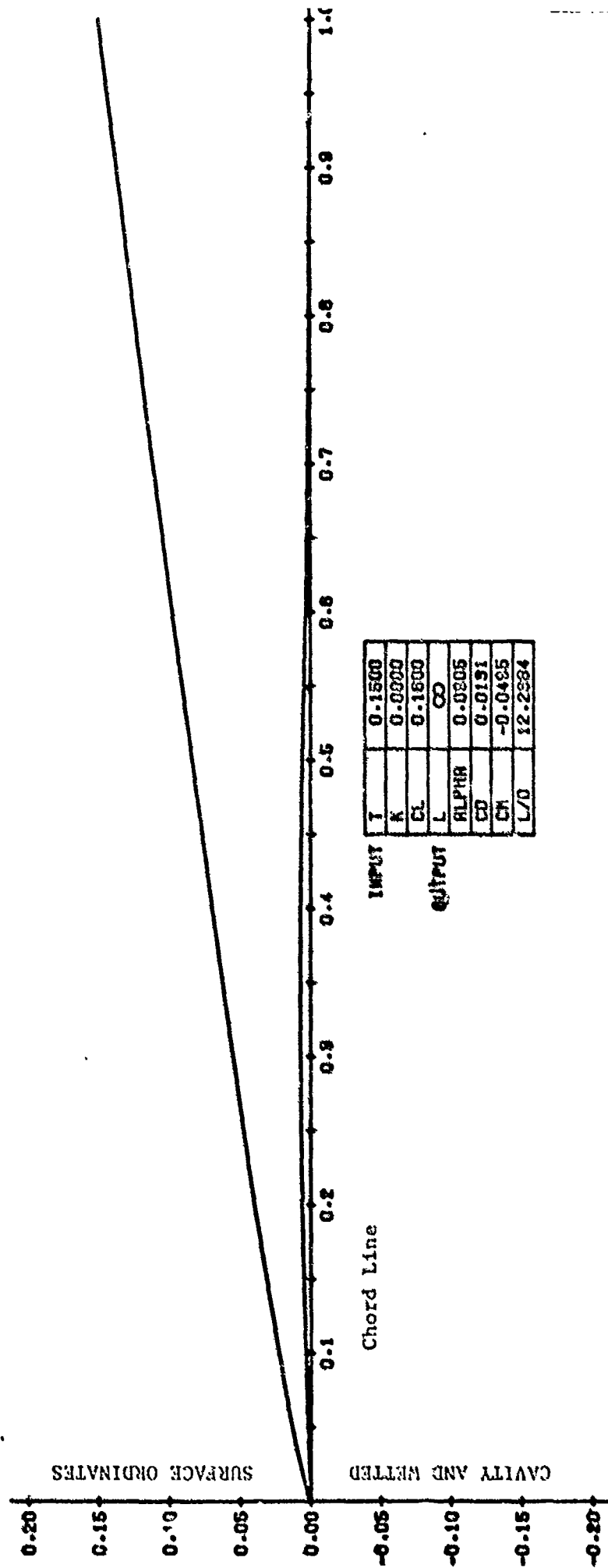
CAVITY AND WETTED

Figure 38 - Cavity and Wetted Surface Geometry
Elliptic Pressure Distribution, Peak Pressure Location $s = .3$.
Second Design Procedure
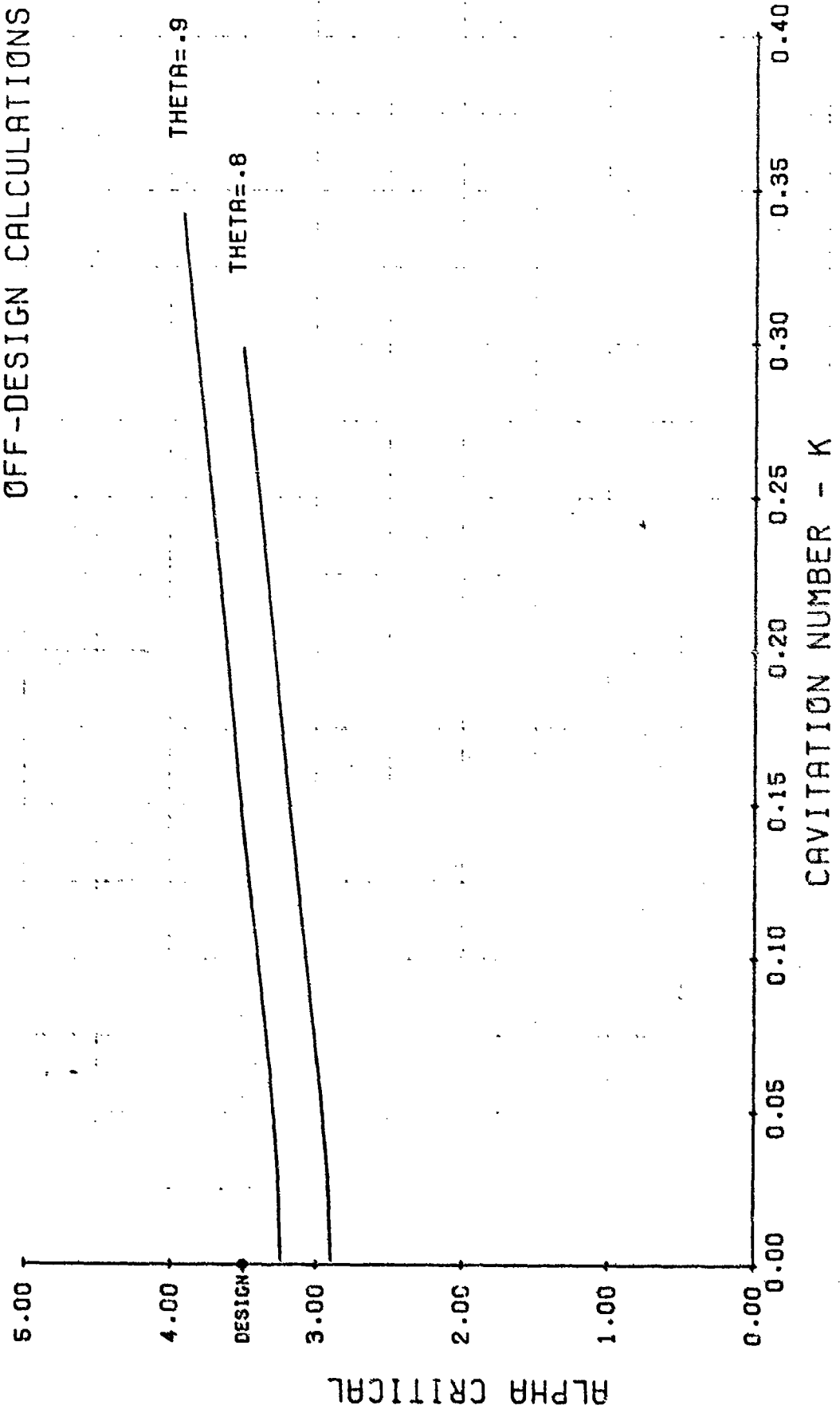
FIGURE-39 ALPHA CRITICAL VERSUS CAVITATION NUMBER. FIRST DESIGN PROCEDURE.

OFF-DESIGN CALCULATIONS

THETA=.9

THETA=.8

CAVITATION NUMBER - K
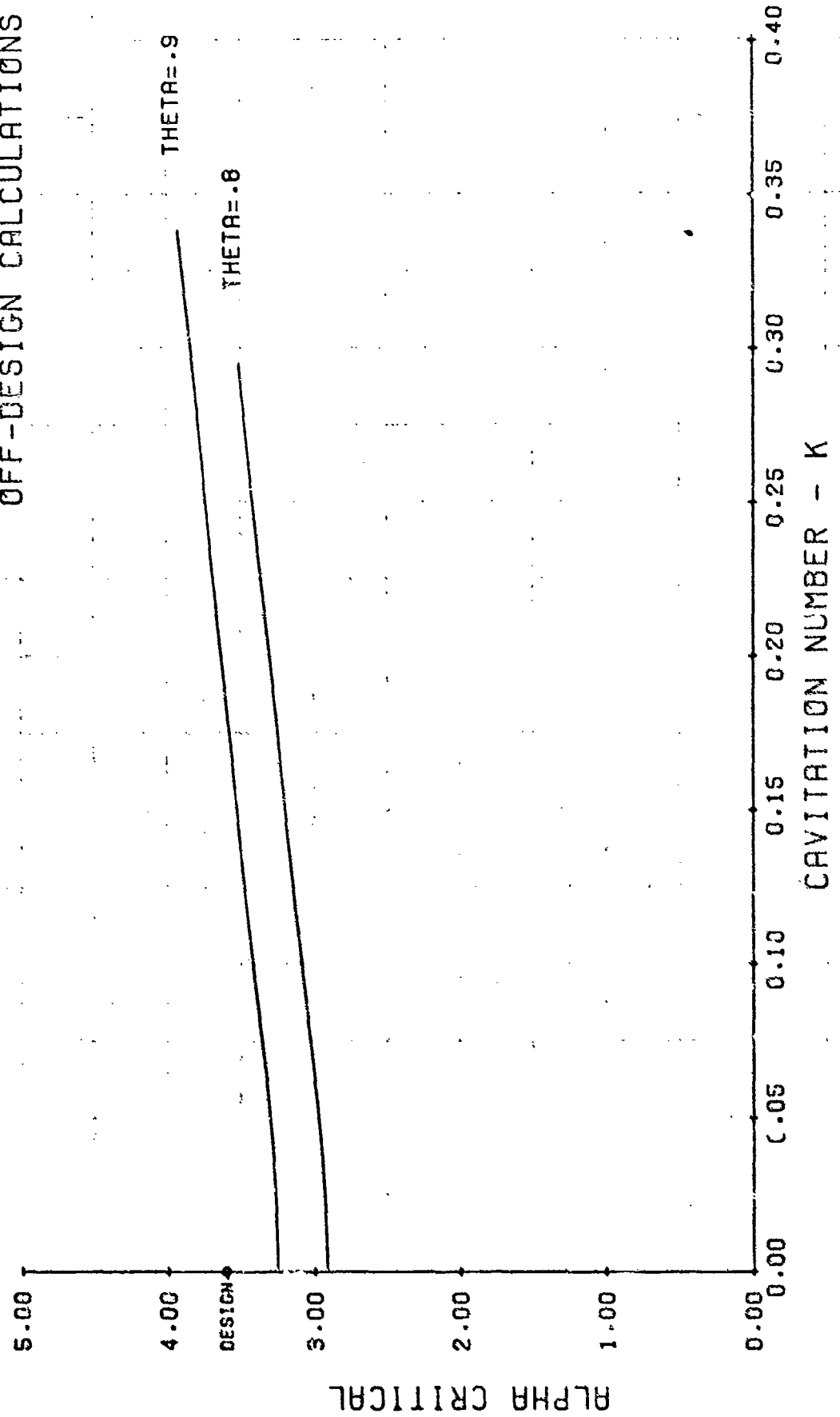
ALPHA CRITICAL

FIGURE-40. ALPHA CRITICAL VERSUS CAVITATION NUMBER. SECOND DESIGN PROCEDURE.
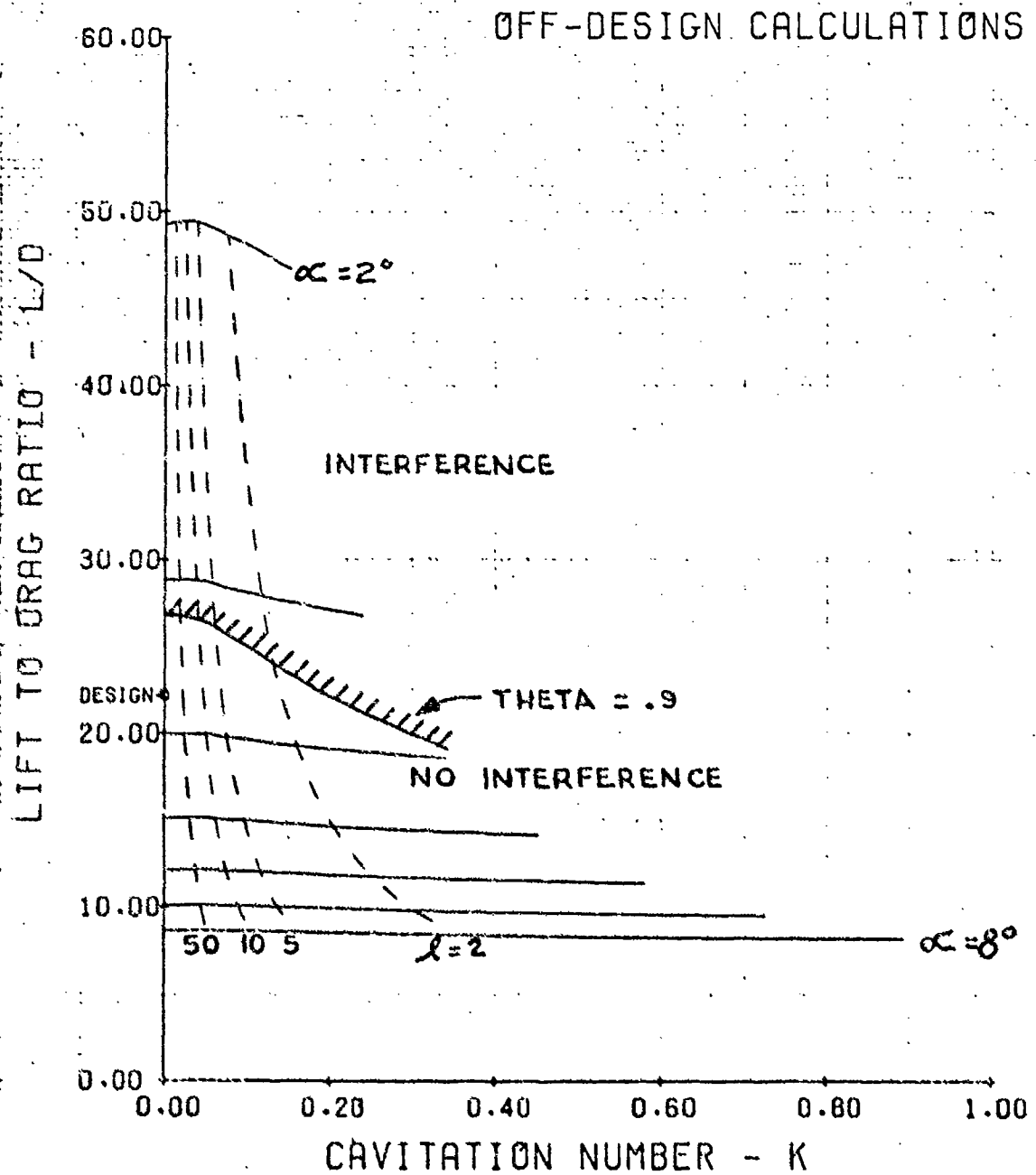
FIFURE-41 LIFT TO DRAG RATIO VERSUS CAVITATION NUMBER.

FIRST DESIGN PROCEDURE.
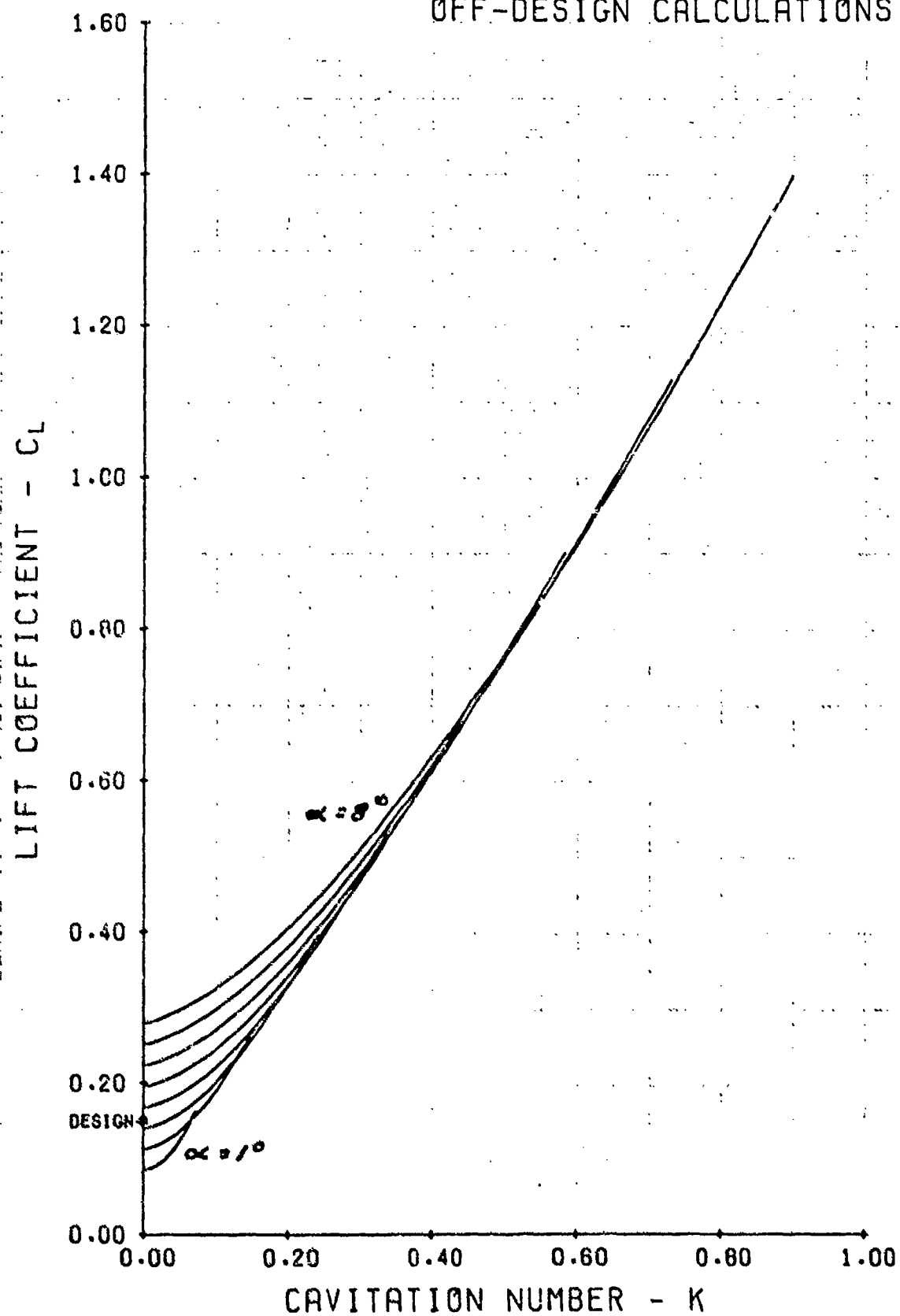
FIGURE-42 LIFT COEFFICIENT VERSUS CAVITATION NUMBER.
FIRST DESIGN PROCEDURE.
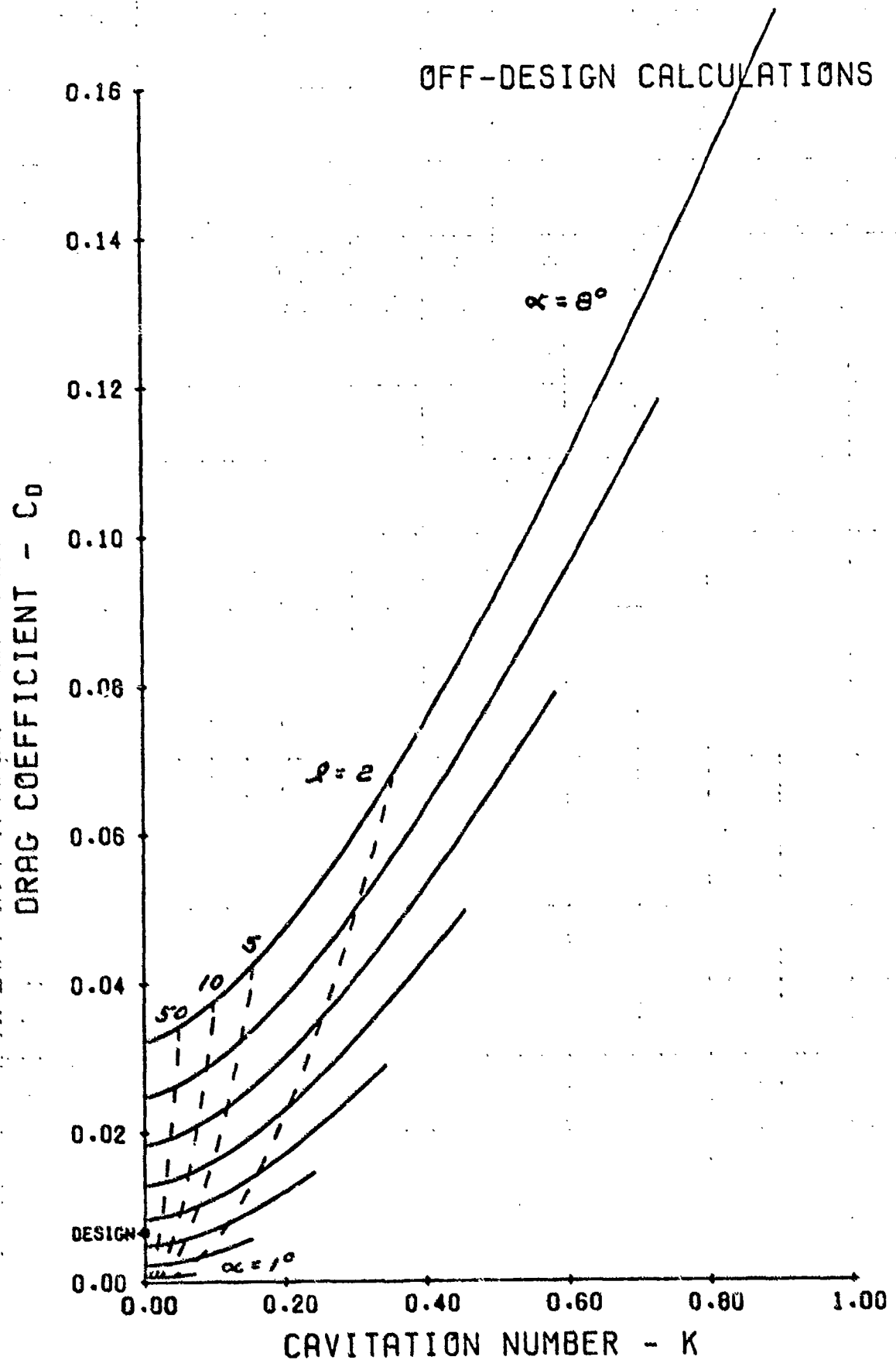
FIGURE-49 DRAG COEFFICIENT VERSUS CAVITATION NUMBER.
FIRST DESIGN PROCEDURE.

OFF-DESIGN CALCULATIONS.
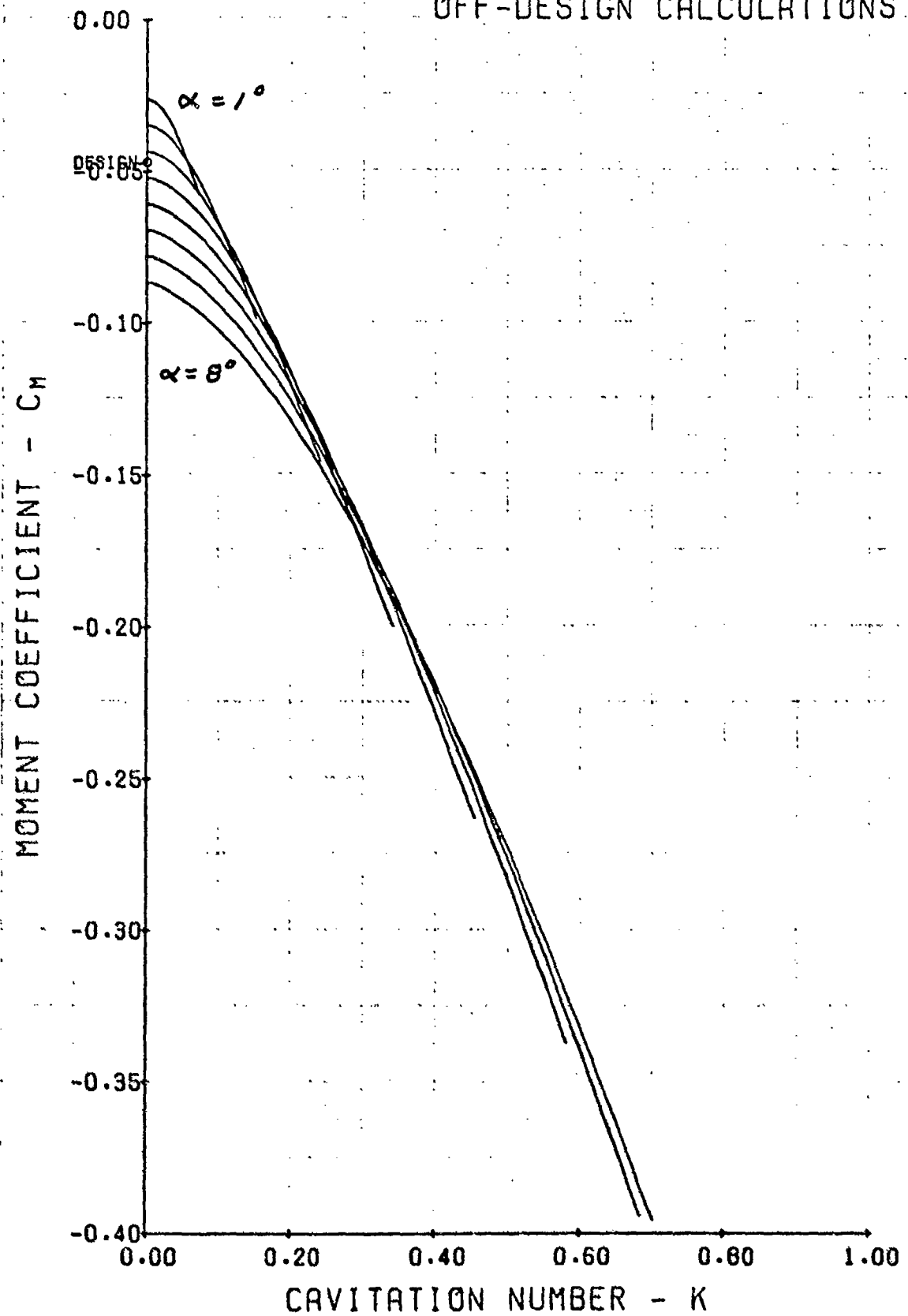
FIGURE-44   MOMENT COEFFICIENT VERSUS CAVITATION NUMBER.
FIRST DESIGN PROCEDURE.
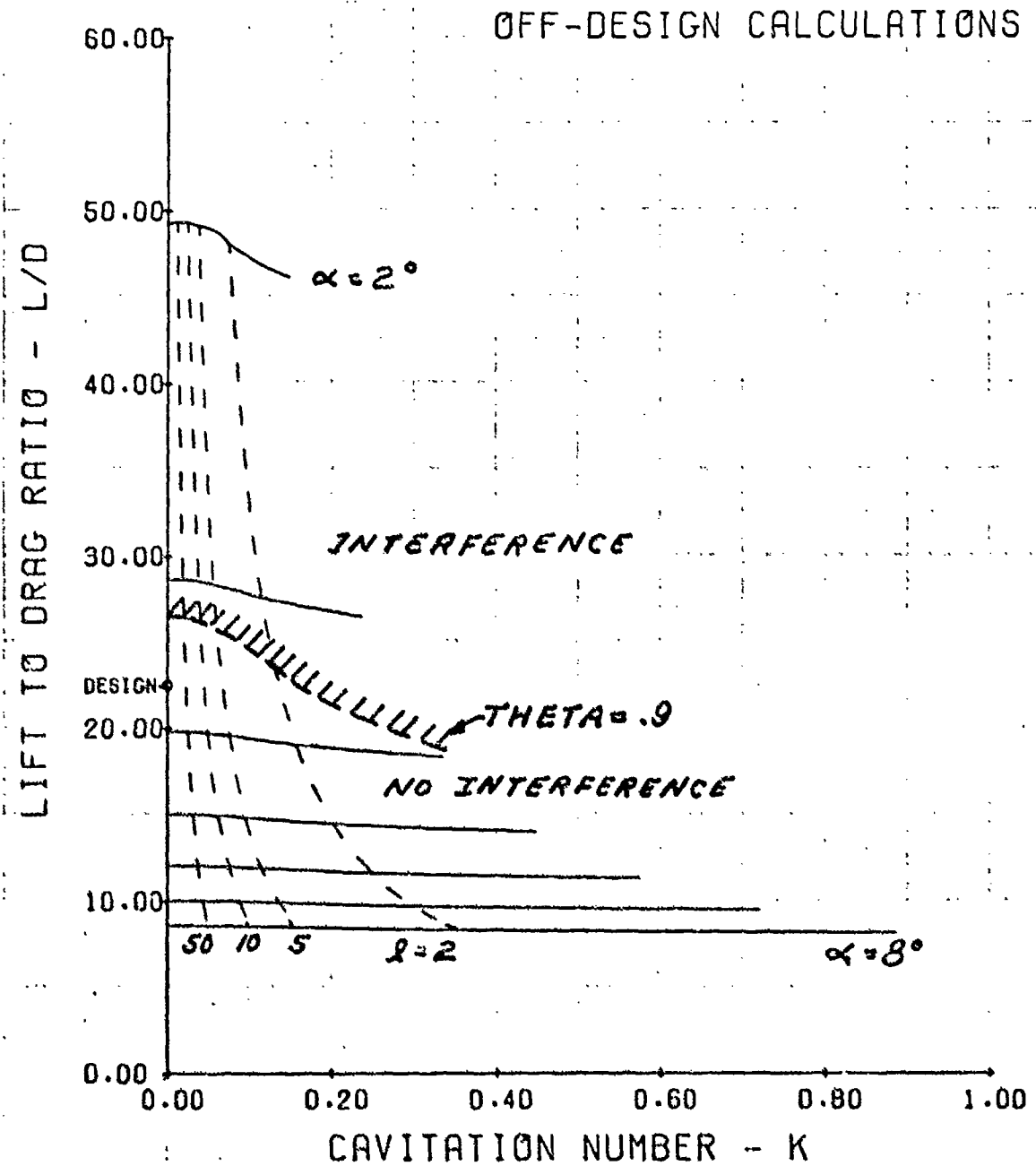
FIGURE-45 LIFT TO DRAG RATIO VERSUS CAVITATION NUMBER.

SECOND DESIGN PROCEDURE.

OFF-DESIGN CALCULATIONS
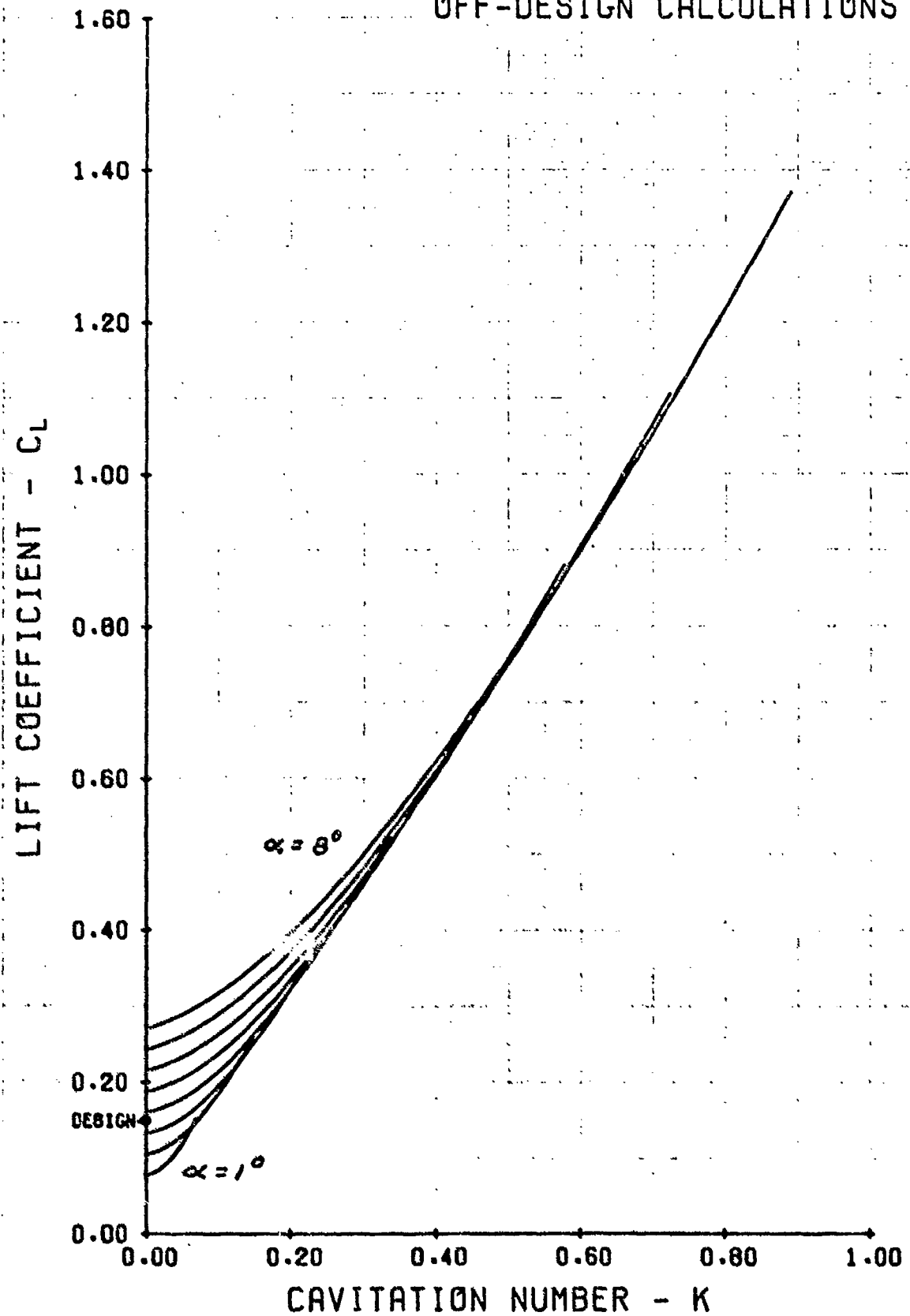
FIGURE-46 LIFT COEFFICIENT VERSUS CAVITATION NUMBER.
SECOND DESIGN PROCEDURE.

OFF-DESIGN CALCULATIONS
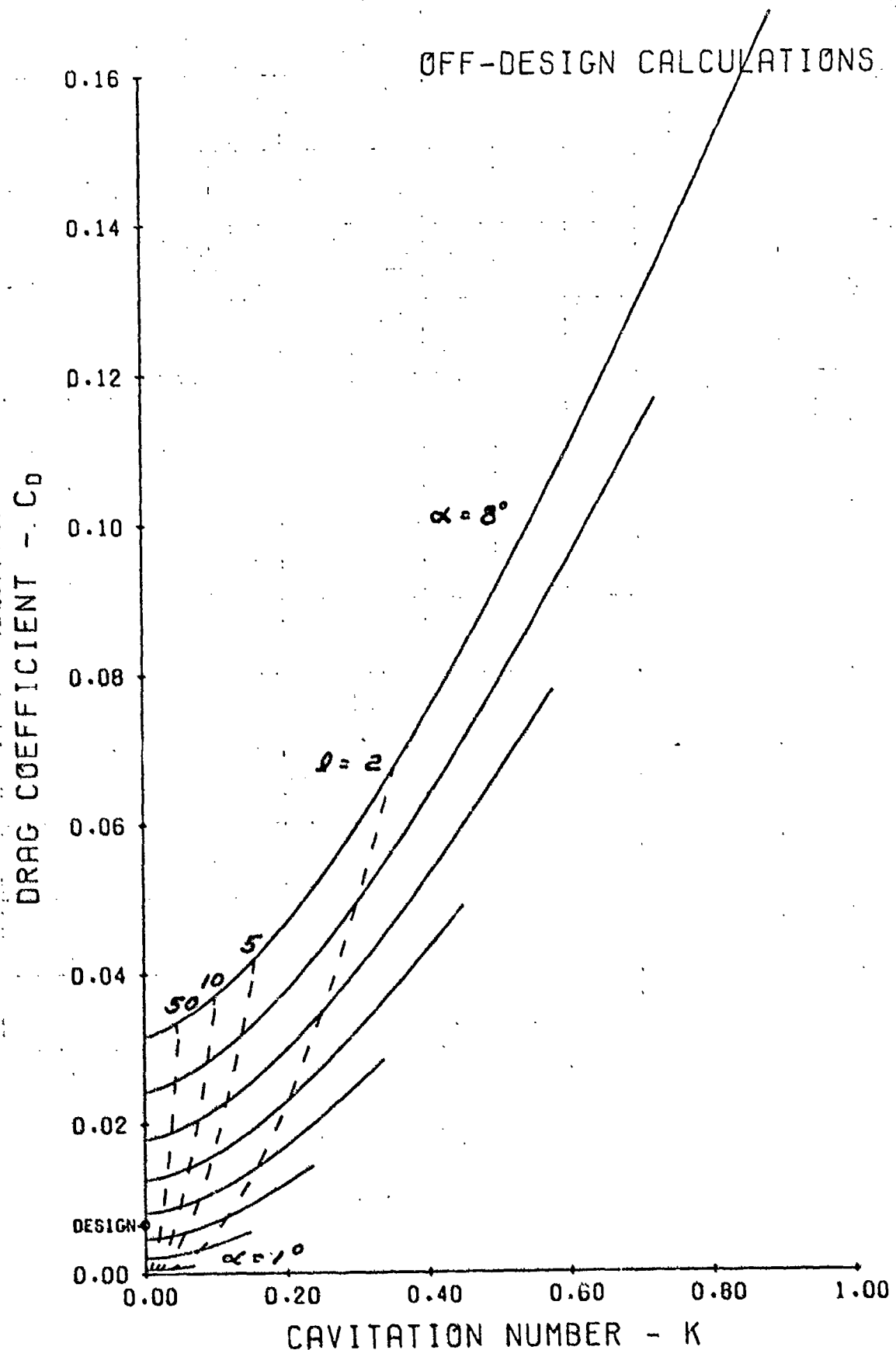
FIGURE-47 DRAG COEFFICIENT VERSUS CAVITATION NUMBER.
SECOND DESIGN PROCEDURE.
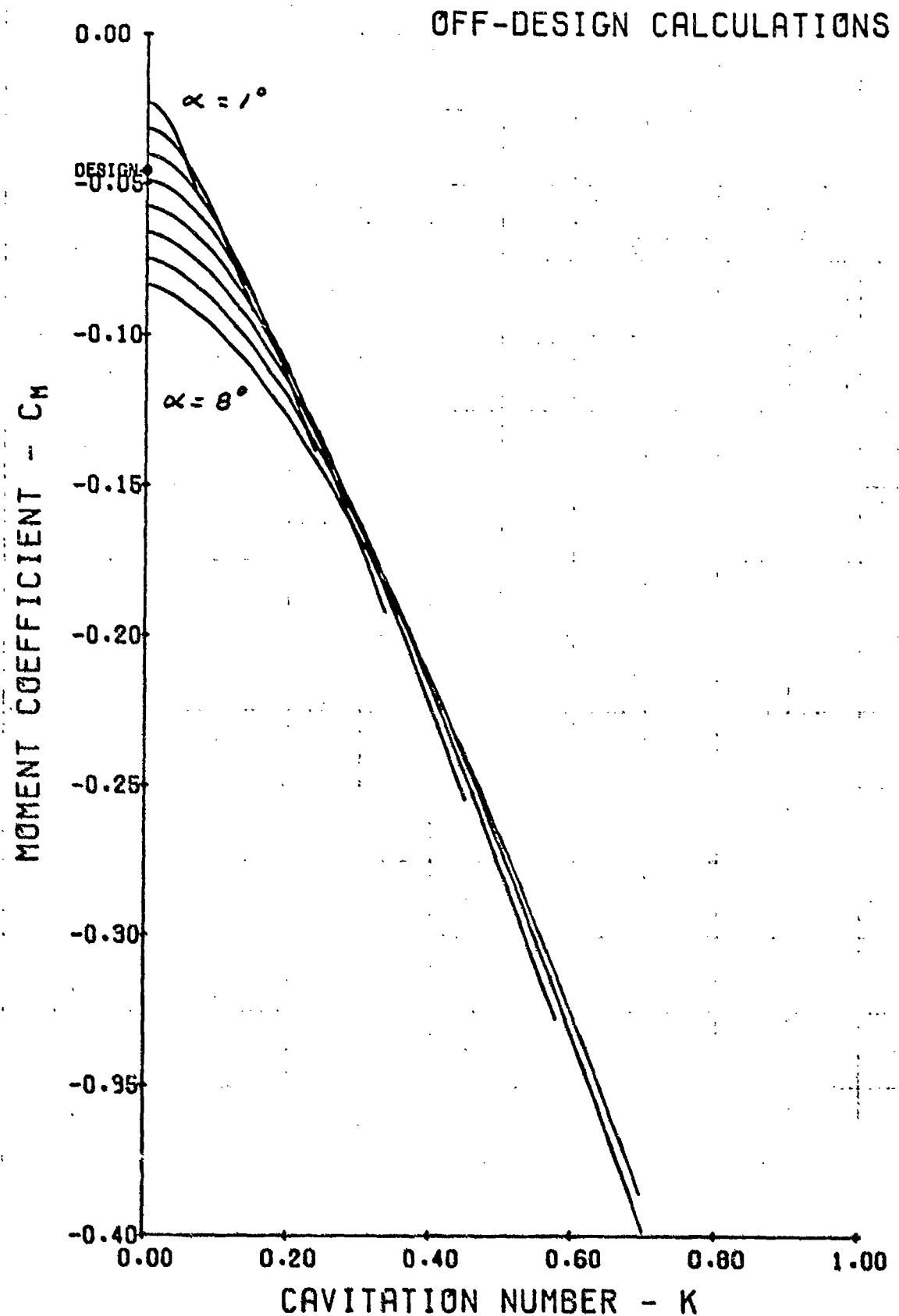
FIGURE-48 MOMENT COEFFICIENT VERSUS CAVITATION NUMBER.
SECOND DESIGN PROCEDURE.

APPENDIX A

Tables of Performance Data - First Design Procedure

Symbols in the following tables are defined as follows:

CAY $\equiv$ Cavitation number, K. See Equation (1) of text.

LAMDA $\equiv$ Double ellipse pressure distribution parameter defined in Figure 2 of text.

CL $\equiv$ Section lift coefficient. See Equation (3) of text.

TEE $\equiv$ Cavity thickness parameter, T, illustrated in Figure 1 of text.

SS $\equiv$ Location of peak pressure, measured from nose of profile. See Figure 1 of text.

LOD $\equiv$ Lift-to-Drag ratio of profile.

ECAP, B, DINT, CO: These are characteristic parameters appearing in the calculations which are described in detail in Ref. 2.

CM $\equiv$ Pitching moment coefficient. See Equation (5) of text.

CD $\equiv$ Drag coefficient. See Equation (4) of text.

ALPHA $\equiv$ Angle of attack in degrees. See Figure 1 of text.

$\bar{x}$ $\equiv$ Center of pressure location, fraction of chord.

FIRST FOIL DESIGN METHOD

DOUBLE ELLIPSE PRESSURE DISTRIBUTION

CAY= 0.000   LAMDA=0.05

CL	TEE	SS	LOD	ECAP	B	CM	DINT	CD	CO	ALPHA	XBAR
0.079	0.099	0.099	16.59984	0.00000	0.00000	-0.01355	0.00000	0.00481	0.06201	3.55311	0.16949
0.079	0.099	0.200	15.92212	0.00000	0.00000	-0.01829	0.00000	0.00502	0.05886	3.37276	0.22665
0.079	0.099	0.300	15.08738	0.00000	0.00000	-0.02524	0.00000	0.00530	0.05592	3.20407	0.31558
0.079	0.099	0.400	14.24224	0.00000	0.00000	-0.03250	0.00000	0.00561	0.05314	3.04498	0.40634
0.079	0.099	0.500	13.19079	0.00000	0.00000	-0.04001	0.00000	0.00606	0.04998	2.86416	0.50012
0.079	0.099	0.600	12.39987	0.00000	0.00000	-0.04745	0.00000	0.00645	0.04679	2.68142	0.59322
0.079	0.099	0.700	11.62884	0.00000	0.00000	-0.05459	0.00000	0.00687	0.04404	2.52353	0.68243
0.079	0.099	0.800	10.77899	0.00000	0.00000	-0.06134	0.00000	0.00742	0.04110	2.35510	0.76682
0.079	0.099	0.900	9.85475	0.00000	0.00000	-0.06583	0.00000	0.00811	0.03772	2.16152	0.82294
0.099	0.099	0.099	19.77921	0.00000	0.00000	-0.01694	0.00000	0.00505	0.06501	3.72534	0.16944
0.099	0.099	0.200	18.79941	0.00000	0.00000	-0.02286	0.00000	0.00531	0.06108	3.49991	0.22560
0.099	0.099	0.300	17.61288	0.00000	0.00000	-0.03155	0.00000	0.00567	0.05740	3.28905	0.31553
0.099	0.099	0.400	16.43288	0.00000	0.00000	-0.04062	0.00000	0.00608	0.05393	3.09019	0.40629
0.099	0.099	0.500	14.99047	0.00000	0.00000	-0.05000	0.00000	0.00667	0.04998	2.86416	0.50007
0.099	0.099	0.600	13.72544	0.00000	0.00000	-0.05931	0.00000	0.00711	0.04600	2.63573	0.59217
0.099	0.099	0.700	12.91105	0.00000	0.00000	-0.06823	0.00000	0.00774	0.04255	2.43837	0.68438
0.099	0.099	0.800	11.91038	0.00000	0.00000	-0.07667	0.00000	0.00846	0.03888	2.22784	0.76677
0.099	0.099	0.900	10.63827	0.00000	0.00000	-0.08228	0.00000	0.00940	0.03465	1.98586	0.82289
0.119	0.099	0.099	22.84796	0.00000	0.00000	-0.02032	0.00000	0.00529	0.06802	3.89758	0.16940
0.119	0.099	0.200	21.34253	0.00000	0.00000	-0.02742	0.00000	0.00562	0.06330	3.62706	0.22957
0.119	0.099	0.300	19.78279	0.00000	0.00000	-0.03786	0.00000	0.00606	0.05888	3.37403	0.31550
0.119	0.099	0.400	18.25401	0.00000	0.00000	-0.04875	0.00000	0.00657	0.05472	3.13540	0.40626
0.119	0.099	0.500	16.42519	0.00000	0.00000	-0.06000	0.00000	0.00730	0.04998	2.86416	0.50004
0.119	0.099	0.600	15.10129	0.00000	0.00000	-0.07117	0.00000	0.00794	0.04520	2.59005	0.59213
0.119	0.099	0.700	13.95227	0.00000	0.00000	-0.08188	0.00000	0.00866	0.04107	2.35321	0.68425
0.119	0.099	0.800	12.52444	0.00000	0.00000	-0.09200	0.00000	0.00958	0.03656	2.10058	0.76674
0.119	0.099	0.900	11.13576	0.00000	0.00000	-0.09874	0.00000	0.01077	0.03159	1.81020	0.82285
0.150	0.099	0.099	26.44214	0.00000	0.00000	-0.02540	0.00000	0.00567	0.07253	4.15594	0.16937
0.150	0.099	0.200	24.61748	0.00000	0.00000	-0.03428	0.00000	0.00609	0.06663	3.81779	0.22854
0.150	0.099	0.300	22.49111	0.00000	0.00000	-0.04732	0.00000	0.00667	0.06111	3.50150	0.31546
0.150	0.099	0.400	20.43358	0.00000	0.00000	-0.06093	0.00000	0.00734	0.05590	3.20320	0.40622
0.150	0.099	0.500	18.04541	0.00000	0.00000	-0.07500	0.00000	0.00831	0.04998	2.86416	0.50001
0.150	0.099	0.600	16.35670	0.00000	0.00000	-0.08896	0.00000	0.00916	0.04400	2.52152	0.59510
0.150	0.099	0.700	14.90108	0.00000	0.00000	-0.10234	0.00000	0.01013	0.03884	2.22548	0.68231
0.150	0.099	0.800	13.17926	0.00000	0.00000	-0.11500	0.00000	0.01138	0.03333	1.90968	0.76670
0.150	0.099	0.900	11.52395	0.00000	0.00000	-0.12342	0.00000	0.01301	0.02699	1.54670	0.82282

FIRST FOIL DESIGN METHOD

DOUBLE ELLIPSE PRESSURE DISTRIBUTION

CAY= 0.000   LAMDA=0.05

CL	TEE	SS	LOD	ECAP	B	CM	DINT	CD	CO	ALPHA	XBAR
0.079	0.150	0.100	7.85068	0.00000	0.00000	-0.01355	0.00000	0.01015	0.08701	4.98550	0.16949
0.079	0.150	0.200	7.65684	0.00000	0.00000	-0.01829	0.00000	0.01044	0.08386	4.90516	0.22865
0.079	0.150	0.300	7.37522	0.00000	0.00000	-0.02524	0.00000	0.01084	0.08092	4.63647	0.31558
0.079	0.150	0.400	7.02269	0.00000	0.00000	-0.03250	0.00000	0.01129	0.07814	4.47738	0.40634
0.079	0.150	0.500	6.70758	0.00000	0.00000	-0.04001	0.00000	0.01192	0.07498	4.29655	0.50012
0.079	0.150	0.600	6.41700	0.00000	0.00000	-0.04745	0.00000	0.01246	0.07179	4.11381	0.59322
0.079	0.150	0.700	6.12612	0.00000	0.00000	-0.05459	0.00000	0.01305	0.06904	3.95592	0.68243
0.079	0.150	0.800	5.79515	0.00000	0.00000	-0.06134	0.00000	0.01380	0.06610	3.78749	0.76682
0.079	0.150	0.900	5.42526	0.00000	0.00000	-0.06593	0.00000	0.01474	0.06272	3.59391	0.82294
0.099	0.150	0.100	9.52951	0.00000	0.00000	-0.01694	0.00000	0.01049	0.09001	5.15774	0.16944
0.099	0.150	0.200	9.19837	0.00000	0.00000	-0.02285	0.00000	0.01087	0.08608	4.93231	0.22860
0.099	0.150	0.300	8.78637	0.00000	0.00000	-0.03195	0.00000	0.01138	0.08240	4.72145	0.31553
0.099	0.150	0.400	8.36357	0.00000	0.00000	-0.04062	0.00000	0.01195	0.07893	4.52258	0.40629
0.099	0.150	0.500	7.83028	0.00000	0.00000	-0.05000	0.00000	0.01277	0.07498	4.29655	0.50007
0.099	0.150	0.600	7.42328	0.00000	0.00000	-0.05931	0.00000	0.01347	0.07100	4.06813	0.59317
0.099	0.150	0.700	7.02144	0.00000	0.00000	-0.06823	0.00000	0.01424	0.06755	3.87076	0.68238
0.099	0.150	0.800	6.57237	0.00000	0.00000	-0.07667	0.00000	0.01521	0.06380	3.66023	0.76677
0.099	0.150	0.900	6.07627	0.00000	0.00000	-0.08228	0.00000	0.01645	0.05965	3.41825	0.82289
0.119	0.150	0.100	11.86836	0.00000	0.00000	-0.02032	0.00000	0.01064	0.09302	5.32997	0.16940
0.119	0.150	0.200	10.61843	0.00000	0.00000	-0.02742	0.00000	0.01130	0.08830	5.05946	0.22857
0.119	0.150	0.300	10.06016	0.00000	0.00000	-0.03786	0.00000	0.01192	0.08388	4.80643	0.31550
0.119	0.150	0.400	9.49625	0.00000	0.00000	-0.04675	0.00000	0.01263	0.07972	4.56779	0.40626
0.119	0.150	0.500	8.79513	0.00000	0.00000	-0.05003	0.00000	0.01364	0.07498	4.29655	0.50004
0.119	0.150	0.600	8.26774	0.00000	0.00000	-0.07117	0.00000	0.01451	0.07020	4.02244	0.59313
0.119	0.150	0.700	7.75361	0.00000	0.00000	-0.08188	0.00000	0.01547	0.06607	3.78561	0.68235
0.119	0.150	0.800	7.18693	0.00000	0.00000	-0.09200	0.00000	0.01669	0.06166	3.53297	0.76674
0.119	0.150	0.900	6.57064	0.00000	0.00000	-0.09874	0.00000	0.01826	0.05659	3.24259	0.82285
0.150	0.150	0.100	13.18797	0.00000	0.00000	-0.02540	0.00000	0.01137	0.09753	5.58833	0.16937
0.150	0.150	0.200	12.53489	0.00000	0.00000	-0.03426	0.00000	0.01196	0.09163	5.25018	0.22854
0.150	0.150	0.300	11.74369	0.00000	0.00000	-0.04732	0.00000	0.01277	0.08611	4.93390	0.31546
0.150	0.150	0.400	10.95551	0.00000	0.00000	-0.06093	0.00000	0.01369	0.08090	4.63560	0.40622
0.150	0.150	0.500	9.99501	0.00000	0.00000	-0.07500	0.00000	0.01500	0.07498	4.29655	0.50001
0.150	0.150	0.600	9.29685	0.00000	0.00000	-0.08896	0.00000	0.01615	0.06900	3.95392	0.59310
0.150	0.150	0.700	8.60846	0.00000	0.00000	-0.10234	0.00000	0.01742	0.06384	3.65787	0.68231
0.150	0.150	0.800	7.87454	0.00000	0.00000	-0.11500	0.00000	0.01904	0.05833	3.34208	0.76670
0.150	0.150	0.900	7.09299	0.00000	0.00000	-0.12342	0.00000	0.02114	0.05199	2.97910	0.82282

FIRST FOIL DESIGN METHOD

DOUBLE ELLIPSE PRESSURE DISTRIBUTION

CAY= 0.000 LAMDA=0.05

CL	TEK	SS	LOG	ECAP	B	CM	DINT	CD	CO	ALPHA	XBAR
0.079	0.200	0.099	4.58532	0.00000	0.00000	-0.01355	0.00000	0.01744	0.11201	6.41789	0.16949
0.079	0.200	0.200	4.08547	0.00000	0.00000	-0.01829	0.00000	0.01763	0.10886	6.23795	0.22365
0.079	0.200	0.300	4.35537	0.00000	0.00000	-0.02524	0.00000	0.01835	0.10592	6.06886	0.31553
0.079	0.200	0.400	4.22446	0.00000	0.00000	-0.03250	0.00000	0.01893	0.10314	5.92977	0.40634
0.079	0.200	0.500	4.05017	0.00000	0.00000	-0.04001	0.00000	0.01975	0.09998	5.72894	0.50012
0.079	0.200	0.600	3.91202	0.00000	0.00000	-0.04745	0.00000	0.02044	0.09679	5.54620	0.59322
0.079	0.200	0.700	3.77338	0.00000	0.00000	-0.05459	0.00000	0.02120	0.09404	5.38831	0.68243
0.079	0.200	0.800	3.61235	0.00000	0.00000	-0.06134	0.00000	0.02214	0.09110	5.21989	0.76682
0.079	0.200	0.900	3.42800	0.00000	0.00000	-0.06583	0.00000	0.02333	0.08772	5.02630	0.82494
0.099	0.200	0.099	5.58819	0.00000	0.00000	-0.01694	0.00000	0.01789	0.11501	6.59013	0.16944
0.099	0.200	0.200	5.43857	0.00000	0.00000	-0.02246	0.00000	0.01838	0.11107	6.36470	0.22360
0.099	0.200	0.300	5.24979	0.00000	0.00000	-0.03155	0.00000	0.01904	0.10740	6.15384	0.31553
0.099	0.200	0.400	5.05290	0.00000	0.00000	-0.04062	0.00000	0.01979	0.10393	5.93497	0.40629
0.099	0.200	0.500	4.79974	0.00000	0.00000	-0.05000	0.00000	0.02083	0.09996	5.72895	0.50007
0.099	0.200	0.600	4.60274	0.00000	0.00000	-0.05931	0.00000	0.02172	0.09500	5.50002	0.59317
0.099	0.200	0.700	4.40432	0.00000	0.00000	-0.06823	0.00000	0.02270	0.09255	5.30316	0.68238
0.099	0.200	0.800	4.17942	0.00000	0.00000	-0.07667	0.00000	0.02392	0.08888	5.09262	0.76677
0.099	0.200	0.900	3.92499	0.00000	0.00000	-0.08228	0.00000	0.02547	0.08465	4.85064	0.82289
0.119	0.200	0.099	6.34007	0.00000	0.00000	-0.02032	0.00000	0.01834	0.11802	6.76237	0.16940
0.119	0.200	0.200	6.13332	0.00000	0.00000	-0.02742	0.00000	0.01894	0.11330	6.49105	0.22857
0.119	0.200	0.300	6.07457	0.00000	0.00000	-0.03706	0.00000	0.01975	0.10888	6.23582	0.31550
0.119	0.200	0.400	5.80756	0.00000	0.00000	-0.04875	0.00000	0.02066	0.10472	6.00018	0.40426
0.119	0.200	0.500	5.45810	0.00000	0.00000	-0.06000	0.00000	0.02194	0.09996	5.72895	0.50004
0.119	0.200	0.600	5.20706	0.00000	0.00000	-0.07117	0.00000	0.02304	0.09520	5.45484	0.59313
0.119	0.200	0.700	4.94756	0.00000	0.00000	-0.08188	0.00000	0.02425	0.09107	5.21800	0.66235
0.119	0.200	0.800	4.65545	0.00000	0.00000	-0.09200	0.00000	0.02577	0.08666	4.95536	0.76674
0.119	0.200	0.900	4.33002	0.00000	0.00000	-0.09274	0.00000	0.02772	0.08159	4.67498	0.82285
0.150	0.200	0.099	7.87839	0.00000	0.00000	-0.02540	0.00000	0.01903	0.12253	7.02073	0.16937
0.150	0.200	0.200	7.57443	0.00000	0.00000	-0.03428	0.00000	0.01980	0.11663	6.69258	0.22654
0.150	0.200	0.300	7.19872	0.00000	0.00000	-0.04732	0.00000	0.02083	0.11111	6.36629	0.31546
0.150	0.200	0.400	6.81629	0.00000	0.00000	-0.05093	0.00000	0.02200	0.10590	6.06799	0.40522
0.150	0.200	0.500	6.33818	0.00000	0.00000	-0.07500	0.00000	0.02368	0.09998	5.72895	0.50001
0.150	0.200	0.600	5.97652	0.00000	0.00000	-0.08896	0.00000	0.02509	0.09400	5.38631	0.59310
0.150	0.200	0.700	5.62255	0.00000	0.00000	-0.10234	0.00000	0.02647	0.08884	5.09026	0.68231
0.150	0.200	0.800	5.23073	0.00000	0.00000	-0.11500	0.00000	0.02867	0.08333	4.77447	0.76670
0.150	0.200	0.900	4.80117	0.00000	0.00000	-0.12342	0.00000	0.03124	0.07699	4.41149	0.82282

FIRST FOIL DESIGN METHOD

DOUBLE ELLIPSE PRESSURE DISTRIBUTION

CAY= 0.050   LAMDA=0.05

CL	TEE	SS	LOD	ECAP	B	CM	DINT	CD	CO	ALPHA	XBAR
0.079	0.099	0.099	13.89169	0.00835	0.00339	-0.01355	-0.00071	0.00575	0.06215	3.52033	0.16949
0.079	0.099	0.200	13.52274	0.01208	0.00251	-0.01829	-0.00027	0.00591	0.05872	3.34857	0.22865
0.079	0.099	0.300	13.01216	0.01424	0.00199	-0.02524	-0.00003	0.00614	0.05567	3.18792	0.31558
0.079	0.099	0.400	12.44940	0.01571	0.00163	-0.03250	0.00011	0.00642	0.05288	3.03640	0.40534
0.079	0.099	0.500	11.69610	0.01679	0.00136	-0.04001	0.00019	0.00683	0.04979	2.86419	0.50012
0.079	0.099	0.600	11.12443	0.01834	0.00102	-0.04745	0.00033	0.00719	0.04662	2.69015	0.59322
0.079	0.099	0.700	10.53655	0.01903	0.00086	-0.05459	0.00037	0.00759	0.04395	2.53978	0.68243
0.079	0.099	0.800	9.85867	0.01946	0.00075	-0.06134	0.00037	0.00811	0.04114	2.37937	0.76682
0.079	0.099	0.900	9.07866	0.01985	0.00066	-0.06583	0.00036	0.00881	0.03794	2.19500	0.82294
0.099	0.099	0.099	16.81744	0.00477	0.00408	-0.01694	-0.00085	0.00594	0.06515	3.68436	0.16944
0.099	0.099	0.200	16.25612	0.00939	0.00300	-0.02286	-0.00033	0.00615	0.06089	3.46967	0.22860
0.099	0.099	0.300	15.49113	0.01209	0.00235	-0.03155	-0.00004	0.00645	0.05709	3.26885	0.31553
0.099	0.099	0.400	14.66172	0.01393	0.00191	-0.04062	0.00012	0.00682	0.05362	3.07946	0.40629
0.099	0.099	0.500	13.57535	0.01529	0.00157	-0.05000	0.00022	0.00736	0.04976	2.86419	0.50007
0.099	0.099	0.600	12.76503	0.01719	0.00117	-0.05931	0.00024	0.00783	0.04582	2.64664	0.59317
0.099	0.099	0.700	11.94848	0.01804	0.00098	-0.06823	0.00040	0.00836	0.04250	2.45867	0.68238
0.099	0.099	0.800	11.02801	0.01860	0.00085	-0.07667	0.00041	0.00906	0.03900	2.25817	0.76677
0.099	0.099	0.900	9.99798	0.01909	0.00073	-0.08228	0.00038	0.01000	0.03500	2.02771	0.82289
0.119	0.099	0.099	19.54137	0.00131	0.00471	-0.02032	-0.00098	0.00614	0.06815	3.84840	0.16940
0.119	0.099	0.200	18.75687	0.00682	0.00344	-0.02742	-0.00038	0.00639	0.06305	3.59077	0.22957
0.119	0.099	0.300	17.70329	0.01005	0.00258	-0.03786	-0.00005	0.00677	0.05851	3.34978	0.31550
0.119	0.099	0.400	16.58018	0.01226	0.00215	-0.04875	0.00013	0.00723	0.05436	3.12251	0.40626
0.119	0.099	0.500	15.14025	0.01390	0.00175	-0.06000	0.00024	0.00792	0.04974	2.86419	0.50004
0.119	0.099	0.600	14.03982	0.01613	0.00129	-0.07117	0.00039	0.00852	0.04503	2.60313	0.59313
0.119	0.099	0.700	13.03982	0.01715	0.00107	-0.08188	0.00043	0.00920	0.04106	2.37757	0.68235
0.119	0.099	0.800	11.88680	0.01782	0.00092	-0.09200	0.00043	0.01009	0.03686	2.13697	0.76674
0.119	0.099	0.900	10.62879	0.01842	0.00079	-0.09874	0.00040	0.01129	0.03206	1.86041	0.82285
0.150	0.099	0.099	23.48053	0.00000	0.00557	-0.02540	-0.00115	0.00858	0.07261	4.09445	0.16937
0.150	0.099	0.200	22.10333	0.00317	0.00403	-0.03428	-0.00044	0.00678	0.06628	3.77241	0.22854
0.150	0.099	0.300	20.56989	0.00719	0.00309	-0.04732	-0.00006	0.00729	0.06064	3.47118	0.31546
0.150	0.099	0.400	18.97626	0.00993	0.00245	-0.06093	0.00015	0.00790	0.05547	3.18709	0.40622
0.150	0.099	0.500	16.99438	0.01201	0.00196	-0.07500	0.00042	0.00882	0.04972	2.86419	0.50001
0.150	0.099	0.600	15.57520	0.01471	0.00143	-0.08896	0.00042	0.00963	0.04386	2.53787	0.59510
0.150	0.099	0.700	14.20945	0.01596	0.00118	-0.10234	0.00045	0.01055	0.03891	2.25592	0.68231
0.150	0.099	0.800	12.74163	0.01679	0.00099	-0.11500	0.00044	0.01177	0.03367	1.95516	0.76670
0.150	0.099	0.900	11.19120	0.01755	0.00084	-0.12342	0.00041	0.01340	0.02768	1.60947	0.82282

FIRST FOIL DESIGN METHOD

DOUBLE ELLIPSE PRESSURE DISTRIBUTION

CAY= 0.050   LAMDA=0.05

CL	TEE	SS	LOD	ECAP	B	CM	DINT	CD	CO	ALPHA	XBAR
0.079	0.150	0.099	7.01946	0.01277	0.00169	-0.01355	-0.00034	0.01139	0.08678	4.95272	0.16949
0.079	0.150	0.200	6.86206	0.01539	0.00127	-0.01829	-0.00013	0.01165	0.08358	4.78097	0.22355
0.079	0.150	0.300	6.65591	0.01691	0.00102	-0.02524	-0.00002	0.01202	0.08066	4.62031	0.31550
0.079	0.150	0.400	6.42891	0.01793	0.00086	-0.03250	-0.00004	0.01244	0.07795	4.46891	0.40634
0.079	0.150	0.500	6.13139	0.01867	0.00073	-0.04001	0.00008	0.01304	0.07490	4.29658	0.50012
0.079	0.150	0.600	5.89979	0.01978	0.00056	-0.04745	0.00015	0.01355	0.07179	4.12254	0.59322
0.079	0.150	0.700	5.66197	0.02027	0.00048	-0.05459	0.00017	0.01412	0.06914	3.97217	0.68243
0.079	0.150	0.800	5.38595	0.02057	0.00043	-0.06134	0.00018	0.01485	0.06634	3.81175	0.76582
0.079	0.150	0.900	5.06505	0.02084	0.00039	-0.06583	0.00018	0.01579	0.06312	3.62740	0.82294
0.099	0.150	0.099	8.54510	0.01013	0.00205	-0.01694	-0.00041	0.01170	0.08972	5.11676	0.16944
0.099	0.150	0.200	8.30755	0.01340	0.00153	-0.02286	-0.00016	0.01203	0.08572	4.90206	0.22860
0.099	0.150	0.300	7.99630	0.01529	0.00123	-0.03155	-0.00003	0.01250	0.08208	4.70124	0.31553
0.099	0.150	0.400	7.66433	0.01657	0.00102	-0.04052	-0.00005	0.01304	0.07869	4.51185	0.40629
0.099	0.150	0.500	7.23145	0.01751	0.00086	-0.05000	0.00010	0.01382	0.07488	4.29658	0.50007
0.099	0.150	0.600	6.89876	0.01888	0.00066	-0.05931	0.00018	0.01449	0.07101	4.07904	0.59517
0.099	0.150	0.700	6.56202	0.01948	0.00056	-0.06823	0.00020	0.01523	0.06770	3.89107	0.68239
0.099	0.150	0.800	6.17716	0.01986	0.00050	-0.07667	0.00021	0.01618	0.06420	3.69056	0.76677
0.099	0.150	0.900	5.73958	0.02021	0.00044	-0.08228	0.00020	0.01742	0.06018	3.46010	0.82289
0.119	0.150	0.099	7.98764	0.00757	0.00239	-0.02032	-0.00048	0.01201	0.09265	5.28079	0.16940
0.119	0.150	0.200	9.65744	0.01147	0.00178	-0.02742	-0.00019	0.01242	0.08786	5.02316	0.22657
0.119	0.150	0.300	9.22898	0.01374	0.00142	-0.03786	-0.00003	0.01304	0.08350	4.78218	0.31550
0.119	0.150	0.400	8.77733	0.01528	0.00117	-0.04875	-0.00005	0.01367	0.07943	4.55490	0.40626
0.119	0.150	0.500	8.19645	0.01642	0.00097	-0.06000	0.00011	0.01464	0.07487	4.29658	0.50004
0.119	0.150	0.600	7.75597	0.01803	0.00074	-0.07117	0.00020	0.01547	0.07023	4.03553	0.59313
0.119	0.150	0.700	7.31586	0.01875	0.00063	-0.08188	0.00022	0.01640	0.06627	3.80997	0.68255
0.119	0.150	0.800	6.82017	0.01922	0.00055	-0.09200	0.00022	0.01759	0.06206	3.56936	0.76674
0.119	0.150	0.900	6.26655	0.01964	0.00048	-0.09874	0.00022	0.01914	0.05724	3.29281	0.82285
0.150	0.150	0.099	12.00479	0.00386	0.00286	-0.02540	-0.00058	0.01249	0.09704	5.52685	0.16937
0.150	0.150	0.200	11.51575	0.00870	0.00212	-0.03428	-0.00023	0.01302	0.09107	5.20480	0.22854
0.150	0.150	0.300	10.89006	0.01153	0.00157	-0.04732	-0.00004	0.01377	0.08562	4.90358	0.31546
0.150	0.150	0.400	10.24161	0.01345	0.00136	-0.06093	-0.00006	0.01464	0.08055	4.61948	0.40622
0.150	0.150	0.500	9.42482	0.01489	0.00112	-0.07500	0.00012	0.01591	0.07486	4.29658	0.50001
0.150	0.150	0.600	8.81573	0.01686	0.00084	-0.08896	0.00022	0.01701	0.06906	3.97026	0.59310
0.150	0.150	0.700	8.22050	0.01776	0.00071	-0.10234	0.00024	0.01824	0.06412	3.66831	0.68231
0.150	0.150	0.800	7.56272	0.01834	0.00061	-0.11500	0.00024	0.01983	0.05887	3.38756	0.76670
0.150	0.150	0.900	6.84462	0.01888	0.00053	-0.12342	0.00023	0.02191	0.05285	3.04186	0.82282

FIRST FOIL DESIGN METHOD

DOUBLE ELLIPSE PRESSURE DISTRIBUTION

CAY= 0.050   LAMBA=0.05

CL	TEE	SS	LOD	ECAP	B	CM	DINT	CD	CO	ALPHA	XBAR
0.075	0.200	0.099	4.19499	0.01530	0.00100	-0.01355	-0.00020	0.01907	0.11164	6.38511	0.16949
0.079	0.200	0.200	4.11717	0.01732	0.00076	-0.01829	-0.00008	0.01943	0.10852	6.21336	0.22865
0.079	0.200	0.300	4.01525	0.01847	0.00062	-0.02524	-0.00001	0.01992	0.10565	6.05270	0.31558
0.079	0.200	0.400	3.90563	0.01925	0.00052	-0.03250	0.00002	0.02048	0.10297	5.90119	0.40634
0.079	0.200	0.500	3.75039	0.01951	0.00045	-0.04001	0.00004	0.02127	0.09993	5.72897	0.50012
0.079	0.200	0.600	3.64556	0.02067	0.00035	-0.04745	0.00009	0.02194	0.09606	5.55494	0.59322
0.079	0.200	0.700	3.52720	0.02104	0.00031	-0.05459	0.00010	0.02258	0.09422	5.40456	0.68243
0.079	0.200	0.800	3.38878	0.02126	0.00028	-0.06134	0.00011	0.02360	0.09141	5.24416	0.76682
0.079	0.200	0.900	3.22721	0.02146	0.00025	-0.06563	0.00011	0.02478	0.08619	5.05979	0.82294
0.099	0.200	0.099	5.13106	0.01322	0.00122	-0.01694	-0.00024	0.01948	0.11455	6.54915	0.16944
0.099	0.200	0.200	5.01324	0.01573	0.00092	-0.02286	-0.00010	0.01994	0.11065	6.33446	0.22860
0.099	0.200	0.300	4.86025	0.01718	0.00075	-0.03155	-0.00002	0.02057	0.10707	6.13364	0.31553
0.099	0.200	0.400	4.59717	0.01816	0.00063	-0.04062	0.00005	0.02128	0.10371	5.94424	0.40629
0.099	0.200	0.500	4.48354	0.01836	0.00054	-0.05000	0.00010	0.02230	0.09993	5.72897	0.50007
0.099	0.200	0.600	4.31646	0.01992	0.00042	-0.05931	0.00012	0.02316	0.09608	5.51143	0.59317
0.099	0.200	0.700	4.14617	0.02038	0.00036	-0.06823	0.00012	0.02411	0.09278	5.32346	0.68238
0.099	0.200	0.800	3.94939	0.02067	0.00032	-0.07667	0.00012	0.02532	0.08928	5.12295	0.75677
0.099	0.200	0.900	3.72320	0.02093	0.00029	-0.08228	0.00012	0.02685	0.08526	4.89249	0.82289
0.119	0.200	0.099	6.02592	0.01119	0.00143	-0.02032	-0.00029	0.01991	0.11745	6.71319	0.16940
0.119	0.200	0.200	5.86155	0.01420	0.00108	-0.02742	-0.00011	0.02047	0.11278	6.45555	0.22857
0.119	0.200	0.300	5.64976	0.01593	0.00087	-0.03786	-0.00002	0.02123	0.10848	6.21457	0.31550
0.119	0.200	0.400	5.42607	0.01710	0.00072	-0.04875	0.00003	0.02211	0.10446	5.98729	0.40626
0.119	0.200	0.500	5.13630	0.01796	0.00062	-0.06000	0.00006	0.02336	0.09992	5.72897	0.50004
0.119	0.200	0.600	4.91208	0.01922	0.00047	-0.07117	0.00012	0.02442	0.09531	5.46792	0.59313
0.119	0.200	0.700	4.68597	0.01977	0.00041	-0.08188	0.00013	0.02550	0.09135	5.24236	0.68235
0.119	0.200	0.800	4.42763	0.02012	0.00036	-0.09200	0.00014	0.02710	0.08715	5.00175	0.75574
0.119	0.200	0.900	4.13486	0.02044	0.00032	-0.09874	0.00014	0.02802	0.08232	4.72520	0.82265
0.150	0.200	0.099	7.29480	0.00923	0.00173	-0.02540	-0.00035	0.02056	0.12181	6.95924	0.16937
0.150	0.200	0.200	7.04994	0.01196	0.00130	-0.03428	-0.00014	0.02227	0.11598	6.63720	0.22854
0.150	0.200	0.300	6.73796	0.01413	0.00103	-0.04732	-0.00002	0.02226	0.11061	6.33597	0.31546
0.150	0.200	0.400	6.41274	0.01560	0.00086	-0.06093	0.00003	0.02339	0.10558	6.05188	0.40622
0.150	0.200	0.500	5.99829	0.01668	0.00072	-0.07500	0.00007	0.02500	0.09995	5.72897	0.50001
0.150	0.200	0.600	5.68238	0.01823	0.00055	-0.08896	0.00013	0.02639	0.09415	5.40265	0.59310
0.150	0.200	0.700	5.36852	0.01892	0.00047	-0.10234	0.00015	0.02794	0.08921	5.12071	0.68231
0.150	0.200	0.800	5.01598	0.01936	0.00041	-0.11500	0.00016	0.02990	0.08396	4.81995	0.76670
0.150	0.200	0.900	4.62400	0.01977	0.00036	-0.12342	0.00015	0.03243	0.07793	4.47425	0.82282

FIRST FOIL DESIGN METHOD

DOUBLE ELLIPSE PRESSURE DISTRIBUTION

CAY= 0.093   LAMDA=0.05

CL	TEE	SS	LOD	ECAP	B	CM	DINT	CD	CO	ALPHA	XBAR
0.079	0.099	0.099	9.65917	0.02253	0.00632	-0.01355	-0.00227	0.00828	0.06320	3.49053	0.16949
0.079	0.099	0.200	9.60036	0.02825	0.00713	-0.01829	-0.00088	0.00833	0.05894	3.32658	0.22865
0.079	0.099	0.300	9.46685	0.03157	0.00349	-0.02524	-0.00000	0.00845	0.05538	3.17323	0.31558
0.079	0.097	0.400	9.27442	0.03383	0.00428	-0.03250	0.00059	0.00862	0.05226	3.02860	0.40634
0.079	0.095	0.500	8.94992	0.03546	0.00352	-0.04001	0.00100	0.00893	0.04698	2.86421	0.50012
0.079	0.099	0.600	8.70437	0.03792	0.00243	-0.04745	0.00153	0.00919	0.04555	2.69809	0.59322
0.079	0.099	0.700	8.41027	0.03899	0.00193	-0.05459	0.00175	0.00951	0.04283	2.55455	0.68243
0.079	0.099	0.800	8.02366	0.03964	0.00163	-0.06134	0.00183	0.00997	0.04007	2.40144	0.76682
0.079	0.099	0.900	7.49815	0.04015	0.00145	-0.06583	0.00178	0.01066	0.03705	2.22545	0.82294
0.099	0.099	0.099	11.96190	0.01682	0.01196	-0.01694	-0.00276	0.00835	0.06641	3.64711	0.16944
0.099	0.099	0.200	11.85616	0.02395	0.00864	-0.02286	-0.00106	0.00843	0.06113	3.44217	0.22860
0.099	0.099	0.300	11.62906	0.02810	0.00662	-0.03155	-0.00001	0.00859	0.05674	3.25048	0.31553
0.099	0.099	0.400	11.30999	0.03192	0.00523	-0.04062	-0.00068	0.00884	0.05289	3.06970	0.40629
0.099	0.099	0.500	10.79744	0.03298	0.00420	-0.05000	0.00114	0.00927	0.04384	2.86421	0.50007
0.099	0.099	0.600	10.39262	0.03600	0.00291	-0.05931	0.00172	0.00962	0.04463	2.65656	0.59317
0.099	0.099	0.700	9.93323	0.03733	0.00233	-0.06823	0.00193	0.01005	0.04129	2.47713	0.68238
0.099	0.099	0.800	9.34834	0.03815	0.00197	-0.07667	0.00199	0.01069	0.03789	2.28574	0.76677
0.099	0.099	0.900	8.59304	0.03681	0.00174	-0.08228	0.00189	0.01164	0.03415	2.06576	0.82289
0.119	0.099	0.099	14.20714	0.01124	0.01597	-0.02032	-0.00321	0.00844	0.06959	3.80369	0.16940
0.119	0.099	0.200	14.03659	0.01975	0.01004	-0.02742	-0.00122	0.00854	0.06332	3.55777	0.22857
0.119	0.099	0.300	13.68631	0.02473	0.00765	-0.03786	-0.00001	0.00876	0.05809	3.32774	0.31546
0.119	0.099	0.400	13.20610	0.02811	0.00603	-0.04875	0.00076	0.00908	0.05353	3.11079	0.40626
0.119	0.099	0.500	12.64263	0.03060	0.00480	-0.06000	0.00125	0.00964	0.04873	2.86421	0.50004
0.119	0.099	0.600	11.87001	0.03418	0.00334	-0.07117	0.00187	0.01010	0.04376	2.61502	0.59313
0.119	0.099	0.700	11.22174	0.03576	0.00267	-0.08188	0.00206	0.01069	0.03981	2.39972	0.68235
0.119	0.099	0.800	10.42131	0.03675	0.00226	-0.09200	0.00209	0.01151	0.03578	2.17005	0.76674
0.119	0.099	0.900	9.42734	0.03757	0.00199	-0.09874	0.00195	0.01272	0.03131	1.90607	0.82285
0.150	0.099	0.099	17.45566	0.00308	0.01677	-0.02540	-0.00383	0.00859	0.07432	4.03856	0.16937
0.150	0.099	0.200	17.15092	0.01366	0.01198	-0.03428	-0.00144	0.00874	0.06657	3.73115	0.22854
0.150	0.099	0.300	16.55952	0.01988	0.00906	-0.04732	-0.00002	0.00905	0.06013	3.44362	0.31546
0.150	0.099	0.400	15.77787	0.02411	0.00708	-0.06093	-0.00085	0.00950	0.05451	3.17244	0.40622
0.150	0.099	0.500	14.58744	0.02725	0.00559	-0.07500	0.00136	0.01028	0.04862	2.86422	0.50001
0.150	0.099	0.600	13.70954	0.03162	0.00309	-0.08896	0.00201	0.01094	0.04253	2.55273	0.59310
0.150	0.099	0.700	12.75413	0.03358	0.00312	-0.10234	0.00218	0.01176	0.03767	2.28350	0.68231
0.150	0.099	0.800	11.62418	0.03483	0.00263	-0.11500	0.00215	0.01290	0.03268	1.99651	0.76670
0.150	0.099	0.900	10.29655	0.03589	0.00228	-0.12342	0.00196	0.01456	0.02712	1.66653	0.82232

FIRST FOIL DESIGN METHOD

DOUBLE ELLIPSE PRESSURE DISTRIBUTION

CAY= 0.099   LAMDA=0.05

CL	TEE	SS	LOD	ECAP	B	CM	DINT	CD	CO	ALPHA	XBAR
0.079	0.150	0.099	5.61164	0.02776	0.00534	-0.01355	-0.00115	0.01425	0.08707	4.92293	0.16949
0.079	0.150	0.200	5.54318	0.03215	0.00397	-0.01829	-0.00045	0.01443	0.08351	4.75898	0.22865
0.079	0.150	0.300	5.43827	0.03468	0.00315	-0.02524	-0.00003	0.01471	0.08041	4.60562	0.31558
0.079	0.150	0.400	5.31331	0.03638	0.00260	-0.03250	-0.00023	0.01505	0.07762	4.46099	0.40634
0.079	0.150	0.500	5.13176	0.03761	0.00218	-0.04001	0.00042	0.01558	0.07456	4.29661	0.50012
0.079	0.150	0.600	4.95158	0.03949	0.00162	-0.04745	0.00068	0.01602	0.07140	4.13048	0.59322
0.079	0.150	0.700	4.83727	0.04030	0.00136	-0.05459	0.00078	0.01653	0.06880	3.98594	0.68243
0.079	0.150	0.800	4.64701	0.04079	0.00120	-0.06134	0.00082	0.01721	0.06608	3.83383	0.76682
0.079	0.150	0.900	4.40697	0.04121	0.00108	-0.06583	0.00082	0.01815	0.06301	3.65784	0.82294
0.099	0.150	0.099	6.90897	0.02330	0.00652	-0.01694	-0.00140	0.01447	0.09005	5.07950	0.16944
0.099	0.150	0.200	6.20103	0.02876	0.00483	-0.02286	-0.00054	0.01470	0.08562	4.87457	0.22860
0.099	0.150	0.300	6.63714	0.03192	0.00382	-0.03155	-0.00004	0.01506	0.08177	4.68288	0.31553
0.099	0.150	0.400	6.44375	0.03406	0.00313	-0.04062	0.00027	0.01551	0.07829	4.50209	0.40629
0.099	0.150	0.500	6.16668	0.03561	0.00261	-0.05000	0.00048	0.01621	0.07450	4.29661	0.50007
0.099	0.150	0.600	5.95444	0.03793	0.00193	-0.05931	0.00078	0.01679	0.07057	4.08895	0.59317
0.099	0.150	0.700	5.72408	0.03894	0.00162	-0.06823	0.00089	0.01747	0.06733	3.90953	0.68238
0.099	0.150	0.800	5.44475	0.03956	0.00142	-0.07667	0.00093	0.01836	0.06395	3.71813	0.76677
0.099	0.150	0.900	5.10135	0.04009	0.00126	-0.08228	0.00091	0.01960	0.06014	3.49815	0.82289
0.119	0.150	0.099	8.16343	0.01893	0.00765	-0.02032	-0.00164	0.01469	0.09303	5.23608	0.16940
0.119	0.150	0.200	8.00709	0.02546	0.00564	-0.02742	-0.00063	0.01498	0.08773	4.99016	0.22857
0.119	0.150	0.300	7.77189	0.02925	0.00444	-0.03786	-0.00005	0.01544	0.08313	4.76013	0.31550
0.119	0.150	0.400	7.49718	0.03182	0.00352	-0.04875	0.00031	0.01600	0.07897	4.54319	0.40626
0.119	0.150	0.500	7.10950	0.03369	0.00299	-0.06000	0.00054	0.01687	0.07444	4.29661	0.50004
0.119	0.150	0.600	6.81446	0.03644	0.00221	-0.07117	0.00087	0.01760	0.06976	4.04742	0.59513
0.119	0.150	0.700	6.49918	0.03765	0.00185	-0.08188	0.00098	0.01846	0.06589	3.83211	0.68235
0.119	0.150	0.800	6.12340	0.03841	0.00161	-0.09200	0.00101	0.01959	0.06186	3.60244	0.76674
0.119	0.150	0.900	5.67179	0.03906	0.00142	-0.09874	0.00097	0.02115	0.05728	3.33846	0.82285
0.150	0.150	0.099	9.95495	0.01253	0.00924	-0.02540	-0.00198	0.01505	0.09746	5.47096	0.16937
0.150	0.150	0.200	9.71953	0.02065	0.00678	-0.03428	-0.00076	0.01543	0.09088	5.16355	0.22854
0.150	0.150	0.300	9.35582	0.02539	0.00529	-0.04762	-0.00006	0.01603	0.08516	4.87601	0.31546
0.150	0.150	0.400	8.93788	0.02860	0.00428	-0.06093	0.00035	0.01678	0.08000	4.60483	0.40622
0.150	0.150	0.500	8.36080	0.03097	0.00351	-0.07500	0.00061	0.01794	0.07437	4.29661	0.50001
0.150	0.150	0.600	7.92748	0.03434	0.00257	-0.08896	0.00097	0.01892	0.06857	3.98512	0.59310
0.150	0.150	0.700	7.47460	0.03585	0.00214	-0.10234	0.00108	0.02006	0.06374	3.71599	0.68231
0.150	0.150	0.800	6.94732	0.03681	0.00185	-0.11500	0.00109	0.02159	0.05874	3.42890	0.76670
0.150	0.150	0.900	6.33413	0.03764	0.00162	-0.12342	0.00104	0.02368	0.05304	3.09892	0.82282

FIRST FOIL DESIGN METHOD

DOUBLE ELLIPSE PRESSURE DISTRIBUTION

CAY= 0.099   LAMDA=0.05

CL	TEE	SS	LOD	ECAP	B	CM	DINT	CD	CO	ALPHA	XBAR
0.079	0.200	0.099	3.58091	0.03137	0.00331	-0.01355	-0.00069	0.02234	0.11161	6.35532	0.16949
0.079	0.200	0.200	3.53493	0.03487	0.00249	-0.01829	-0.00027	0.02263	0.10833	6.19137	0.22865
0.079	0.200	0.300	3.47002	0.03687	0.00201	-0.02524	-0.00003	0.02305	0.10541	6.03801	0.31558
0.079	0.200	0.400	3.39631	0.03822	0.00168	-0.03250	0.00011	0.02355	0.10273	5.89339	0.40634
0.079	0.200	0.500	3.29357	0.03919	0.00144	-0.04001	0.00022	0.02428	0.09976	5.72900	0.50012
0.079	0.200	0.600	3.21287	0.04069	0.00110	-0.04745	0.00037	0.02489	0.09671	5.56288	0.59322
0.079	0.200	0.700	3.12631	0.04133	0.00095	-0.05459	0.00043	0.02558	0.09414	5.41934	0.68243
0.079	0.200	0.800	3.02152	0.04171	0.00085	-0.06134	0.00046	0.02647	0.09144	5.26622	0.76582
0.079	0.200	0.900	2.89271	0.04205	0.00077	-0.06583	0.00046	0.02765	0.08837	5.09023	0.82294
0.099	0.200	0.099	4.40773	0.02774	0.00405	-0.01694	-0.00084	0.02268	0.11450	6.51190	0.16944
0.099	0.200	0.200	4.33665	0.03210	0.00304	-0.02286	-0.00033	0.02305	0.11041	6.30696	0.22860
0.099	0.200	0.300	4.23694	0.03461	0.00245	-0.03155	-0.00004	0.02360	0.10677	6.11527	0.31553
0.099	0.200	0.400	4.12459	0.03630	0.00204	-0.04062	0.00014	0.02424	0.10343	5.93448	0.40629
0.099	0.200	0.500	3.95962	0.03752	0.00173	-0.05000	0.00026	0.02519	0.09972	5.72900	0.50007
0.099	0.200	0.600	3.84874	0.03938	0.00132	-0.05931	0.00044	0.02598	0.09592	5.52134	0.59313
0.099	0.200	0.700	3.72051	0.04018	0.00113	-0.06823	0.00050	0.02687	0.09272	5.34192	0.68238
0.099	0.200	0.800	3.56716	0.04067	0.00101	-0.07667	0.00053	0.02803	0.08935	5.15053	0.76677
0.099	0.200	0.900	3.38184	0.04110	0.00091	-0.08228	0.00053	0.02956	0.08551	4.93054	0.82289
0.119	0.200	0.099	5.20805	0.02418	0.00477	-0.02032	-0.00099	0.02304	0.11738	6.66848	0.16940
0.119	0.200	0.200	5.10692	0.02940	0.00357	-0.02742	-0.00039	0.02349	0.11249	6.42255	0.22857
0.119	0.200	0.300	4.96589	0.03241	0.00286	-0.03785	-0.00005	0.02416	0.10813	6.19252	0.31550
0.119	0.200	0.400	4.80824	0.03444	0.00237	-0.04875	0.00016	0.02495	0.10413	5.97558	0.40626
0.119	0.200	0.500	4.59301	0.03592	0.00200	-0.06000	0.00029	0.02612	0.09969	5.72900	0.50004
0.119	0.200	0.600	4.42654	0.03812	0.00152	-0.07117	0.00050	0.02710	0.09513	5.47981	0.59313
0.119	0.200	0.700	4.25169	0.03909	0.00129	-0.08188	0.00057	0.02822	0.09131	5.26451	0.68235
0.119	0.200	0.800	4.04511	0.03968	0.00115	-0.09200	0.00059	0.02966	0.08727	5.03483	0.76574
0.119	0.200	0.900	3.79958	0.04020	0.00103	-0.09874	0.00058	0.03158	0.08268	4.77085	0.82285
0.150	0.200	0.099	6.36003	0.01896	0.00580	-0.02540	-0.00121	0.02358	0.12169	6.90335	0.16937
0.150	0.200	0.200	6.20496	0.02545	0.00431	-0.03428	-0.00047	0.02417	0.11559	6.59594	0.22854
0.150	0.200	0.300	5.99085	0.02921	0.00343	-0.04732	-0.00006	0.02503	0.11016	6.30841	0.31546
0.150	0.200	0.400	5.75442	0.03176	0.00282	-0.06093	0.00018	0.02606	0.10518	6.03723	0.40622
0.150	0.200	0.500	5.43663	0.03352	0.00236	-0.07500	0.00034	0.02759	0.09964	5.72900	0.50001
0.150	0.200	0.500	5.19372	0.03634	0.00178	-0.08896	0.00057	0.02888	0.09397	5.41751	0.59310
0.150	0.200	0.700	4.94257	0.03754	0.00151	-0.10234	0.00064	0.03034	0.08920	5.14838	0.68231
0.150	0.200	0.800	4.65097	0.03830	0.00133	-0.11500	0.00066	0.03225	0.08417	4.86129	0.76670
0.150	0.200	0.900	4.31233	0.03897	0.00117	-0.12342	0.00064	0.03478	0.07843	4.53132	0.82282

FIRST FOIL DESIGN METHOD

DOUBLE ELLIPSE PRESSURE DISTRIBUTION

CAY= 0.150   LAMDA=0.05

CL	TEE	SS	LOD	ECAP	B	CM	DINT	CD	CO	ALPHA	XBAR
0.079	0.099	0.099	6.41655	0.04021	0.01595	-0.01355	-0.00413	0.01246	0.06458	3.46333	0.16949
0.079	0.099	0.200	6.45108	0.04679	0.01133	-0.01829	-0.00169	0.01240	0.05939	3.30650	0.22865
0.079	0.099	0.300	6.46448	0.05062	0.00844	-0.02524	-0.00001	0.01237	0.05516	3.15982	0.31558
0.079	0.099	0.400	6.44961	0.05323	0.00641	-0.03250	0.00124	0.01240	0.05148	3.02148	0.40634
0.079	0.099	0.500	6.37574	0.05512	0.00484	-0.04001	0.00228	0.01254	0.04770	2.86424	0.50012
0.079	0.099	0.600	6.32432	0.05802	0.00283	-0.04745	0.00345	0.01264	0.04376	2.70534	0.59322
0.079	0.099	0.700	6.23378	0.05930	0.00188	-0.05459	0.00407	0.01283	0.04074	2.56804	0.68243
0.079	0.099	0.800	6.07785	0.06005	0.00131	-0.06134	0.00446	0.01316	0.03779	2.42158	0.76682
0.079	0.099	0.900	5.78939	0.06058	0.00111	-0.06583	0.00448	0.01381	0.03484	2.25325	0.82294
0.099	0.099	0.099	8.05084	0.03358	0.01957	-0.01694	-0.00504	0.01242	0.06810	3.61310	0.16944
0.099	0.099	0.200	8.09775	0.04177	0.01386	-0.02286	-0.00204	0.01234	0.06168	3.41707	0.22860
0.099	0.099	0.300	8.10652	0.04656	0.01030	-0.03155	-0.00001	0.01233	0.05645	3.23371	0.31553
0.099	0.099	0.400	8.06627	0.04981	0.00781	-0.04062	0.00148	0.01239	0.05193	3.06079	0.40629
0.099	0.099	0.500	7.92194	0.05218	0.00590	-0.05000	0.00266	0.01262	0.04732	2.86424	0.50007
0.099	0.099	0.600	7.81469	0.05577	0.00353	-0.05931	0.00398	0.01279	0.04254	2.66561	0.59317
0.099	0.099	0.700	7.64537	0.05734	0.00243	-0.06823	0.00462	0.01307	0.03890	2.49399	0.68238
0.099	0.099	0.800	7.37198	0.05823	0.00180	-0.07667	0.00495	0.01356	0.03537	2.31092	0.76677
0.099	0.099	0.900	6.90480	0.05895	0.00158	-0.08228	0.00484	0.01448	0.03181	2.10050.	0.82289
0.119	0.099	0.099	9.69052	0.02701	0.02304	-0.02032	-0.00591	0.01238	0.07158	3.76287	0.16940
0.119	0.099	0.200	9.74737	0.03682	0.01627	-0.02742	-0.00237	0.01231	0.06394	3.52764	0.22857
0.119	0.099	0.300	9.74218	0.04256	0.01205	-0.03786	-0.00001	0.01231	0.05774	3.30761	0.31550
0.119	0.099	0.400	9.65895	0.04647	0.00913	-0.04875	0.00169	0.01242	0.05240	3.10010	0.40626
0.119	0.099	0.500	9.41264	0.04932	0.00691	-0.06000	0.00298	0.01274	0.04700	2.86424	0.50004
0.119	0.099	0.600	9.22511	0.05357	0.00421	-0.07117	0.00440	0.01300	0.04142	2.62588	0.59313
0.119	0.099	0.700	8.94724	0.05544	0.00299	-0.08188	0.00503	0.01341	0.03720	2.41994	0.68235
0.119	0.099	0.800	8.51952	0.05656	0.00230	-0.09200	0.00528	0.01408	0.03312	2.20025	0.76674
0.119	0.099	0.900	7.86153	0.05738	0.00204	-0.09874	0.00505	0.01526	0.02894	1.94775	0.82285
0.150	0.099	0.099	12.14644	0.01732	0.02797	-0.02540	-0.00712	0.01234	0.07672	3.98752	0.16937
0.150	0.099	0.200	12.21040	0.02953	0.01967	-0.03428	-0.00282	0.01228	0.06729	3.69348	0.22854
0.150	0.099	0.300	12.15982	0.03670	0.01450	-0.04732	-0.00000	0.01233	0.05966	3.41845	0.31546
0.150	0.099	0.400	11.97350	0.04158	0.01095	-0.06093	0.00196	0.01252	0.05316	3.15906	0.40622
0.150	0.099	0.500	11.50968	0.04516	0.00829	-0.07500	0.00334	0.01303	0.04664	2.86424	0.50001
0.150	0.099	0.500	11.15110	0.05039	0.00517	-0.08896	0.00486	0.01345	0.03992	2.56630	0.59310
0.150	0.099	0.700	10.66232	0.05270	0.00378	-0.10234	0.00543	0.01406	0.03486	2.30886	0.68231
0.150	0.099	0.800	9.97368	0.05409	0.00302	-0.11500	0.00555	0.01503	0.02995	2.03426	0.76670
0.150	0.099	0.900	8.93419	0.05515	0.00269	-0.12342	0.00514	0.01669	0.02484	1.71863	0.82282

FIRST FOIL DESIGN METHOD

DOUBLE ELLIPSE PRESSURE DISTRIBUTION

CAY= 0.150   LAMDA=0.05

CL	TEE	SS	LOD	ECAP	B	CM	DINT	CD	CO	ALPHA	XBAR
0.079	0.150	0.099	4.27040	0.04462	0.00925	-0.01355	-0.00215	0.01873	0.08759	4.89572	0.16949
0.079	0.150	0.200	4.25472	0.05002	0.00679	-0.01829	-0.00084	0.01880	0.08355	4.73890	0.22865
0.079	0.150	0.300	4.21896	0.05314	0.00529	-0.02524	-0.00000	0.01896	0.08015	4.59221	0.31558
0.079	0.150	0.400	4.16731	0.05525	0.00424	-0.03250	-0.00058	0.01919	0.07715	4.45387	0.40634
0.079	0.150	0.500	4.07877	0.05677	0.00346	-0.04001	0.00102	0.01961	0.07396	4.29663	0.50012
0.079	0.150	0.600	4.01219	0.05717	0.00239	-0.04745	0.00158	0.01993	0.07062	4.13773	0.59322
0.079	0.150	0.700	3.93041	0.06013	0.00190	-0.05459	0.00185	0.02035	0.06796	4.00043	0.62243
0.079	0.150	0.800	3.81913	0.06074	0.00160	-0.06134	0.00200	0.02094	0.06525	3.85398	0.76682
0.079	0.150	0.900	3.65836	0.06120	0.00143	-0.06583	0.00201	0.02186	0.06230	3.68564	0.82294
0.099	0.150	0.099	5.30769	0.03909	0.01141	-0.01694	-0.00263	0.01884	0.09069	5.04549	0.16944
0.099	0.150	0.200	5.28047	0.04582	0.00832	-0.02286	-0.00102	0.01893	0.08566	4.84946	0.22860
0.099	0.150	0.300	5.22084	0.04972	0.00645	-0.03155	-0.00000	0.01915	0.08144	4.66611	0.31553
0.099	0.150	0.400	5.13596	0.05236	0.00517	-0.04062	0.00069	0.01947	0.07772	4.49318	0.40529
0.099	0.150	0.500	4.99299	0.05426	0.00420	-0.05000	0.00119	0.02002	0.07379	4.29663	0.50007
0.099	0.150	0.600	4.88477	0.05717	0.00292	-0.05931	0.00185	0.02047	0.06967	4.09800	0.59317
0.099	0.150	0.700	4.75417	0.05843	0.00233	-0.05823	0.00213	0.02103	0.06639	3.92638	0.68238
0.099	0.150	0.800	4.58019	0.05919	0.00197	-0.07667	0.00227	0.02183	0.06305	3.74331	0.76677
0.099	0.150	0.900	4.33727	0.05978	0.00176	-0.08228	0.00225	0.02305	0.05940	3.53289	0.82289
0.119	0.150	0.099	6.33032	0.03363	0.01346	-0.02032	-0.00309	0.01895	0.09377	5.19526	0.16940
0.119	0.150	0.200	6.28751	0.04159	0.00977	-0.02742	-0.00120	0.01908	0.08776	4.96003	0.22657
0.119	0.150	0.300	6.19660	0.04637	0.00756	-0.03786	-0.00001	0.01936	0.08274	4.74000	0.31550
0.119	0.150	0.400	6.05900	0.04953	0.00604	-0.04875	0.00079	0.01977	0.07831	4.53249	0.40626
0.119	0.150	0.500	5.85797	0.05183	0.00489	-0.06000	0.00135	0.02048	0.07363	4.29663	0.50004
0.119	0.150	0.600	5.69796	0.05528	0.00343	-0.07117	0.00207	0.02106	0.06875	4.05828	0.59313
0.119	0.150	0.700	5.50615	0.05579	0.00273	-0.08188	0.00236	0.02178	0.06487	3.85233	0.63235
0.119	0.150	0.800	5.26037	0.05770	0.00231	-0.09200	0.00248	0.02281	0.06091	3.63265	0.76574
0.119	0.150	0.900	4.92554	0.05843	0.00205	-0.09874	0.00242	0.02436	0.05657	3.38014	0.82265
0.150	0.150	0.099	7.83444	0.02559	0.01639	-0.02540	-0.00375	0.01914	0.09835	5.41992	0.16937
0.150	0.150	0.200	7.75949	0.03562	0.01187	-0.03428	-0.00144	0.01933	0.09090	5.12588	0.22854
0.150	0.150	0.300	7.60685	0.04146	0.00912	-0.04732	-0.00002	0.01971	0.08468	4.85085	0.31546
0.150	0.150	0.400	7.39734	0.04542	0.00724	-0.06093	0.00091	0.02027	0.07921	4.59146	0.40622
0.150	0.150	0.500	7.05962	0.04831	0.00583	-0.07500	0.00154	0.02124	0.07344	4.29663	0.50001
0.150	0.150	0.600	6.80430	0.05257	0.00407	-0.08896	0.00234	0.02204	0.06744	3.99869	0.59310
0.150	0.150	0.700	6.50933	0.05444	0.00327	-0.10234	0.00263	0.02304	0.06266	3.74126	0.68231
0.150	0.150	0.800	6.13543	0.05559	0.00278	-0.11500	0.00271	0.02444	0.05779	3.46665	0.76670
0.150	0.150	0.900	5.65247	0.05653	0.00246	-0.12342	0.00258	0.02653	0.05240	3.15102	0.82282

FIRST FOIL DESIGN METHOD

DOUBLE ELLIPSE PRESSURE DISTRIBUTION

CAY= 0.150   LAMDA=0.05

CL	TEE	SS	LOD	ECAP	B	CM	DINT	CD	CO	ALPHA	XBAR
0.079	0.200	0.099	2.93908	0.04822	0.00602	-0.01355	-0.00132	0.02721	0.11176	6.32811	0.16949
0.079	0.200	0.200	2.91798	0.05271	0.00448	-0.01829	-0.00051	0.02741	0.10822	6.17129	0.22665
0.079	0.200	0.300	2.88379	0.05528	0.00357	-0.02524	-0.00002	0.02774	0.10517	6.02460	0.31558
0.079	0.200	0.400	2.84158	0.05702	0.00294	-0.03250	0.00030	0.02815	0.10243	5.88627	0.40634
0.079	0.200	0.500	2.77786	0.05825	0.00248	-0.04001	0.00054	0.02879	0.09944	5.72902	0.50012
0.079	0.200	0.600	2.72859	0.06020	0.00182	-0.04745	0.00087	0.02931	0.09634	5.57012	0.59322
0.079	0.200	0.700	2.67255	0.06103	0.00152	-0.05459	0.00101	0.02993	0.09380	5.43283	0.68243
0.079	0.200	0.800	2.60098	0.06152	0.00134	-0.06134	0.00109	0.03075	0.09116	5.28637	0.76682
0.079	0.200	0.900	2.50575	0.06192	0.00121	-0.06583	0.00111	0.03192	0.08821	5.11803	0.82294
0.099	0.200	0.099	3.64039	0.04357	0.00741	-0.01694	-0.00162	0.02746	0.11468	6.47788	0.16944
0.099	0.200	0.200	3.60676	0.04916	0.00550	-0.02286	-0.00063	0.02772	0.11027	6.28186	0.22860
0.099	0.200	0.300	3.55279	0.05237	0.00436	-0.03155	-0.00003	0.02814	0.10647	6.09850	0.31553
0.099	0.200	0.400	3.48649	0.05455	0.00359	-0.04062	0.00036	0.02868	0.10305	5.92557	0.40529
0.099	0.200	0.500	3.38729	0.05610	0.00301	-0.05000	0.00064	0.02952	0.09934	5.72902	0.50007
0.099	0.200	0.600	3.31091	0.05851	0.00221	-0.05931	0.00102	0.03020	0.09549	5.35878	0.59317
0.099	0.200	0.700	3.22478	0.05955	0.00184	-0.06823	0.00118	0.03100	0.09233	5.35878	0.63438
0.099	0.200	0.800	3.11518	0.06017	0.00162	-0.07667	0.00127	0.03209	0.08906	5.17570	0.76677
0.099	0.200	0.900	2.97467	0.06068	0.00146	-0.08228	0.00127	0.03361	0.08538	4.96528	0.82269
0.119	0.200	0.099	4.32780	0.03897	0.00876	-0.02032	-0.00191	0.02772	0.11758	6.62766	0.16940
0.119	0.200	0.200	4.27360	0.04566	0.00648	-0.02742	-0.00074	0.02804	0.11231	6.39242	0.22657
0.119	0.200	0.300	4.20018	0.04952	0.00512	-0.03786	-0.00004	0.02857	0.10777	6.17240	0.31550
0.119	0.200	0.400	4.10451	0.05213	0.00420	-0.04875	0.00041	0.02923	0.10369	5.96488	0.40626
0.119	0.200	0.500	3.96289	0.05401	0.00350	-0.06000	0.00072	0.03028	0.09926	5.72902	0.50004
0.119	0.200	0.600	3.85394	0.05688	0.00257	-0.07117	0.00116	0.03113	0.09466	5.49067	0.59313
0.119	0.200	0.700	3.73255	0.05812	0.00214	-0.08188	0.00133	0.03214	0.09089	5.28473	0.63235
0.119	0.200	0.800	3.58142	0.05887	0.00188	-0.09200	0.00141	0.03350	0.08698	5.06504	0.76674
0.119	0.200	0.900	3.38835	0.05949	0.00168	-0.09874	0.00139	0.03541	0.08259	4.81254	0.82285
0.150	0.200	0.099	5.33244	0.03220	0.01069	-0.02540	-0.00233	0.02812	0.12192	6.85231	0.16937
0.150	0.200	0.200	5.25406	0.04053	0.00788	-0.03428	-0.00090	0.02854	0.11536	6.55827	0.22354
0.150	0.200	0.300	5.13034	0.04535	0.00620	-0.04743	-0.00005	0.02923	0.10972	6.28324	0.31546
0.150	0.200	0.400	4.76107	0.04862	0.00505	-0.06093	0.00048	0.03011	0.10464	6.02385	0.40622
0.150	0.200	0.500	4.76349	0.05099	0.00418	-0.07500	0.00084	0.03148	0.09914	5.72903	0.50001
0.150	0.200	0.600	4.59713	0.05453	0.00306	-0.08896	0.00134	0.03262	0.09344	5.43108	0.59310
0.150	0.200	0.700	4.41479	0.05607	0.00255	-0.10234	0.00151	0.03397	0.08877	5.17365	0.68231
0.150	0.200	0.800	4.19203	0.05702	0.00222	-0.11500	0.00158	0.03578	0.08392	4.89905	0.76670
0.150	0.200	0.900	3.91547	0.05782	0.00198	-0.12342	0.00153	0.03830	0.07845	4.58341	0.82282

FIRST FOIL DESIGN METHOD

DOUBLE ELLIPSE PRESSURE DISTRIBUTION

CAY = 0.200   LAMDA = 0.05

CL	TEE	SS	LOD	ECAP	B	CM	DINT	CD	CO	ALPHA	XBAR
0.079	0.099	0.099	4.37244	0.05886	0.02114	-0.01355	-0.00600	0.01827	0.06601	3.43839	0.16949
0.079	0.099	0.200	4.42001	0.06573	0.01477	-0.01829	-0.00263	0.01809	0.06002	3.28810	0.22865
0.079	0.099	0.300	4.46203	0.06976	0.01070	-0.02524	-0.00021	0.01792	0.05515	3.14753	0.31558
0.079	0.099	0.400	4.49622	0.07251	0.00774	-0.03250	0.00175	0.01779	0.05086	3.01495	0.40634
0.079	0.099	0.500	4.51434	0.07452	0.00534	-0.04001	0.00361	0.01772	0.04687	2.86426	0.50012
0.079	0.099	0.600	4.53303	0.07763	0.00235	-0.04745	0.00553	0.01764	0.04179	2.71198	0.59322
0.079	0.099	0.700	4.53257	0.07902	0.00082	-0.05459	0.00676	0.01765	0.03827	2.58040	0.68243
0.079	0.099	0.800	4.49718	0.07986	-0.00015	-0.06134	0.00772	0.01778	0.03486	2.44005	0.76682
0.079	0.099	0.900	4.36366	0.08040	-0.00046	-0.06583	0.00810	0.01833	0.03166	2.27873	0.82294
0.099	0.099	0.099	5.52309	0.05190	0.02605	-0.01694	-0.00737	0.01810	0.06988	3.58192	0.16944
0.099	0.099	0.200	5.58602	0.06048	0.01816	-0.02286	-0.00321	0.01790	0.06245	3.39406	0.22650
0.099	0.099	0.300	5.64763	0.06550	0.01314	-0.03155	-0.00024	0.01770	0.05641	3.21834	0.31553
0.099	0.099	0.400	5.69380	0.06894	0.00951	-0.04062	0.00213	0.01756	0.05114	3.05262	0.40629
0.099	0.099	0.500	5.70578	0.07145	0.00660	-0.05030	0.00430	0.01752	0.04568	2.86426	0.50007
0.099	0.099	0.600	5.72003	0.07531	0.00305	-0.05931	0.00651	0.01748	0.04015	2.67391	0.59315
0.099	0.099	0.700	5.63954	0.07702	0.00129	-0.06823	0.00784	0.01754	0.03595	2.50944	0.68238
0.099	0.099	0.800	5.61539	0.07804	0.00023	-0.07667	0.00878	0.01780	0.03195	2.33400	0.76677
0.099	0.099	0.900	5.37660	0.07871	-0.00003	-0.08228	0.00897	0.01859	0.02824	2.13234	0.82289
0.119	0.099	0.099	6.68539	0.04698	0.03081	-0.02032	-0.00868	0.01794	0.07370	3.72545	0.16940
0.119	0.099	0.200	6.77360	0.05526	0.02144	-0.02742	-0.00375	0.01771	0.06484	3.50002	0.22857
0.119	0.099	0.300	6.85590	0.06128	0.01548	-0.03786	-0.00026	0.01750	0.05766	3.28916	0.31550
0.119	0.099	0.400	6.91019	0.06541	0.01120	-0.04875	0.00249	0.01736	0.05144	3.09029	0.40626
0.119	0.099	0.500	6.93443	0.06842	0.00783	-0.06000	0.00490	0.01738	0.04508	2.86426	0.50004
0.119	0.099	0.600	6.90229	0.07300	0.00378	-0.07117	0.00735	0.01738	0.03865	2.63554	0.59315
0.119	0.099	0.700	6.84246	0.07504	0.00183	-0.08188	0.00872	0.01753	0.03383	2.43847	0.68235
0.119	0.099	0.800	6.68417	0.07624	0.00072	-0.09200	0.00957	0.01795	0.02930	2.22794	0.76674
0.119	0.099	0.900	6.30716	0.07704	-0.00049	-0.09874	0.00953	0.01902	0.02512	1.98596	0.82285
0.150	0.099	0.099	8.46025	0.03469	0.03769	-0.02540	-0.01055	0.01772	0.07933	3.94074	0.16937
0.150	0.099	0.200	8.59024	0.04751	0.02615	-0.03428	-0.00450	0.01746	0.06836	3.65895	0.22854
0.150	0.099	0.300	8.70208	0.05503	0.01881	-0.04732	-0.00027	0.01723	0.05953	3.39538	0.31545
0.150	0.099	0.400	8.75832	0.06018	0.01362	-0.06093	0.00298	0.01712	0.05194	3.14680	0.40622
0.150	0.099	0.500	8.69195	0.06395	0.00959	-0.07500	0.00567	0.01725	0.04431	2.86426	0.50001
0.150	0.099	0.600	8.63619	0.06960	0.00489	-0.08896	0.00836	0.01736	0.03664	2.57873	0.59310
0.150	0.099	0.700	8.47842	0.07210	0.00273	-0.10234	0.00970	0.01769	0.03099	2.32203	0.68231
0.150	0.099	0.800	8.15597	0.07258	0.00157	-0.11500	0.01035	0.01839	0.02575	2.06886	0.76670
0.150	0.099	0.900	7.52029	0.07458	0.00138	-0.12342	0.00995	0.01994	0.02087	1.76638	0.82282

FIRST FOIL DESIGN METHOD

DOUBLE ELLIPSE PRESSURE DISTRIBUTION

CAY= 0.200   LAMDA=0.05

CL	TEE	SS	LCD	ECAP	B	CM	DINT	CD	CO	ALPHA	XBAR
0.079	0.150	0.099	3.22670	0.06227	0.01287	-0.01355	-0.00320	0.02479	0.08821	4.87078	0.16949
0.079	0.150	0.200	3.23200	0.06820	0.00927	-0.01829	-0.00128	0.02475	0.08367	4.72049	0.22865
0.079	0.150	0.300	3.22852	0.07164	0.00705	-0.02524	0.00000	0.02477	0.07993	4.57992	0.31558
0.079	0.150	0.400	3.21526	0.07397	0.00549	-0.03250	0.00097	0.02488	0.07664	4.44734	0.40534
0.079	0.150	0.500	3.18160	0.07565	0.00429	-0.04001	0.00177	0.02514	0.07321	4.29665	0.50012
0.079	0.150	0.600	3.15819	0.07827	0.00268	-0.04745	0.00272	0.02533	0.06961	4.14437	0.59322
0.079	0.150	0.700	3.12306	0.07942	0.00190	-0.05459	0.00324	0.02561	0.06679	4.01280	0.68243
0.079	0.150	0.800	3.06672	0.08010	0.00142	-0.06134	0.00360	0.02608	0.06397	3.87244	0.76682
0.079	0.150	0.900	2.96386	0.08058	0.00121	-0.06583	0.00370	0.02699	0.06106	3.71112	0.82294
0.099	0.150	0.099	4.03469	0.05619	0.01587	-0.01694	-0.00393	0.02478	0.09145	5.01431	0.16944
0.099	0.150	0.200	4.04116	0.06359	0.01141	-0.02286	-0.00157	0.02474	0.08580	4.82645	0.22860
0.099	0.150	0.300	4.03276	0.06788	0.00866	-0.03155	0.00000	0.02479	0.08116	4.65074	0.31553
0.099	0.150	0.400	4.00834	0.07079	0.00673	-0.04062	0.00117	0.02494	0.07710	4.48501	0.40629
0.099	0.150	0.500	3.94956	0.07289	0.00526	-0.05000	0.00210	0.02531	0.07288	4.29665	0.50000
0.099	0.150	0.600	3.90735	0.07615	0.00332	-0.05931	0.00321	0.02555	0.06845	4.10630	0.59317
0.099	0.150	0.700	3.84616	0.07757	0.00240	-0.06823	0.00378	0.02599	0.06501	3.94183	0.68438
0.099	0.150	0.800	3.74798	0.07841	0.00185	-0.07667	0.00413	0.02668	0.06159	3.76639	0.76677
0.099	0.150	0.900	3.59368	0.07902	0.00160	-0.08228	0.00418	0.02782	0.05802	3.56474	0.82289
0.119	0.150	0.099	4.84173	0.05016	0.01879	-0.02032	-0.00464	0.02478	0.09456	5.15784	0.16940
0.119	0.150	0.200	4.84851	0.05902	0.01348	-0.02742	-0.00184	0.02474	0.08793	4.93241	0.22857
0.119	0.150	0.300	4.83206	0.06417	0.01020	-0.03786	0.00000	0.02483	0.08239	4.72155	0.31550
0.119	0.150	0.400	4.79152	0.06766	0.00792	-0.04875	0.00135	0.02504	0.07757	4.52269	0.40626
0.119	0.150	0.500	4.69874	0.07019	0.00619	-0.06000	0.00240	0.02553	0.07258	4.29665	0.50004
0.119	0.150	0.600	4.63014	0.07406	0.00394	-0.07117	0.00363	0.02591	0.06736	4.06823	0.59313
0.119	0.150	0.700	4.55083	0.07576	0.00290	-0.08188	0.00423	0.02648	0.06332	3.87087	0.68235
0.119	0.150	0.800	4.39136	0.07676	0.00228	-0.09200	0.00457	0.02732	0.05930	3.66034	0.75574
0.119	0.150	0.900	4.16263	0.07750	0.00200	-0.09874	0.00454	0.02882	0.05511	3.41835	0.82285
0.150	0.150	0.099	6.04770	0.04123	0.02301	-0.02540	-0.00565	0.02480	0.09943	5.37314	0.16937
0.150	0.150	0.200	6.05239	0.05227	0.01645	-0.03428	-0.00223	0.02478	0.09109	5.09135	0.22354
0.150	0.150	0.300	6.01773	0.05869	0.01241	-0.04732	0.00001	0.02492	0.08424	4.82778	0.31546
0.150	0.150	0.400	5.94148	0.06206	0.00961	-0.06093	0.00160	0.02524	0.07831	4.57919	0.40622
0.150	0.150	0.500	5.77957	0.06624	0.00750	-0.07500	0.00278	0.02595	0.07220	4.29665	0.50001
0.150	0.150	0.600	5.55358	0.07102	0.00484	-0.08896	0.00416	0.02653	0.06584	4.01113	0.59310
0.150	0.150	0.700	5.49083	0.07311	0.00362	-0.10234	0.00478	0.02730	0.06091	3.76442	0.68231
0.150	0.150	0.800	5.25900	0.07436	0.00291	-0.11500	0.00506	0.02852	0.05604	3.50126	0.76670
0.150	0.150	0.900	4.90705	0.07530	0.00258	-0.12342	0.00490	0.03056	0.05092	3.19878	0.82282

FIRST FOIL DESIGN METHOD

DOUBLE ELLIPSE PRESSURE DISTRIBUTION

CAY= 0.200   LAMDA=0.05

CL	TEE	SS	LOD	ECAP	B	CM	DINT	CD	CO	ALPHA	XBAR
0.079	0.200	0.099	2.37702	0.06544	0.00865	-0.01355	-0.00199	0.03365	0.11200	6.30317	0.16949
0.079	0.200	0.200	2.37035	0.07053	0.00636	-0.01829	-0.00078	0.03375	0.10817	6.15288	0.22865
0.079	0.200	0.300	2.35573	0.07347	0.00498	-0.02524	-0.00000	0.03395	0.10494	6.01231	0.31558
0.079	0.200	0.400	2.34489	0.07545	0.00402	-0.03250	0.00054	0.03426	0.10207	5.87974	0.40634
0.079	0.200	0.500	2.29939	0.07686	0.00331	-0.04001	0.00097	0.03479	0.09901	5.72905	0.50012
0.079	0.200	0.600	2.27279	0.07909	0.00230	-0.04745	0.00152	0.03519	0.09580	5.57677	0.59322
0.079	0.200	0.700	2.24000	0.08005	0.00163	-0.05459	0.00180	0.03571	0.09323	5.44519	0.68243
0.079	0.200	0.800	2.19495	0.08062	0.00154	-0.06134	0.00198	0.03644	0.09060	5.30484	0.76682
0.079	0.200	0.900	2.12826	0.08105	0.00138	-0.06583	0.00203	0.03758	0.08773	5.14351	0.82294
0.099	0.200	0.099	2.95861	0.06015	0.01068	-0.01694	-0.00245	0.03379	0.11497	6.44670	0.16944
0.099	0.200	0.200	2.94740	0.06650	0.00783	-0.02286	-0.00096	0.03392	0.11019	6.25885	0.22860
0.099	0.200	0.300	2.92342	0.07017	0.00612	-0.03155	-0.00000	0.03420	0.10617	6.08313	0.31553
0.099	0.200	0.400	2.88760	0.07264	0.00493	-0.04062	0.00065	0.03460	0.10261	5.91741	0.40629
0.099	0.200	0.500	2.83255	0.07442	0.00404	-0.05000	0.00116	0.03530	0.09865	5.72905	0.50007
0.099	0.200	0.600	2.78954	0.07719	0.00282	-0.05951	0.00181	0.03584	0.09485	5.53969	0.59317
0.099	0.200	0.700	2.73710	0.07838	0.00225	-0.06823	0.00212	0.03653	0.09167	5.37423	0.68238
0.099	0.200	0.800	2.66507	0.07909	0.00191	-0.07667	0.00231	0.03750	0.08842	5.19878	0.76677
0.099	0.200	0.900	2.56366	0.07963	0.00171	-0.08228	0.00233	0.03900	0.08487	4.99713	0.82289
0.119	0.200	0.099	3.53639	0.05491	0.01265	-0.02032	-0.00290	0.03395	0.11792	6.59024	0.16940
0.119	0.200	0.200	3.51715	0.06252	0.00926	-0.02742	-0.00113	0.03411	0.11221	6.36431	0.22857
0.119	0.200	0.300	3.48107	0.06692	0.00721	-0.03786	-0.00001	0.03447	0.10741	6.15394	0.31550
0.119	0.200	0.400	3.43068	0.06989	0.00580	-0.04875	0.00076	0.03497	0.10317	5.95508	0.40626
0.119	0.200	0.500	3.34662	0.07203	0.00475	-0.06000	0.00133	0.03585	0.09893	5.72905	0.50004
0.119	0.200	0.600	3.28299	0.07532	0.00332	-0.07117	0.00207	0.03655	0.09393	5.50063	0.59313
0.119	0.200	0.700	3.20633	0.07675	0.00266	-0.08188	0.00240	0.03742	0.09015	5.30326	0.68235
0.119	0.200	0.800	3.10398	0.07760	0.00226	-0.09200	0.00258	0.03865	0.08630	5.09273	0.76674
0.119	0.200	0.900	2.95993	0.07827	0.00202	-0.09874	0.00258	0.04054	0.08207	4.85074	0.82285
0.150	0.200	0.099	4.38645	0.04716	0.01551	-0.02540	-0.00355	0.03419	0.12233	6.80553	0.16937
0.150	0.200	0.200	4.35706	0.05664	0.01132	-0.03428	-0.00137	0.03442	0.11523	6.52374	0.22854
0.150	0.200	0.300	4.29735	0.06213	0.00878	-0.04732	-0.00001	0.03490	0.10927	6.26017	0.31546
0.150	0.200	0.400	4.21509	0.06585	0.00704	-0.06093	0.00090	0.03558	0.10401	6.01159	0.40622
0.150	0.200	0.500	4.08029	0.06853	0.00574	-0.07500	0.00155	0.03676	0.09843	5.72905	0.50001
0.150	0.200	0.600	3.97797	0.07251	0.00402	-0.08896	0.00239	0.03779	0.09260	5.43352	0.59310
0.150	0.200	0.700	3.85594	0.07439	0.00324	-0.10234	0.00275	0.03889	0.08794	5.19681	0.68231
0.150	0.200	0.800	3.69868	0.07546	0.00276	-0.11500	0.00291	0.04055	0.08319	4.93365	0.76670
0.150	0.200	0.900	3.48373	0.07631	0.00246	-0.12342	0.00285	0.04305	0.07797	4.63117	0.82282

APPENDIX B

Tables of Performance Data - Second Design Procedure

The symbols in this table are the same as those of Appendix A except for ACAP and EM. These are defined in Reference 2 as:

ACAP $\equiv$ A, the strength of the leading edge singularity due to the increase of the design attack angle above the value for shockless entry.

EM $\equiv$ m, the fraction of C_L which is carried by the prescribed pressure distribution. The fraction of C_L carried by the angle of attack term is 1-M.

ALPHA $\equiv$ Angle of Attack in radians (note that in Appendix A this quantity is expressed in degrees).

SECOND FOIL DESIGN METHOD

ELLIPTICAL PRESSURE DISTRIBUTION

CAM= 0.000

CL	TEE	SS	LCD	ACAP	EM	CM	DINT	CD	CO	ALPHA	XBAR
0.120	0.100	0.200	20.80032	-0.02886	0.62219	-0.02908	0.02886	0.00577	0.03554	0.06385	0.24436
0.120	0.100	0.300	19.77785	-0.04491	0.41205	-0.03690	0.04491	0.00606	0.01646	0.06113	0.30750
0.120	0.100	0.400	17.20459	-0.05105	0.33165	-0.04098	0.05105	0.00624	0.00899	0.05982	0.34157
0.120	0.100	0.500	15.47691	-0.05478	0.28282	-0.04375	0.05478	0.00644	0.00404	0.05874	0.36549
0.120	0.100	0.600	15.63976	-0.05825	0.23749	-0.04568	0.05825	0.00650	-0.00012	0.05808	0.38074
0.120	0.100	0.700	15.13493	-0.05982	0.21556	-0.04749	0.05962	0.00661	-0.00259	0.05748	0.39277
0.120	0.100	0.800	17.40246	-0.06133	0.19707	-0.04899	0.06133	0.00674	-0.00458	0.05686	0.40828
0.120	0.100	0.900	17.25259	-0.06304	0.17471	-0.04973	0.06204	0.00695	-0.00652	0.05613	0.41443
0.130	0.100	0.200	22.42972	-0.01751	0.79025	-0.02903	0.01751	0.00584	0.04493	0.06549	0.22555
0.130	0.100	0.300	20.05721	-0.03941	0.52370	-0.03980	0.03941	0.00626	0.02265	0.06175	0.30615
0.130	0.100	0.400	19.95271	-0.04747	0.42151	-0.04542	0.04787	0.00651	0.01239	0.05995	0.34945
0.130	0.100	0.500	19.21277	-0.05301	0.35945	-0.04938	0.05301	0.00676	0.00557	0.05846	0.37925
0.130	0.100	0.600	18.45523	-0.05777	0.30184	-0.05190	0.05778	0.00688	-0.00016	0.05754	0.39923
0.130	0.100	0.700	14.47850	-0.06248	0.27397	-0.05438	0.06208	0.00703	-0.00329	0.05672	0.41833
0.130	0.100	0.800	13.01494	-0.06202	0.25547	-0.05645	0.06203	0.00721	-0.00605	0.05596	0.43423
0.130	0.100	0.900	17.29433	-0.06443	0.22205	-0.05746	0.06438	0.00751	-0.00895	0.05486	0.44205
0.140	0.100	0.200	23.61917	-0.00576	0.93932	-0.02898	0.00575	0.00592	0.06233	0.06713	0.20706
0.140	0.100	0.300	21.66022	-0.03391	0.61941	-0.04254	0.03392	0.00646	0.04886	0.06256	0.30497
0.140	0.100	0.400	20.51522	-0.04466	0.49656	-0.04986	0.04469	0.00679	0.01574	0.06007	0.34921
0.140	0.100	0.500	19.47149	-0.05123	0.42414	-0.05492	0.05123	0.00711	0.00710	0.05817	0.39215
0.140	0.100	0.600	19.40346	-0.05730	0.35700	-0.05811	0.05730	0.00726	-0.00021	0.05701	0.41505
0.140	0.100	0.700	19.36206	-0.06127	0.32404	-0.06127	0.06024	0.00747	-0.00420	0.05556	0.43767
0.140	0.100	0.800	13.17017	-0.06390	0.29625	-0.06360	0.06272	0.00770	-0.00768	0.05497	0.45048
0.140	0.100	0.900	17.27642	-0.06521	0.26263	-0.06521	0.06572	0.00810	-0.01137	0.05353	0.46272

SECOND FOIL DESIGN METHOD

ELLIPTICAL PRESSURE DISTRIBUTION

CAY= 0.000

CL	TEE	SS	LOD	ACAP	EM	CM	DINT	CD	CO	ALPHA	XBAR
0.150	0.100	0.300	2?.49731	-0.02842	0.70236	-0.04559	0.02842	0.00666	0.03506	0.06298	0.37398
0.150	0.100	0.400	21.21690	-0.04150	0.56530	-0.05430	0.04151	0.00707	0.01918	0.06019	0.??
0.150	0.100	0.500	20.06458	-0.04945	0.48207	-0.06042	0.04945	0.00747	0.00863	0.05789	0.40463
0.150	0.100	0.600	19.55830	-0.05613	0.40431	-0.06431	0.05683	0.00766	-0.00025	0.05648	0.42831
0.150	0.100	0.700	18.94484	-0.06040	0.36743	-0.06816	0.06040	0.00791	-0.00510	0.05520	0.45443
0.150	0.100	0.800	18.26863	-0.06341	0.35591	-0.07136	0.06341	0.00821	-0.00934	0.05387	0.47576
0.150	0.100	0.900	17.21014	-0.06705	0.29780	-0.07293	0.06705	0.00871	-0.01380	0.05232	0.4862?
0.150	0.100	0.300	23.27904	-0.02292	0.77495	-0.04839	0.02292	0.00687	0.04127	0.06360	0.303??
0.150	0.100	0.400	21.75781	-0.03832	0.62372	-0.05874	0.03832	0.00735	0.02258	0.06031	0.3671?
0.160	0.100	0.500	20.39658	-0.04768	0.53189	-0.06594	0.04768	0.00784	0.01016	0.05760	0.41216
0.160	0.100	0.600	19.81740	-0.05636	0.44664	-0.07053	0.05636	0.00807	-0.00031	0.05594	0.440?
0.160	0.100	0.700	19.09795	-0.06056	0.37040	-0.07505	0.06056	0.00837	-0.00609	0.05445	0.46910
0.150	0.100	0.800	13.32405	-0.06410	0.37063	-0.07882	0.06410	0.00873	-0.01100	0.05288	0.49263
0.150	0.100	0.900	17.14159	-0.06838	0.32657	-0.08067	0.06839	0.00933	-0.01619	0.05105	0.50419
0.150	0.150	0.200	11.87903	-0.07793	0.18390	-0.04376	0.07793	0.01262	0.01313	0.09086	0.29476
0.150	0.150	0.300	11.72916	-0.08386	0.12179	-0.04665	0.08836	0.01278	0.00608	0.08985	0.31401
0.150	0.150	0.400	11.64199	-0.08613	0.09802	-0.04816	0.08613	0.01288	0.00332	0.08937	0.32108
0.150	0.150	0.500	11.55789	-0.08750	0.08359	-0.04922	0.08751	0.01297	0.00149	0.08897	0.32815
0.150	0.150	0.600	11.51960	-0.08878	0.07019	-0.04989	0.08879	0.01302	-0.00004	0.08872	0.33266
0.150	0.150	0.800	11.47003	-0.08940	0.06371	-0.05056	0.08940	0.01307	-0.00088	0.08850	0.33710
0.150	0.150	0.800	11.41333	-0.08992	0.05824	-0.05112	0.08993	0.01314	-0.00161	0.08827	0.34030
0.150	0.150	0.900	11.31914	-0.09056	0.05163	-0.05139	0.09056	0.01325	-0.00240	0.08800	0.34261
0.150	0.150	0.200	12.55386	-0.06638	0.34829	-0.04371	0.06638	0.01274	0.02653	0.09250	0.27322
0.160	0.150	0.300	12.23844	-0.07836	0.23065	-0.04954	0.07836	0.01307	0.01268	0.09047	0.30967
0.160	0.150	0.400	12.05855	-0.08294	0.18564	-0.05260	0.08295	0.01326	0.00672	0.08949	0.32676
0.160	0.150	0.500	11.58547	-0.08573	0.15830	-0.05474	0.08573	0.01346	0.00302	0.08868	0.34215
0.160	0.150	0.600	11.60715	-0.08931	0.13293	-0.05611	0.08831	0.01355	-0.00069	0.08819	0.35069
0.150	0.150	0.700	11.70755	-0.08956	0.12066	-0.05745	0.08956	0.01366	-0.00178	0.06774	0.35710
0.150	0.150	0.800	11.59386	-0.09062	0.11031	-0.05857	0.09062	0.01380	-0.00327	0.08728	0.36610
0.150	0.150	0.900	11.43765	-0.09189	0.09779	-0.05912	0.09189	0.01402	-0.00462	0.08673	0.36954

SECOND FOIL DESIGN METHOD

ELLIPTICAL PRESSURE DISTRIBUTION

CL	TEE	SS	LDD	ACAP	EX	CM	DINT	CD	CO	ALPHA	XBAR
0.120	0.100	0.200	13.01576	-0.04928	0.27523	-0.03397	0.04682	0.00666	0.01337	0.06220	0.28516
0.120	0.100	0.300	17.63741	-0.05635	0.18232	-0.03745	0.05530	0.00680	0.00574	0.06104	0.31414
0.120	0.100	0.400	17.43764	-0.05842	0.14702	-0.03927	0.05777	0.00688	0.00271	0.06049	0.32729
0.120	0.100	0.500	17.23840	-0.06032	0.12578	-0.04056	0.05928	0.00696	0.00074	0.06032	0.33799
0.120	0.100	0.600	17.14457	-0.06173	0.10567	-0.04137	0.06069	0.00700	-0.00094	0.05974	0.34482
0.120	0.100	0.700	17.03363	-0.06241	0.09512	-0.04219	0.06137	0.00704	-0.00188	0.05948	0.35160
0.120	0.100	0.800	16.94451	-0.06299	0.08615	-0.04287	0.06195	0.00710	-0.00273	0.05921	0.35731
0.120	0.100	0.900	16.71095	-0.06369	0.07651	-0.04323	0.06265	0.00718	-0.00376	0.05889	0.36027
0.130	0.100	0.200	19.46024	-0.03908	0.47546	-0.03380	0.03814	0.00668	0.02567	0.06380	0.26007
0.130	0.100	0.300	18.70387	-0.05119	0.31519	-0.04032	0.05025	0.00695	0.01138	0.06163	0.31019
0.130	0.100	0.400	18.30777	-0.05592	0.25412	-0.04373	0.05489	0.00710	0.00570	0.06059	0.33639
0.130	0.100	0.500	17.62145	-0.05854	0.21726	-0.04613	0.05771	0.00725	0.00202	0.05973	0.35488
0.130	0.100	0.600	17.74193	-0.06126	0.18260	-0.04760	0.06034	0.00732	0.00114	0.05919	0.36667
0.130	0.100	0.700	17.52989	-0.06256	0.16608	-0.04918	0.06162	0.00741	-0.00290	0.05871	0.37837
0.130	0.100	0.800	17.26802	-0.06364	0.15228	-0.05047	0.06271	0.00752	-0.00450	0.05820	0.38623
0.130	0.100	0.900	16.52770	-0.06496	0.13558	-0.05113	0.06402	0.00768	-0.00641	0.05760	0.39932
0.140	0.100	0.200	20.49568	-0.02828	0.64798	-0.03363	0.02742	0.00670	0.03798	0.06540	0.24028
0.140	0.100	0.300	19.71091	-0.04603	0.42896	-0.04319	0.04519	0.00710	0.01703	0.06223	0.30353
0.140	0.100	0.400	19.10951	-0.05282	0.34550	-0.04818	0.05198	0.00732	0.00671	0.06070	0.34418
0.140	0.100	0.500	18.52718	-0.05666	0.29572	-0.05170	0.05612	0.00755	0.00331	0.05943	0.36933
0.140	0.100	0.600	18.25380	-0.06093	0.24842	-0.05365	0.05999	0.00766	-0.00133	0.05865	0.38537
0.140	0.100	0.700	17.94492	-0.06270	0.22592	-0.05616	0.06186	0.00780	-0.00391	0.05725	0.40128
0.140	0.100	0.800	17.56105	-0.06429	0.20711	-0.05805	0.06345	0.00797	-0.00624	0.05720	0.41467
0.140	0.100	0.900	17.06987	-0.06622	0.18433	-0.05901	0.06537	0.00820	-0.00905	0.05632	0.42156
0.150	0.100	0.200	22.32182	-0.01747	0.79703	-0.03347	0.01671	0.00672	0.05029	0.06700	0.22313
0.150	0.100	0.300	20.66960	-0.04096	0.52746	-0.04506	0.04012	0.00725	0.02270	0.06282	0.30709
0.150	0.100	0.400	19.34711	-0.04981	0.42515	-0.05264	0.04907	0.00755	0.01173	0.06080	0.35093
0.150	0.100	0.500	18.76250	-0.05527	0.36352	-0.05727	0.05451	0.00786	0.00451	0.05913	0.38184
0.150	0.100	0.600	18.70406	-0.06037	0.30537	-0.06023	0.05962	0.00802	-0.00150	0.05811	0.40105
0.150	0.100	0.700	18.28800	-0.06284	0.27767	-0.06316	0.06209	0.00820	-0.00490	0.05718	0.42110
0.150	0.100	0.800	17.78494	-0.06494	0.25451	-0.06563	0.06418	0.00843	-0.00797	0.05620	0.43753
0.150	0.100	0.900	17.15059	-0.06748	0.22646	-0.06689	0.06671	0.00874	-0.01166	0.05504	0.44297

SECOND FOIL DESIGN METHOD

ELLIPTICAL PRESSURE DISTRIBUTION

CAM   0.100

CL	TEE	SS	LOD	ACAP	EM	CM	DINT	CD	CO	ALPHA	XBAR
0.140	0.100	0.200	15.43129	-0.06792	0.00732	-0.04462	0.06380	0.00909	-0.00136	0.06244	0.31875
0.140	0.100	0.300	15.39573	-0.06910	0.00484	-0.04473	0.06398	0.00909	-0.00157	0.05240	0.31953
0.140	0.100	0.400	15.39251	-0.05816	0.00392	-0.04479	0.06405	0.00909	-0.00166	0.05239	0.31794
0.140	0.100	0.500	15.38900	-0.06820	0.00337	-0.04483	0.06409	0.00909	-0.00171	0.05237	0.32023
0.140	0.100	0.600	15.38744	-0.06824	0.00284	-0.04485	0.06413	0.00909	-0.00176	0.05236	0.32042
0.140	0.100	0.700	15.38533	-0.06826	0.00259	-0.04488	0.06415	0.00910	-0.00179	0.05236	0.32060
0.140	0.100	0.800	15.38248	-0.06428	0.00239	-0.04490	0.06417	0.00910	-0.00181	0.05235	0.32077
0.140	0.100	0.900	15.37799	-0.06830	0.00215	-0.04492	0.06419	0.00910	-0.00184	0.05234	0.32066
0.150	0.100	0.200	16.53548	-0.05803	0.20854	-0.04419	0.05417	0.00907	0.00988	0.06405	0.29465
0.150	0.100	0.300	16.35240	-0.06339	0.13796	-0.04753	0.05961	0.00917	0.00337	0.06298	0.31685
0.150	0.100	0.400	16.24701	-0.06543	0.11158	-0.04926	0.06168	0.00923	0.00078	0.06247	0.32845
0.150	0.100	0.500	16.12947	-0.06667	0.09603	-0.05050	0.06296	0.00930	-0.00091	0.06204	0.33671
0.150	0.100	0.600	16.07800	-0.06785	0.08073	-0.05129	0.06415	0.00933	-0.00237	0.06178	0.34199
0.150	0.100	0.700	16.01021	-0.06843	0.07375	-0.05209	0.06474	0.00937	-0.00321	0.06153	0.34730
0.150	0.100	0.800	15.91772	-0.06892	0.06806	-0.05278	0.06526	0.00942	-0.00398	0.06127	0.35188
0.150	0.100	0.900	15.77373	-0.06953	0.05121	-0.05317	0.06587	0.00951	-0.00492	0.06095	0.35450
0.160	0.100	0.200	17.67436	-0.04814	0.38459	-0.04376	0.04453	0.00905	0.02112	0.05566	0.27355
0.160	0.100	0.300	17.28514	-0.05867	0.25422	-0.05032	0.05521	0.00925	0.00835	0.05356	0.31455
0.160	0.100	0.400	17.06195	-0.06268	0.20555	-0.05374	0.05928	0.00937	0.00326	0.06255	0.33569
0.160	0.100	0.500	16.81529	-0.06513	0.17684	-0.05617	0.06179	0.00951	-0.00007	0.06171	0.35410
0.160	0.100	0.600	16.70706	-0.06745	0.14865	-0.05773	0.06413	0.00957	-0.00293	0.06119	0.36081
0.160	0.100	0.700	15.56601	-0.06858	0.13575	-0.05929	0.06529	0.00965	-0.00457	0.06072	0.37057
0.160	0.100	0.800	16.37581	-0.06956	0.12523	-0.06063	0.06629	0.00977	-0.00608	0.06020	0.37898
0.160	0.100	0.900	16.08731	-0.07075	0.11253	-0.06140	0.06750	0.00994	-0.00791	0.05958	0.38976

SECOND FOIL DESIGN METHOD

ELLIPTICAL PRESSURE DISTRIBUTION

CAVE   0.050

CL	TEE	SS	LOD	ACAP	EM	CM	DINT	CD	CO	ALPHA	XBAR
0.150	0.100	0.200	23.73923	-0.00666	0.92742	-0.03330	0.00600	0.00674	0.06260	0.06860	0.20813
0.150	0.100	0.300	21.57959	-0.03569	0.61356	-0.04893	0.03503	0.00741	0.04837	0.06341	0.30285
0.150	0.100	0.400	20.52658	-0.04680	0.49449	-0.05709	0.04614	0.00779	0.01476	0.06091	0.35683
0.150	0.100	0.500	19.53359	-0.05357	0.42274	-0.06484	0.05290	0.00819	0.00593	0.05884	0.39477
0.150	0.100	0.600	19.08472	-0.05991	0.35510	-0.06651	0.05924	0.00838	-0.00166	0.05757	0.41970
0.160	0.100	0.700	18.56933	-0.06298	0.32206	-0.07014	0.06230	0.00861	-0.05588	0.05642	0.43841
0.160	0.100	0.800	17.94969	-0.06558	0.29589	-0.07320	0.06490	0.00891	-0.00969	0.05520	0.45750
0.160	0.100	0.900	17.19045	-0.06874	0.26322	-0.07476	0.06804	0.00931	-0.01427	0.05377	0.46726
0.150	0.150	0.200	11.44972	-0.08496	0.10104	-0.04833	0.08419	0.01397	0.06655	0.09074	0.30208
0.160	0.150	0.300	11.36075	-0.08329	0.06594	-0.05003	0.08743	0.01403	0.00274	0.09018	0.31268
0.150	0.150	0.400	11.31387	-0.08944	0.05393	-0.05091	0.08867	0.01414	0.00123	0.08991	0.31823
0.150	0.150	0.500	11.26762	-0.09019	0.04606	-0.05154	0.08942	0.01420	0.00025	0.08968	0.32214
0.150	0.150	0.600	11.24545	-0.09089	0.03869	-0.05194	0.09013	0.01422	-0.00058	0.08954	0.32463
0.160	0.150	0.700	11.21949	-0.09123	0.03515	-0.05233	0.09047	0.01426	-0.00104	0.08942	0.32710
0.160	0.150	0.800	11.18735	-0.09152	0.03219	-0.05266	0.09075	0.01430	-0.00146	0.08929	0.32916
0.150	0.150	0.900	11.14599	-0.09187	0.02860	-0.05283	0.09110	0.01435	-0.00196	0.08913	0.33020

APPENDIX C

Pressure Distributions for Fully Cavitating
Hydrofoil Profiles Which Use the
Stratford Pressure Rise

We have seen that fully cavitating hydrofoils have the best L/D
if the center of pressure on the wetted surface is as near to the pro-
file nose as possible when cavity thickness constraints are specifi-
cally accounted for in the design. Even so, there may be some situa-
tions when tail loading may be desired. Then it is necessary to avoid
turbulent separation and to make certain that it will not occur at the
very beginning of the design process.

In particular, if one specifies the cavitation number, the Reynolds
number, and the profile lift coefficient, he needs to know how close to
the trailing edge he can locate the center of pressure and still main-
tain a prescribed value of the cavity thickness. In order to move the
center of pressure to the rear, one needs to specify adverse pressure
gradients on the wetted surface which become steeper and steeper as the
center of pressure moves aft. At the same time, turbulent separation
must be avoided. It is the avoidance of turbulent separation along with
other design considerations noted above which has led to the following
considerations. For nose-loaded profiles such considerations are not needed.

Fortunately, the problem of turbulent-separation avoidance was solved
by B. S. Stratford in 1959 [12]. In two papers in the Journal of Fluid
Mechanics he has given a solution for the form of pressure rise in a tur-
bulent boundary layer which is just on the verge of separating during the
whole time that a typical boundary-layer fluid particle experiences a
rising pressure. Although such a boundary layer flow is a very special

one, it obviously has great technical interest, because it is not possible
to prescribe steeper pressure increases without producing turbulent sepa-
ration. Of equal importance for applications, Stratford was able to pro-
duce such a flow experimentally and to measure the important boundary-
layer flow quantities.

Since Stratford's pioneering efforts, his results have been applied
in this country, principally by engineers at Douglas [13, 14, 15, 16], to
the design of very efficient high-lift airfoils. Moreover, they have
verified the correctness of their methods in a series of wind tunnel tests
which showed excellent agreement between calculated and measured perfor-
mance. On the basis of these results, there is every reason to believe
that the work of Stratford can be applied to the hydrodynamic design of
certain supercavitating hydrofoils.

On the other hand, the design considerations appropriate to cavity
flows are somewhat different from those for airfoils. Therefore, it is
necessary for us to adapt some of the methods of Stratford and of Liebeck
to the present inverse design prodedure [2]. In this note, we consider
only profiles designed in accordance with the first profile design proce-
dure. The use of the Stratford recovery for the second design procedure
will differ from that given below. We will not consider it here because
of its complexity and its limited usefullness.

Prescribed Pressure Distribution

Figure C-1 shows
schematically the kind
of pressure distribu-
tion under study. The
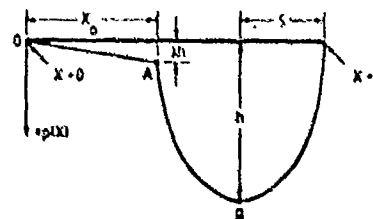wetted surface of the

Figure C-1

hydrofoil is of unit chord, and it lies on the X-axis as shown. The dotted contour illustrates the upper surface of the cavity which originates at the profile nose. The lower surface of the cavity leaves the profile trailing edge at $X = 1$. The cavitation number K is

$$K = \frac{P_\infty - P_c}{1/2\rho\, U_\infty^2} \quad ,$$

where P_∞ and U_∞ are the steady upstream flow conditions. The cavity pressure P_c is the lowest pressure in the flow field, and ρ is the liquid density. The disturbance pressure in Ref. 2 is $P(X) - P_c + p(X) \cdot 1/2\rho\, U_\infty^2$, where $P(X)$ is the static pressure on the foil and the distrubance pressure is $p(X)$. The pressure coefficient C_p is

$$C_p = \frac{P(X) - P_\infty}{1/2\rho\, U_\infty} = -K + p(X) \ .$$

Note that $p(X) = 0$ on the cavity. Moreover, the velocity magnitude on the cavity is

$$q_c = U_\infty \sqrt{1 + K}$$

and, if all disturbance velocities (u,v) are normalized with respect to this cavity speed, we have

$$U(X) = q_c\, [1 + u(X)]$$

and, to terms of first order,

$$p(X) = -2\, (1+K)\, u(X) \ .$$

We can now discuss the pressure distribution shown above in terms of this notation. Note that this diagram shows three regions:

(i) from $X = 0$ to $X = X_o$ at A, where $p(X_o) = \lambda h$, $\lambda \ll 1$.

Two shapes for this region are considered:

$$p(X) = \frac{X}{X_o} \lambda h \qquad \text{linear rise,}$$

or

$$p(X) = \lambda h \sqrt{\frac{X}{X_o}} \qquad \text{parabolic rise.}$$

$$(C-1)$$

This region of small positive perturbation pressure is required to give the profiles resulting from the design process some tolerance to angle of attack variations without wetted surface cavitation occurring.

(ii) from A to B $[X_o \leq X \leq (1-S)]$, "Stratford Recovery" region. This is considered more fully below.

(iii) from B to C $[(1-S) \leq X \leq 1]$. This region of falling pressure will have an elliptic contour:

$$p(X) = \frac{h}{S} \sqrt{(1-X)(2S-1+X)} \ . \qquad (C-2)$$

This particular shape has been chosen to have zero slope at B, where $p = h$, and to behave like $p \sim \sqrt{1-X}$ near the trailing edge. This latter condition characterizes the trailing edge condition of the flows studied in [2].

Canonical Pressure Distribution:

For boundary layer calculations in the Stratford region, the so-called canonical pressure distribution is most useful. It is based on the pressure
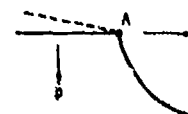

Figure C-2

at A, $P_o = P(X_o)$, just at the start of the pressure rise. Note that this definition varies somewhat from airfoil [13, 14, 15, 16] usage in which P_o is taken to be the _lowest_ pressure on the foil. Our definition is consistent with the requirement that, except for the leading and trailing edges, the wetted surface of the profile must have a positive perturbation pressure. The canonical pressure distribution is defined as follows:

$$\overline{C}_p = \frac{P(X) - P_o}{1/2 \, U_o^2} \quad .$$

We can now translate this quantity into those which we will need for hydrofoil design. Thus,

$$\overline{C}_p = \left[\frac{P(X) - P_c}{1/2\rho \, U_\infty^2} + \frac{P_c - P_o}{1/2\rho \, U_\infty^2} \right] \frac{U_\infty^2}{U_o^2} = [p(X) - p_o] \frac{U_\infty^2}{U_o^2} \quad ,$$

where p_o is the perturbation pressure at $X = X_o$.

Moreover,

$$\frac{U_\infty^2}{U_o^2} = \frac{U_\infty^2}{q_c^2 [1 + u(X_o)]^2} = \frac{1}{(1 + K) \, [1 - p_o/2(1 + K)]^2}$$

$$= \frac{1}{1 + K - p_o + p_o^2/4(1 + K)} \quad .$$

But $1 > p_o > \dfrac{p_o^2}{4(1 + K)}$ and we can neglect the second order term compared to 1. Moreover, in the present case $p_o = \lambda h$. So, the final result which we require to translate specifications on perturbation pressure $p(X)$ into canonical pressure distributions, $\overline{C}_p(X)$, is

$$\overline{C}_p(X) = \frac{p(X) - \lambda h}{1 + K - \lambda h} \qquad . \tag{C-3}$$

The perturbation pressure is needed to calculate the lift coefficient, C_L, and the canonical pressure coefficient is needed for boundary layer calculations.

Now the boundary layer flow state at the start of the Stratford recovery is characterized by the momentum thickness at point A [10, 11]. Moreover, Stratford's experiments and his theory pertain to a pressure recovery region which is preceded by flat region of x_o. In the pressure recovery region normalized coordinates are x/x_o with origin at $x = 0$. To start the pressure rise, Stratford gives formulae, based on matching the momentum thickness at $x/x_o = 1$, to account for other than flat pressure distributions ahead of X_o for both laminar and turbulent boundary layers. In the present application, we will assume that the boundary layer is turbulent from the nose of the foil to the point X_o. Then, the "effective" flat region x_o is

$$x_o = \int_0^{X_o} \left(\frac{U}{U_o} \right)^3 dX = \int_0^{X_o} \left(\frac{2(1 + K) - p(X)}{2(1 + K) - p_o} \right) dX \quad . \tag{C-4}$$

For the linear pressure distribution, we get

$$x_o = X_o \left[1 + \frac{3}{4} \frac{\lambda h}{1 + K} + \frac{5}{8} \left(\frac{\lambda h}{1 + K} \right)^2 + \dots \right] \quad ,$$

and for the parabolic nose pressure, we have

$$x_o = X_o \left[1 + \frac{1}{2} \frac{\lambda h}{1 + K} + \frac{3}{2} \left(\frac{\lambda h}{1 + K} \right)^2 + \dots \right] \quad .$$

In either of these cases, we can write

$$x_o = X_o \frac{1}{\tau} \, . \tag{C-5}$$

The quantity τ is defined by one or the other of the above functions of $\lambda h/(1 + K)$.

The Stratford Recovery

The chief result of Stratford's investigation is contained in his canonical pressure distribution [12]. It is

$$\overline{C}_p \left(\frac{x}{x_o} \right) = \begin{cases} 0.49 \left\{ Re_o^{1/5} \left[\left(\frac{x}{x_o} \right)^{1/5} - 1 \right] \right\}^{1/3}, \ \overline{C}_p \leq \frac{4}{7} \\ \\ 1 - \dfrac{a}{\sqrt{(x/x_o)+b}} \qquad\qquad , \ \overline{C}_p > \frac{4}{7} \end{cases} \tag{C-6}$$

where $Re_o = \dfrac{U_o x_o}{\nu} = \dfrac{U_\infty X_o}{\nu} \ \dfrac{\sqrt{1 + K}}{\tau}$

and where the constants a and b are chosen to match $\overline{C}_p$ and $d\overline{C}_p/dx$ when $\overline{C}_p = 4/7$. Now, the above formulae are written for a hydrofoil of unit chord. Naturally, we will be dealing with foils of chord c. All we need to relate Re_o for this case to the Reynolds number based on chord c is to put

$$Re_o = \left(\frac{U_\infty c}{\nu} \right) \frac{X_o \ \sqrt{1 + K}}{\tau} = Re \ \frac{X_o \ \sqrt{1 + K}}{\tau} \quad , \tag{C-7}$$

where now, Re and Re_o are based on actual distances.

Coordinates and Lift Coefficient

As we have seen, there are two sets of coordinates: those which

measure actual distances along the unit chord of the profile, designated by X, X_o etc., and those which relate to the canonical pressure distribution, designated by x, x_o etc. We must determine the relationships between these coordinates in order to continue the analysis. We have already obtained one result in the form of the Equation (C-5) which is

$$X_o = x_o \tau \quad .$$

However, this relationship holds only at the point A on the foil. That is, when $X = X_o$ and $x = x_o$. But we know that in going from A to B, we follow the Stratford Recovery and, in particular, when we are at B, $X = (1 - S)$. Moreover, at B we know that $p(X) = h$, and so the canonical pressure coefficient from Equation (3) is

$$\overline{C}_p = \frac{(1 - \lambda)h}{1 + K - \lambda h} \quad . \tag{C-8}$$

This value of C_p can be put into the Stratford Recovery and the corresponding value of x/x_o found. Denote this value of x/x_o, corresponding to $X = 1 - S$, by Z. Then, we find that

$$
Z = \begin{cases}
\left\{ 1 + \dfrac{1}{(Re_o)^{1/5}} \left[\dfrac{(1 - \lambda)h}{.49(1 + K - \lambda h)} \right]^3 \right\}^5 \quad , \quad \dfrac{(1 - \lambda)h}{1 + K - \lambda h} \leq \dfrac{4}{7} \\[20pt]
\left(\dfrac{a}{1 - \dfrac{(1 - \lambda)h}{1 + K - \lambda h}} \right)^2 \quad , \quad \dfrac{(1 - \lambda)h}{1 + K - \lambda h} > \dfrac{4}{7} \quad .
\end{cases}
\tag{C-9}
$$

We now have two pairs of corresponding points:

at A $\quad \dfrac{x}{x_o} = 1, \dfrac{X}{X_o} = 1$; and at B $\quad \dfrac{x}{x_o} = Z, \dfrac{X}{X_o} = \dfrac{1 - S}{x_o} \quad .$

Evidentially, as one traverses the distance from A to B on the wetted

surface x goes from x_o to Zx_o. Therefore, the distance is $(Z-1)x_o = (Z-1)X_o/\tau$. But, the profile has unit chord. Hence, the sum of the distances from 0 to A, A to B and B to C is

$$1 = X_o + (Z-1)X_o/\tau + S$$

or

$$(1-S)\tau = (\tau + Z - 1)X_o \tag{C-10}$$

This is a fundamental geometrical constraint on the variables of the problem which we will need later.

In order to consider further the relationship between the boundary layer coordinate x and the hydrofoil coordinate X, let us take a point Q in the Stratford Recovery region between A and B. Suppose Q has the foil coordinate X and the boundary layer coordinate x. Then, it must follow that

$$X - X_o = x - x_o \quad .$$

Now we can divide this relationship by x_o:

$$\frac{X}{x_o} - \frac{X_o}{x_o} = \frac{x}{x_o} - 1 \quad .$$

Next, we can apply Eq. (C-5) to this result to obtain

$$\frac{x}{x_o} = \frac{X}{x_o} + 1 - \tau \quad . \tag{C-11}$$

Equation (C-5) relates the boundary layer variable $z = x/x_o$, appearing in the Stratford Recovery equations, to the geometric coordinate X on the profile.

It is the coordinate X, along with the perturbation pressure p(X), which allows us to calculate the lift coefficient. Moreover, since the quantity x_o is determined by Eqs. (C-1) or (C-2), we can use it to relate the boundary layer coordinate in the Stratford region to the geometric coordinate X without ambiguity. In particular, we can write

$$C_L = \int_0^1 p(X) dX \quad .$$

Then, with the help of Eqs. (C-1), (C-2), and (C-3), this formula becomes

$$C_L = \lambda h[(1-S) - \frac{1}{2} X_o] + \frac{\pi S h}{4} + (1 + K - \lambda h) \frac{X_o}{\tau} \int_\tau^{\tau + Z - 1} \overline{C}_p(\frac{X}{x_o} + 1 - \tau) \, d(\frac{X}{x_o})$$

$$(C-12)$$

for the linear nose pressure distribution and for the parabolic case,

$$C_L = \lambda h[1 - S - \frac{1}{3} X_o] + \frac{\pi S h}{4} + (1 + K - \lambda h) \frac{X_o}{\tau} \int_\tau^{\tau + Z - 1} \overline{C}_p(\frac{X}{x_o} + 1 - \tau) \, d(\frac{X}{x_o})$$

$$(C-13)$$

Note that Eq. (C-11) and the considerations leading to Eq. (C-10) have been used to put the integrals in Eqs. (C-12) and (C-13) in a form suitable for direct use of the Stratford Recovery as specified by Eqs. (C-6)

Further Details of the Solution

The preceding sections provide all essential ingredients necessary for the determination of the prescribed pressure distribution on the profile. However, in order to implement these results, a number of subsidiary calculations must be completed. For example, we have noted that

the Stratford Recovery requires that a joining of profile shapes occurs at $\overline{C}_p = 4/7$. At this pressure, $\overline{C}_p(z)$ and $d\overline{C}_p/dz$ are to be continuous. These two conditions permit us to calculate the constants a and b of Eqs. (C-6). At the point of joining, let us put

$$z = z_0 \quad \text{for} \quad \overline{C}_p = \frac{4}{7} \ .$$

Then, from the first of Eqs. (C-6), we have,

$$z_0 = \left[\frac{1.586}{(Re_0)^{1/5}} \right]^5 \ .$$

Then, it follows that

$$a = \frac{1.206}{Re_0^{1/5}} z_0^{4/5} (z_0^{1/5} - 1)^{2/3}$$

$$b = \frac{6.563 \, z_0^{4/5} (z_0^{1/5} - 1)^{2/3}}{Re_0^{1/5}} - z_0$$

Now, we can continue with the determination of the matching of the Stratford Recovery to other prescribed conditions on the pressure distribution. We require that the lift coefficient be specified in advance. However, the point X_0 is as yet undetermined, and the value of h, the maximum pressure on the wetted surface, is also unknown. We know that the Stratford Recovery allows for the steepest possible pressure rise without turbulent separation. Thus, we can specify a family of pressure distributions, depending on the parameter S. Members of this family will all have the same values of C_L, K and Reynolds number.

The values X_0 and h must be determined by trial and error. We can use the basic geometrical constraint and either Eqs. (C-12) or (C-13)

for C_L to guide the iteration in a Newton-Raphson procedure. Thus, we can write Eq. (C-10) as

$$G\ (X_o,h) = \frac{1-S}{X_o} - 1 - Z + 1 = 0 \quad ,$$

and Eq. (C-12), for example, as

$$C_L(X_o,h) = \lambda[1 - S - \frac{1}{2}\ X_o] + \pi Sh/4 + I \quad .$$

Then, we suppose that, in the process of iteration, we find at some step a difference in the calculated value of C_L from that specified. Let this difference be ΔC_L. Then we have

$$\frac{\partial C_L}{\partial h}\ \Delta h + \frac{\partial C_L}{\partial X_o}\ \Delta X_o = \Delta C_L$$

and

$$\frac{\partial G}{\partial h}\ \Delta h + \frac{\partial G}{\partial X_o}\ \Delta X_o = 0 \quad .$$

Evidentally, one can solve for Δh and ΔX_o and use them to determine the next value of h and X_o in the iteration. This is a standard procedure. It needs no further discussion here. The calculation of all the partial derivatives from the formulae of the preceding sections is rather tedious. We shall, therefore, proceed to the discussion of results.

These results are contained in Figure (C-3) which shows the variation of L/D for a range of peak pressure locations at zero cavitation number. For each value of cavity thickness T three values of C_L are used. Note that the trends show that the nose loading, corresponding to large values of S, lead to more favorable L/D values than the tail-loaded

profile obtained at small values of S. As we have already explained the

chief value of the Stratford recovery is for tail-loaded profiles which

are not as efficient as those having nose loading. Therefore we have

discarded this kind of pressure distribution in favor of the simple

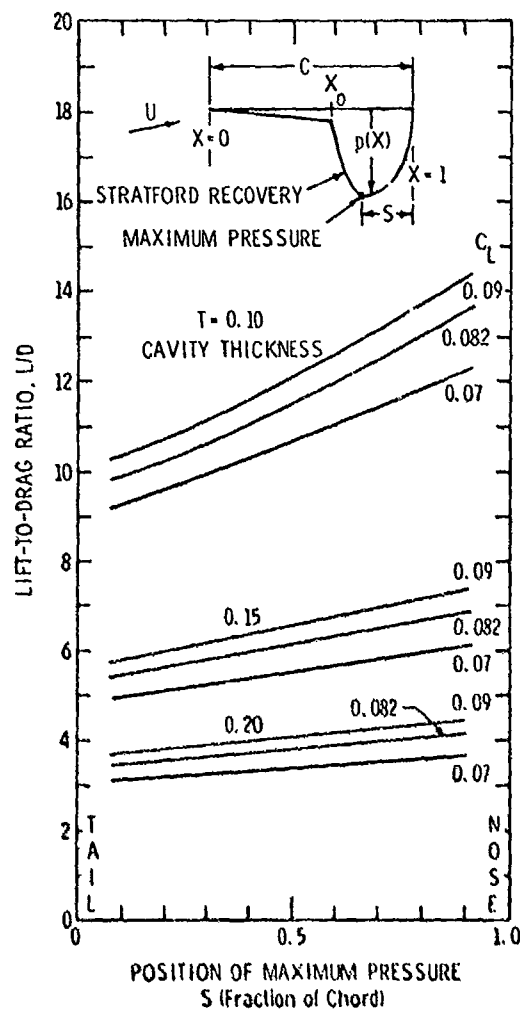double elliptical form which has been used in the body of this study.

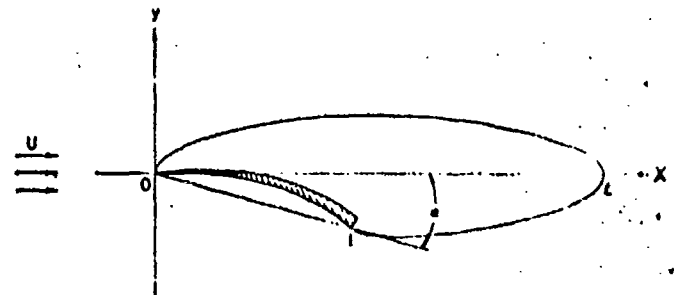Figure C-3 — Lift-to-drag ratio of a profile using a Stratford recovery for three prescribed lift coefficients and three cavity thicknesses.

APPENDIX D

Fig. 1 Schematic diagram of cavity flow past a hydrofoil

the x-axis. The chord of the profile is inclined at an angle of attack α with respect to the undisturbed flow. The shape of the wetted surface, measured from the x-axis, is defined by the function $f(x)$. The cavity extends back over the upper surface of the foil. Generally, the static pressure of the gas or vapor inside the cavity P_b will be less than the free stream static pressure P_∞ and the cavity will close at a finite distance of abscissa l, behind the hydrofoil nose. When $l > 1$ the flow is called fully cavitating. Partial cavitation is said to exist when the cavity closes on the upper surface of the profile. Only fully cavitating flows are considered in this paper. In such flows the flow state is characterized by the cavitation number,

$$ K = \frac{P_\infty - P_b}{\frac{1}{2} \rho U^2} \tag{1} $$

In this section we shall consider those special flows for which $K = 0$. In this limiting case the cavity length l becomes infinite and the flow speed on the cavity surface is equal to the free stream speed, U.

Let the flow at any point in the x, y-plane be given by the velocity vector $q(x, y)$. Next, as is customary, we introduce the x and y components of the disturbance velocity caused by the foil. These are $u(x, y)$ and $v(x, y)$, respectively. The perturbation velocities are related to the vector q by

$$ q = U[1 + u, v]. \tag{2} $$

In accordance with the linearization scheme we must have $u, v \ll 1$. We shall also assume that the cavity surfaces and the wetted surface of the hydrofoil lie close enough to the x-axis so that in the z-plane ($z = x + iy$) the boundary conditions on the complex velocity,

$$ w(z) = u - iv, \tag{3} $$

Hydrofoils at Zero Cavitation Number and Related Airfoils [2]

Consider the steady rectilinear flow of a liquid of density ρ past a fully cavitating hydrofoil of unit chord in two dimensions. As illustrated in Fig. 1, the profile nose is at the origin of coordinates and the free stream velocity has magnitude U and flows parallel to
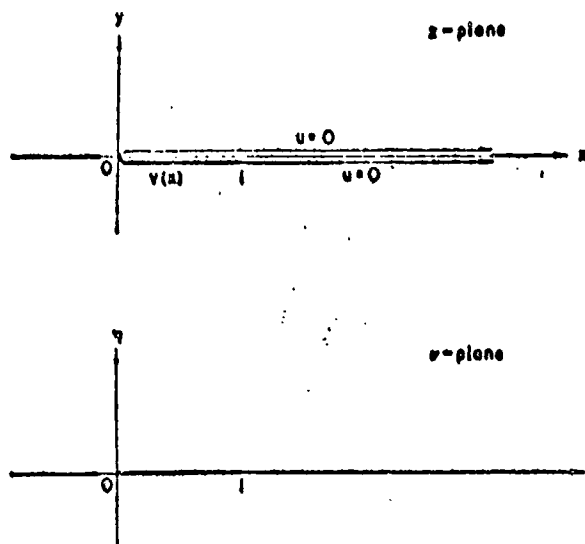
Fig. 2 Boundary conditions in the physical plane (z-plane) and corresponding boundaries in the transformed plane (ν-plane) for zero cavitation number

Fig. 3 Geometric parameters for a circular-arc hydrofoil

can be applied on the x-axis. The linearized boundary conditions for the analytic function $w(z)$ are shown in Fig. 2. These conditions can be summarized as follows:

$$\left.\begin{array}{ll} u(x, 0+) = 0 & \text{for } x > 0, \\ v(x, 0-) = f'(x) & \text{for } 0 \le x \le 1, \\ u(x, 0-) = 0 & \text{for } x > 1, \\ u = v = 0 & \text{as } |z| \to \infty. \end{array}\right\} \tag{4}$$

By means of the conformal transformation,

$$\nu = \xi + i\eta = -z^{1/2}, \tag{5}$$

the whole z-plane is mapped into the lower half of the ν-plane with the solid surface lying on the real ν-axis between $\xi = 0$ and $\xi = 1$. The cavity boundaries lie along the remainder of the real axis. The ν-plane and the transformed boundary conditions are also illustrated in Fig. 2. It is to be noted that we have chosen w to be invariant under the mapping, that is

$$w(z) = u(x, y) - iv(x, y) = w(\nu^2) = w^*(\nu)$$
$$= u^*(\xi, \eta) - iv^*(\xi, \eta). \tag{6}$$

We can obtain the related airfoil formulas by noting that on part of the real ν-axis $u = u^* = 0$. Therefore $w^*(\nu)$ can be continued analytically into the upper half of the ν-plane by the Riemann-Schwartz principle of reflection [6]. For the present flow we can write

$$w^*(\bar{\nu}) = -\overline{w^*(\nu)}, \tag{7}$$

so that u^* is odd and v^* is even in η. After the analytic continuation the flow in the ν-plane will be recognized as the flow past an airfoil of zero thickness with w^* being the disturbance created by the airfoil in an otherwise uniform stream of velocity $V^* = U$. As a consequence of the invariance indicated by equation (6), the shape of the transformed solid boundary in the ν-plane, determined by $v^*(\xi, 0)$, will generally be different from the wetted surface shape in the z-plane. Let the shape of the new related airfoil be denoted by

$$\eta = \varphi(\xi). \tag{8}$$

Then from equation (6) it follows that

$$\frac{df(x)}{dx} = v(x, 0-) = v^*(\xi, 0\pm) = \frac{d\varphi(\xi)}{d\xi}, \quad \text{for } 0 < x = \xi^2 < 1.$$
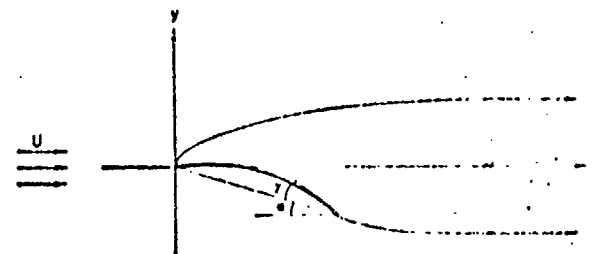
Hence, the shape of the related airfoil is given by

$$\varphi(\xi) = \int_0^\xi \frac{1}{2t} \frac{df(t^2)}{dt} dt \tag{9}$$

for $0 < \xi < 1$.

For example, if we take

$$f(x) = ax + bx^2 + cx^3 + \ldots, \quad 0 \le x \le 1,$$

we find that

$$\varphi(\xi) = a\xi + \frac{2b}{3}\xi^3 + \frac{3c}{5}\xi^5 + \ldots, \quad 0 \le \xi \le 1.$$

Evidently, an inclined flat plate, defined by $f(x) = ax$, is mapped into itself. In the general case the shape of the related airfoil and even its angle of attack will be different from those of the original hydrofoil.

Corresponding to the disturbance velocity, we shall define the perturbation pressure coefficient $p(x, y)$ by

$$p(x, y) = \frac{P(x, y) - P_i}{\frac{1}{2}\rho U^2}, \tag{10}$$

where $P(x, y)$ denotes the static pressure at any point in the flow. Use of the linearized Bernoulli equation shows that $p(x, y) = -2u(x, y)$. The lift, drag, and moment[*] coefficients are

$$\begin{pmatrix} C_L \\ C_D \\ C_M \end{pmatrix} = \int_0^1 \begin{pmatrix} 1 \\ f'(x) \\ -x \end{pmatrix} p(x, 0-) dx$$

$$= -2 \int_0^1 \begin{pmatrix} 1 \\ v'(x, 0-) \\ -x \end{pmatrix} u(x, 0-) dx$$

$$= \int_0^1 \begin{pmatrix} 1 \\ v^*(\xi, 0-) \\ -\xi^2 \end{pmatrix} u^*(\xi, 0-)\xi d\xi \tag{11}$$

The expression for C_D can be simplified by means of the Poisson integral formula [7]

$$v^*(\xi, 0-) = \frac{1}{\pi} \text{P.V.} \int_0^1 \frac{u^*(t, 0-)}{t - \xi} dt,$$

where P.V. stands for the Cauchy principle value of the integral. Thus,

$$C_D = -\frac{4}{\pi} \text{P.V.} \int_0^1 u^*(\xi, 0-) d\xi \int_0^1 \frac{u^*(t, 0-)}{t - \xi} [(\xi - t) + t] dt$$

$$= \frac{4}{\pi} \left\{ \int_0^1 u^*(\xi, 0-) d\xi \right\}^2 + 4 \int_0^1 v^*(t, 0-) u^*(t, 0-) dt$$

Hence

$$C_D = \frac{2}{\pi} \left\{ \int_0^1 u^*(\xi, 0-) d\xi \right\}^2. \tag{12}$$

---

[*] Moments are counted positive if they tend to increase the angle of attack. Note that the moment is taken about the nose of the profile.

On the other hand, the lift, moment, and the third moment of the related airfoil are

$$\begin{pmatrix} C_L^* \\ C_M^* \\ C_{3M}^* \end{pmatrix} = \int_0^1 \begin{pmatrix} 1 \\ \xi \\ -\xi^2 \end{pmatrix} [p^*(\xi, 0-) - p^*(\xi, 0+)] d\xi$$

$$= -4 \int_0^1 \begin{pmatrix} 1 \\ \xi \\ \xi^2 \end{pmatrix} u^*(\xi, 0-) d\xi \qquad (13)$$

Therefore, by comparison with equations (11) and (12) we find

$$C_L = C_M^*, \qquad C_M = -C_{3M}^*, \qquad C_z = C_L^{*2}/2\pi. \qquad (14)$$

The location of the center of pressure, expressed as a fraction of the chord from the hydrofoil nose, is

$$C.P. = -C_M/C_L = -C_{3M}^*/C_M^*. \qquad (14a)$$

These equivalence relationships between the hydrofoil and the related airfoil are due to Tulin and Burkart [1, 2].

From the direct problem of thin airfoil theory [8], it is known that C_L^*, C_M^*, and C_{3M}^* can be expressed in terms of the Fourier coefficients of $v^*(\xi, 0\pm)$. Write

$$-v^*(\xi, 0\pm) = \frac{a_0}{2} + \sum_{n=1}^{\infty} a_n \cos n\theta, \qquad (15)$$

where

$$\xi = (1 + \cos \theta)/2, \qquad -\pi < \theta < \pi,$$

and where

$$a_n = -\frac{2}{\pi} \int_0^\pi v^*(\xi, 0\pm) \cos n\theta \, d\theta. \qquad (15a)$$

It is also shown that

$$p^*(\xi, 0-) = -2v^*(\xi, 0-) = -a_0 \tan \frac{\theta}{2}$$

$$- 2 \sum_{n=1}^{\infty} a_n \sin n\theta, \qquad -\pi < \theta < 0, \qquad (15b)$$

and hence, from equation (13) that

$$\left.\begin{array}{l} C_L^* = \pi(a_0 + a_1), \qquad C_M^* = \frac{\pi}{4}(a_0 + 2a_1 + a_2) \\[2mm] \text{and} \\[2mm] C_{3M}^* = \frac{\pi}{32}\left[\frac{5}{2}a_0 + 7(a_1 + a_2) + 3a_3 + \frac{1}{2}a_4\right]. \end{array}\right\} \qquad (16)$$

Therefore, from equations (14) and (16), the hydrodynamic reactions on the hydrofoil are determined by quadratures.

It is important to note that for vaporous cavitation the cavity pressure must be the lowest pressure in the flow. Therefore, on the wetted surface of the foil, the disturbance pressure, $p(x, 0-) = p^*(\xi, 0-)$, must be nonnegative. Accordingly, the coefficient a_0 must be such that the right-hand side of equation (15b) is nonnegative. Otherwise the flow configuration will not correspond to that which we have postulated. (This requirement is one which should be added to those summarized in equation (4).) In particular, it is necessary that $a_0 \geq 0$. This coefficient determines the strength of the mean singularity. When it vanishes, the flow is said to exhibit smooth or "shockless" entry. If a_0 were to become negative the cavity would change sides at least near the profile leading edge.

The preceding development of the linearized theory for $K = 0$ permits us to consider three specific examples. First, in order to give a basis for subsequent comparison we will treat the flat plate

hydrofoil. Next, to show the effects of camber, we will apply theory to circular arc hydrofoils. Finally, we will consider optimum design problem for fully cavitating hydrofoils at K

Example 1. Flat-Plate Hydrofoil. For a flat-plate hydrofoil angle of attack, α, we have $f(x) = -\alpha x$ and

$$v^*(\xi, 0-) = v(x, 0-) = -\alpha.$$

From equations (11) it follows that

$$a_0 = 2\alpha, \qquad a_n = 0, \qquad n = 1, 2, \ldots.$$

Hence, from equations (14) and (16) we obtain

$$C_L = \frac{\pi}{2}\alpha, \qquad C_D = \frac{\pi}{2}\alpha^2,$$

$$C_M = -\frac{5\pi}{32}\alpha \quad \text{and} \quad C.P. = \frac{5}{16}$$

These results show the total force on the fully cavitating flat to be normal to the plate, as it should be. Also C.P., the al of the center of pressure, is $5/16$ chord from the leading These values for the coefficients will be recognized as a line form of Kirchoff's exact solution [9] for small values of x.

Example 2. Circular-Arc Hydrofoil. The circular-arc which subtends a total angle of 2γ at the center of the circle which is at an angle of attack α, is defined for small values of

$$f(x) = -\alpha x + \gamma x(1 - x).$$

Then we have

$$v^*(\xi, 0-) = v(x, 0-) = \gamma - \alpha - 2\gamma x = \gamma - \alpha - 2\gamma\xi$$

$$= \left(\frac{\gamma}{4} - \alpha\right) - \gamma \cos \theta - \frac{\gamma}{4}$$

where θ is defined in equation (15). From equation (11) tain

$$a_0 = 2\alpha - \frac{\gamma}{2}, \qquad a_1 = \gamma, \qquad a_2 = \gamma/4,$$

$$a_3 = a_4 = \ldots = 0$$

From equations (14) and (16) it follows that

$$C_L = \frac{\pi}{2}\left(\alpha + \frac{7\gamma}{8}\right), \qquad C_D = \frac{\pi}{2}\left(\alpha + \frac{\gamma}{4}\right)^2,$$

$$C_M = -\frac{5\pi}{32}\left(\alpha + \frac{3}{2}\gamma\right)$$

and

$$C.P. = \frac{5}{16}\left(\alpha + \frac{3}{2}\gamma\right)\Big/\left(\alpha + \frac{7\gamma}{8}\right).$$

Moreover the requirement that $a_0 \geq 0$ implies that

$$\alpha \geq \frac{\gamma}{4}$$

if the solution is to be valid. When this condition is sati we see that at a given value of α, an increasing positive camber always increases the lift, drag, and moment and moves the center of pressure farther to the rear from the f location. In particular,

$$\frac{\partial C_L}{\partial \gamma} = \frac{7\pi}{16}, \qquad \frac{\partial C_D}{\partial \gamma} = \frac{\pi}{4}\left(\alpha + \frac{\gamma}{4}\right), \qquad \frac{\partial C_M}{\partial \gamma} = -\frac{15}{0}$$

A point of interest is the favorable increase of C_L due to in γ for fully cavitating hydrofoils. For fixed α, the lift-d is a maximum at

$$\gamma\big|_{opt} = \frac{12}{7}\,\alpha,\qquad (25)$$

giving

$$\frac{L}{D}\bigg|_{max} = \frac{40}{40}\,\frac{1}{\alpha}. \qquad (26)$$

This value of L/D is a 22.5 percent increase over the flat-plate value of $1/\alpha$.

Example 3. Optimum Profile Design. From the results of the preceding example we are led to consider the design of the optimum profile. To do this one attempts to determine that profile shape which, for prescribed drag coefficient and attack angle α, will produce the highest lift. From the general formulas we have

$$C_L = \frac{\pi}{4}\,(a_0 + 2a_1 + a_2) \qquad (27)$$

and

$$C_D = \frac{\pi}{8}\,(a_0 + a_1)^2. \qquad (28)$$

When the value of α is prescribed we must have $f(0) = 0, f(1) = -\alpha$ which constrains the form of the Fourier coefficients as follows:

$$f(1) = -\alpha = \int_0^1 v(x,0-)dx = 2\int_0^1 v^*(\xi,0-)\xi d\xi,$$

or upon using equation (15) we find after term by term integration that

$$\alpha = \frac{a_0}{2} - \sum_1^\infty \frac{a_{2n}}{4n^2 - 1} - \sum_1^\infty \frac{a_{2n-1}}{(2n+1)(2n-3)}. \qquad (29)$$

Moreover, since $p(x, 0-)$ must be nonnegative at every point on the foil we have from equation (15b), that $a_0 \geqslant 0$, and that

$$\frac{a_0}{2}\tan\frac{\theta}{2} + \sum_1^\infty a_n \sin n\theta \geqslant 0 \text{ for } 0 \leq \theta < \pi. \qquad (30)$$

It is clear on physical grounds that if the whole underside of the profile is to be wetted, from the nose to the trailing edge, we must have $v(1) \leq 0$, or by equation (15) that

$$a_0 + 2\sum_1^\infty a_n \geqslant 0. \qquad (31)$$

Since C_L and C_D depend upon the first three coefficients only, the problem of finding a unique set of values of the a_n's corresponding to the highest C_L for prescribed C_D and α, and which also satisfies conditions (30) and (31) is not a mini-max problem.

For practical engineering purposes we shall confine ourselves to the special class of profiles for which $a_3 = a_4 = \ldots = 0$. Then equations (27) through (29) can be solved for a_0, a_1, and a_2. The solution is

$$\left.\begin{array}{l} a_0 = -\dfrac{8C_L}{\pi} + 6\sqrt{\dfrac{8C_D}{\pi}} - 6\alpha, \\[3mm] a_1 = \dfrac{8C_L}{\pi} - 5\sqrt{\dfrac{8C_D}{\pi}} + 6\alpha, \\[3mm] a_2 = -\dfrac{4C_L}{\pi} + 4\sqrt{\dfrac{8C_D}{\pi}} - 6\alpha. \end{array}\right\} \qquad (32)$$

The condition that $a_0 \geqslant 0$ and conditions (30) and (31) lead to

$$\left.\begin{array}{l} 2\sqrt{\dfrac{8C_D}{\pi}} \geqslant 3\alpha, \\[3mm] C_L \leqslant \dfrac{3\pi}{4}\left[\sqrt{\dfrac{8C_D}{\pi}} - \alpha\right]. \end{array}\right\} \qquad (33)$$

If the flow configuration is to remain as postulated, the first inequality shows that C_D and α cannot both be prescribed arbitrarily. When this first condition is satisfied the second inequality gives the largest attainable value of C_L. To proceed with the analysis let us write

$$\left.\begin{array}{l} \sqrt{\dfrac{8C_D}{\pi}} = \dfrac{3}{2}\,\epsilon\alpha \\[3mm] \dfrac{4C_L}{\pi} = 3\delta\left(\sqrt{\dfrac{8C_D}{\pi}} - \alpha\right), \end{array}\right\} \qquad (34)$$

where $\epsilon \geqslant 1$ and $0 < \delta \leqslant 1$. For a fixed value of δ, it is found that C_L/C_D is a maximum when $\epsilon = 4/3$. The limit $\delta = 1$ leads to $a_0 = 0$, which corresponds to the smooth entry configuration. In practice it may be desirable to retain the leading edge singularity since smooth entry is difficult to maintain or even to realize. To retain the nose singularity we simply choose δ slightly less than unity.

For instance if we take $\epsilon = 4/3, \delta = 14/15$, then for engineering purposes we have the following optimum values:

$$\left.\begin{array}{l} C_{D_0} = \dfrac{\pi}{2}\,\alpha^2 \\[3mm] C_{L_0} = \dfrac{7\pi}{10}\,\alpha. \end{array}\right\} \qquad (35)$$

The ratio $C_{L_0}/C_{D_0} = 7/(5\alpha)$ is greater than the flat plate case by 40 percent and it surpasses the maximum L/D of the circular arc by 14.4 percent. Now from equations (35) and (32) we obtain

$$a_0 = \frac{2}{5}\,\alpha, \quad a_1 = \frac{8}{5}\,\alpha \text{ and } a_2 = -\frac{4}{5}\,\alpha. \qquad (36)$$

Finally, the pressure condition, equation (30), becomes

$$\frac{a_0}{2}\tan\frac{\theta}{2} + a_1\sin\theta + a_2\sin 2\theta$$

$$= \frac{1}{5}\csc\theta(1 - \cos\theta)(1 + 8\sin^2\theta) > 0$$

for $0 < \theta < \pi$, so that this condition is fulfilled. The corresponding shape of the wetted surface is found to be

$$f(x) = -\frac{a_0}{2}\,x + a_1 x\left(1 - \frac{4}{3}\sqrt{x}\right) - \frac{a_2}{3}\,x(3 - 10\sqrt{x} + 15x)$$

$$= \frac{\alpha}{5}\,x(11 - 32\sqrt{x} + 10x), \quad 0 < x < 1. \qquad (37)$$

The camber function of the wetted surface, measured from the chord is

$$h(x) = f(x) + \alpha x = \frac{10\alpha}{5}\,x(1 - \sqrt{x})^2, \quad 0 < x < 1. \qquad (38)$$

The last point to check is to see whether or not there is interference between the upper surface of the foil and the camber line. From the general solution,
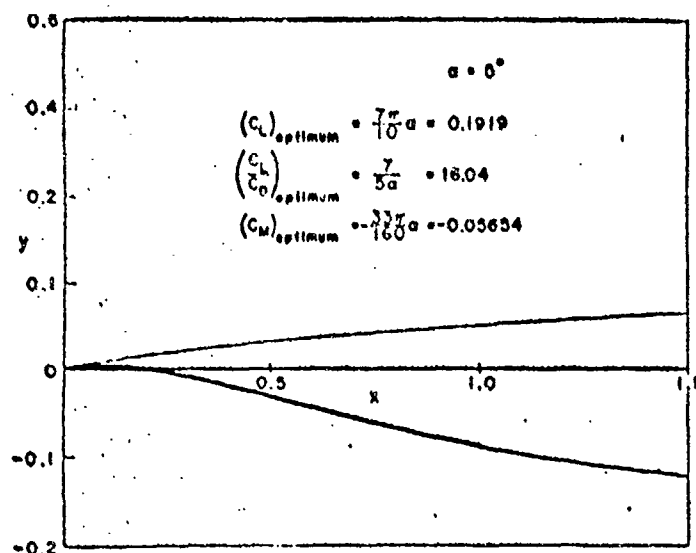
Fig. 4 Profile and cavity contours of a low-drag hydrofoil at $K = 0$. Note magnified vertical scale.

$$w^*(\nu) = u^* - i w^* = \frac{i a_0}{2}\left(1 - \sqrt{\frac{\nu - 1}{\nu}}\right)$$
$$+ i \sum_1^\infty a_n \left[2\nu - 1 - 2\sqrt{\nu(\nu - 1)}\right]^n,$$

in which the branches are chosen to make $\sqrt{(\nu - 1)/\nu} \to 1$ and $\sqrt{\nu(\nu - 1)} \to \nu$ as $|\nu| \to \infty$. We find the upper and lower boundaries of the cavity from

$$h_+(x) = \int_0^x v(x, 0+)dx \quad \text{for} \quad x > 0,$$

and

$$h_-(x) = -\alpha + \int_1^x v(x, 0-)dx \quad \text{for} \quad x > 1.$$

When the values of a_n for this example are put in the general solution and when the values for $v(x, 0\pm)$ are substituted in the integrals above the final result is

$$h_+(x) = \frac{\alpha}{10}\left\{(7 - 2\sqrt{x} - 48x - 32x^{1/4})\sqrt{x + \sqrt{x}}\right.$$
$$- 7\log\left(\sqrt{1 + \sqrt{x}} + x^{1/4}\right) + 22x + 64x^{1/4} + 32x^2\right\}, \quad (39)$$

$$h_-(x) = \alpha + \frac{\alpha}{10}\left\{(7 + 2\sqrt{x} - 48x + 32x^{1/4})\sqrt{x - \sqrt{x}}\right.$$
$$+ 7\log\left(\sqrt{\sqrt{x} - 1} + x^{1/4}\right) - 22(x - 1)$$
$$+ 64(x^{1/4} - 1) - 32(x^2 - 1)\right\}. \quad (40)$$

The profile and the upper surface of the cavity calculated from equations (38) and (39) are shown to scale in Fig. 4. It is seen that the cavity does clear the lower surface of the hydrofoil.

References

1. B. R. Parkin and R. S. Grote, "Inverse Methods in the Linearized
    Theory of Fully-Cavitating Hydrofoils," Trans. ASME, Journal of
    Basic Engineering, Vol. 86, Series D, No. 4, December 1974,
    p. 641-654.

2. B. R. Parkin, "The Inverse Problem of the Linearized Theory of
    Fully-Cavitating Hydrofoils," Research Memorandum RM-3566 PR,
    The Rand Corporation, Santa Monica, California, September 1964,
    AD 606 038.

3. R. S. Grote, "Numerical Methods and Program Description for the
    Inverse Problem of Linearized, Fully-Cavitating, Hydrofoil Theory,"
    The Rand Corporation, RM-3563, September 1974, AD 606 062.

4. A. G. Fabula, "Fundamental Step Profiles in Thin Airfoil Theory
    with Hydrofoil Application," Journal of the Aerospace Sciences,
    Vol. 28, No. 6, June 1961.

5. L. M. Milne-Thomson, Theoretical Aerodynamics, Fourth Edition,
    Dover Publications, New York, 1973, p. 147-156.

6. M. A. Biot, "Some Simplified Methods in Airfoil Theory," Journal
    of the Aeronautical Sciences, Vol. 9, No. 5, March 1942, p. 185.

·7. H. J. Stewart, "A Simplified Two-Dimensional Theory of Thin Air-
    foils," Journal of the Aeronautical Sciences, Vol. 9, No. 12,
    October 1942, p. 452.

8. R. F. Davis and J. Fernandez, "Computer Program Description for
    Supercavitating Hydrofoil Section Design According to Linearized
    Theory," Technical Memorandum, 75-221, September 1975.

9. M. P. Tulin, "Supercavitating Flow Past Foils and Struts,"
    Cavitation in Hydrodynamics, National Physical Laboratory,
    H. M. Stationery Office, London, 1956, p. 16-1.

10. B. R. Parkin, "Munk Integrals for Fully-Cavitating Hydrofoils,"
    Journal of the Aerospace Sciences, Vol. 29, No. 7, July 1962,
    p. 775.

11. T. Cebeci, G. T. Mosinskis and A. M. O. Smith, "Calculation of
    Separation Points in Incompressible Turbulent Flows," Journal
    of Aircraft, Vol. 9, No. 9, September 1972, p. 618.

References (Cont.)

12. B. S. Stratford, "The Prediction of Separation of the Turbulent
    Boundary Layer," Journal of Fluid Mechanics, Vol. 5, p. 1-16, 1959.

    _____, "An Experimental Flow with Zero Skin Friction
    Throughout its Region of Pressure Rise," Journal of Fluid Mechanics,
    Vol. 5, p. 17-35.

13. R. H. Liebeck and A. I. Ormsbee, "Optimization of Airfoils for
    Maximum Lift," Journal of Aircraft, Vol. 7, No. 5, Sept.-Oct. 1970,
    p. 409.

14. R. H. Liebeck, "A Class of Airfoils Designed for High Lift in
    Incompressible Flow," Journal of Aircraft, Vol. 10, No. 10,
    October, 1973, p. 610.

15. A. M. O. Smith, "Aerodynamics of High-Lift Airfoil Systems,"
    AGARD Conference Preprint No. 102 on Fluid Dynamics of Aircraft
    Stalling, AGARD Conference Proceedings No. 4, May 1968.

16. A. M. O. Smith, "High-Lift Aerodynamics," J. Aircraft, Vol. 12, No.
    6, June, 1975, p. 501.

DISTRIBUTION LIST FOR UNCLASSIFIED TM 75-170 by B. R. Parkin, R. F. Davis and J. Fernandez (dated June 30, 1975)

Commander
Naval Sea Systems Command
Department of the Navy
Washington, DC 20362
Attn: Library
     Code SEA-09G32
(Copies 1 and 2)

Naval Sea Systems Command
Attn: T. E. Peirce
     Code SEA-0351
(Copy No. 3)

Naval Sea Systems Command
Attn: Code SEA-03412
(Copy No. 4)

Naval Sea Systems Command
Attn: Code PMS-303
(Copy No. 5)

Commander
Naval Ship Engineering Center
Prince Georges Center
Hyattsville, MD 20782
Attn: Code SEC-6110
(Copy No. 6)

Naval Ship Engineering Center
Attn: Code SEC-6136
(Copy No. 7)

Commanding Officer
Naval Underwater Systems Center
Newport, RI 02840
Attn: J. F. Brady
(Copy No. 8)

Commanding Officer
Naval Undersea Center
San Diego, CA 92132
Attn: J. W. Hoyt
     Code 2501
(Copy No. 9)

Commanding Officer
David W. Taylor Naval Ship R&D Center
Department of the Navy
Bethesda, MD 20084
Attn: Code 115
(Copy No. 10)

David W. Taylor Naval Ship R&D Center
Attn: Code 15
(Copy No. 11)

David W. Taylor Naval Ship R&D Center
Attn: Code 152
(Copy No. 12)

David W. Taylor Naval Ship R&D Center
Attn: Y. T. Shen
     Code 1524
(Copy No. 13)

David W. Taylor Naval Ship R&D Center
Attn: Code 1532
(Copies 14 and 15)

David W. Taylor Naval Ship R&D Center
Attn: Code 1542
(Copy No. 16)

David W. Taylor Naval Ship R&D Center
Attn: Code 1556
(Copies 17 and 18)

David W. Taylor Naval Ship R&D Center
Attn: Code 1572
(Copies 19 and 20)

David W. Taylor Naval Ship R&D Center
Attn: Code 1576
(Copy No. 21)

Dr. Allen J. Acosta
Prof. of Mech. Eng.
Div. of Engineering & Applied Science
California Institute of Tech.
Pasadena, CA 91109
(Copy No. 22)

Mr. T. F. Ogilivie
University of Michigan
Ann Arbor, MI 48105
(Copy No. 23)

Mr. C. T. Ray
Boeing Aerospace Company
Seattle, WA 98124
(Copies 24, 25 and 26)

Mr. H. R. Wright
Grumman Aircraft
Bethpage, Long Island
New York 11714
(Copy No. 27)

Defense Documentation Center
5010 Duke Street
Cameron Station
Alexandria, VA 22314

Via: Commander (SEA-09G32)
      Naval Sea Systems Command
      Department of the Navy
      Washington, DC 20362
(Copies 28-39)

Chief, Naval Material
Department of the Navy
Washington, DC 20360
Attn: MAT-033
(Copy No. 40)

Dr. Blaine R. Parkin
The Pennsylvania State University
Applied Research Laboratory
P. O. Box 30
State College, PA 16801
(Copy No. 41)

Dr. J. William Holl
The Pennsylvania State University
Applied Research Laboratory
P. O. Box 30
State College, PA 16801
(Copy No. 42)

Mr. Robert F. Davis
The Pennsylvania State University
Applied Research Laboratory
P. O. Box 30
State College, PA 16801
(Copy No. 43)

Mr. J. Fernandez
The Pennsylvania State University
Applied Research Laboratory
P. O. Box 30
State College, PA 16801
(Copy No. 44)